Stellar atmospheres

Academic year 2017 – 2018

Gregor Rauw
University of Liège

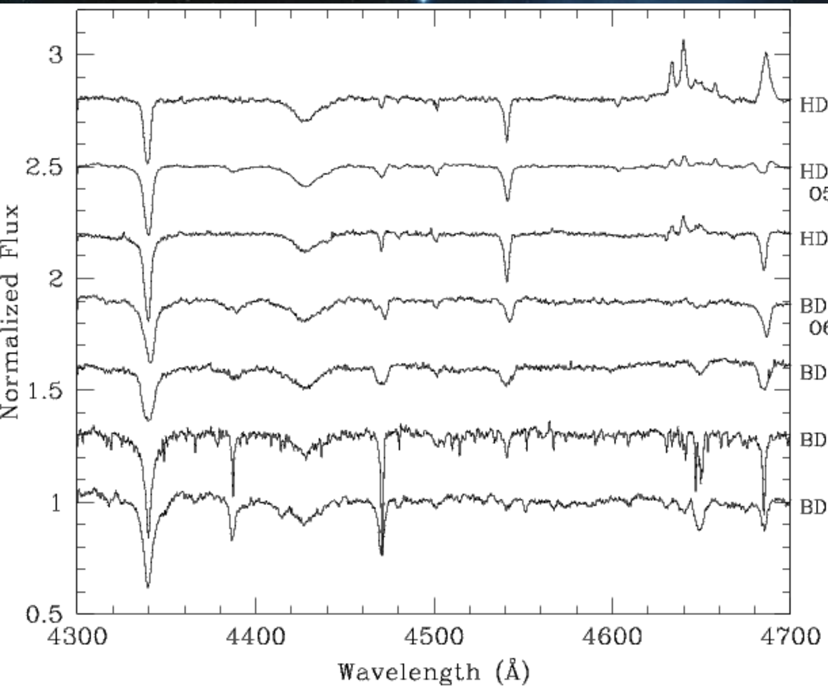

I. Introduction

- The whole light that we receive from stars arises in their atmosphere = narrow transition zone between the stellar interior and the interstellar medium.
- Solar atmosphere: photosphere, chromosphere, transition zone, corona.
- Photosphere = region where the visible light arises. In the case of the Sun: 1000 km (1 $R_\odot$ = 6.96 10^5 km). The temperature varies between 4000 and 8000 K.

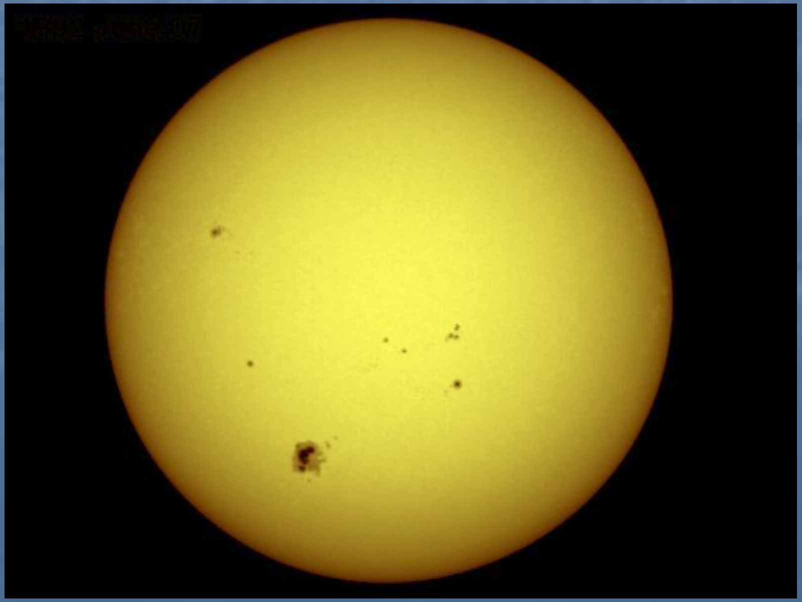

I. Introduction

- Chromosphere (height of about 2500 km in the case of the Sun). Temperature increases to about 50 000 K.
- The chromosphere produces Hα emission as well as emissions of Ca II at 3934 Å.

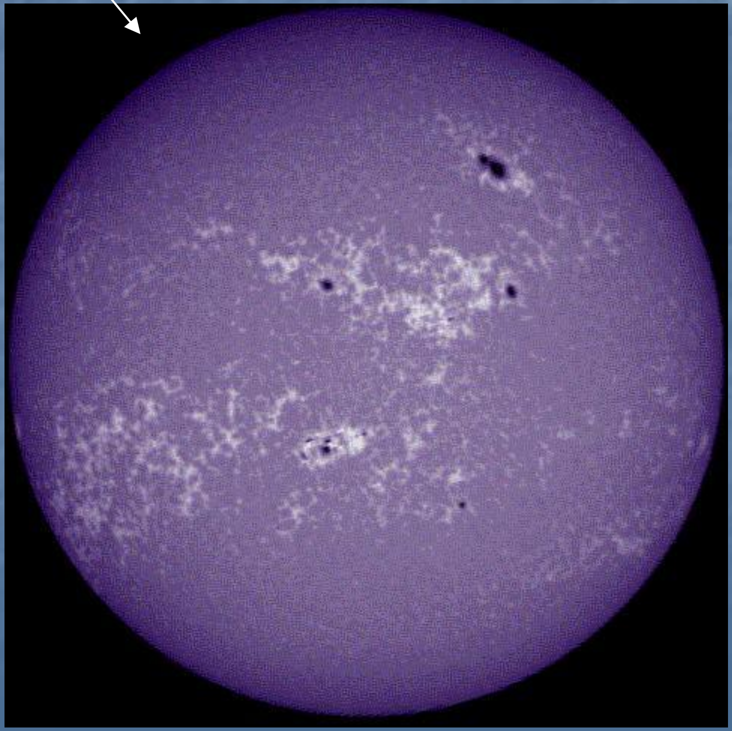

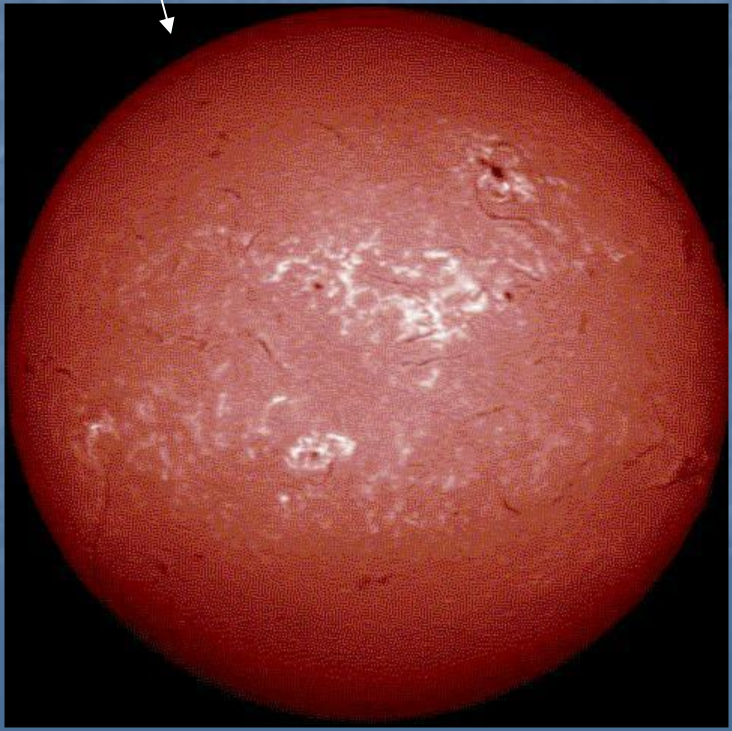

I. Introduction

- In the transition zone (100 km width in the case of the Sun), the temperature increases rapidly.
- In the corona, the temperature reaches several million degrees. The exact heating mechanism (of magnetic origin) of the corona remains currently unknown.

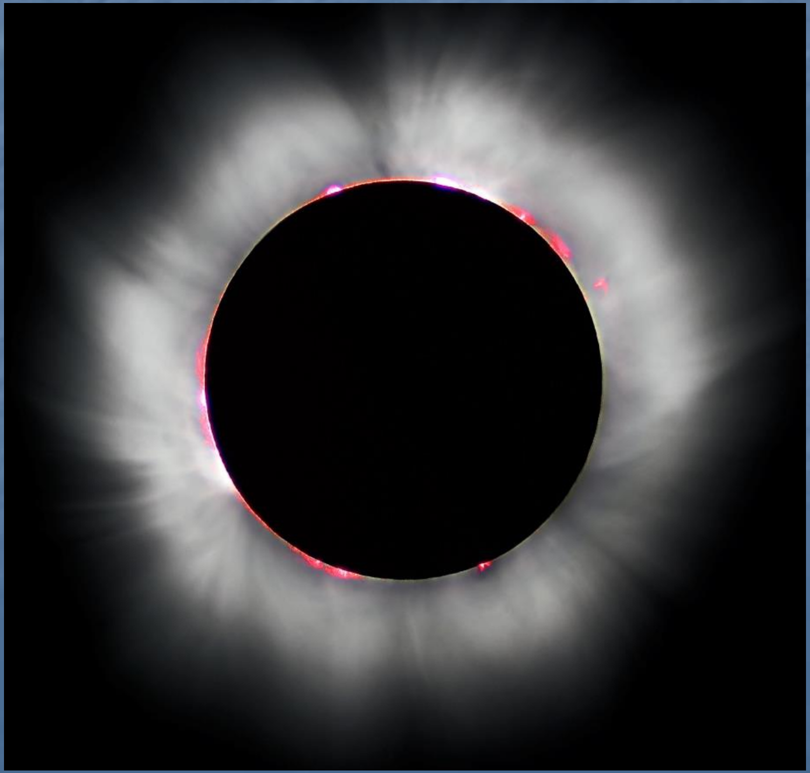

I. Introduction

- In this course, we are mainly interested in the photosphere and, to some extent, in expanding atmospheres (stellar winds of hot stars).
- The physical conditions in the photosphere depend on the star's surface gravity and on the radiative flux that crosses the atmosphere.
- Total radiated power: $$\int_0^\infty \mathcal{F}_\nu \, d\nu = \sigma \, T_{\text{eff}}^4$$
- Bolometric luminosity (integrated over the full electro-magnetic spectrum): $$L_{\text{bol}} = 4 \, \pi \, R_*^2 \, \sigma \, T_{\text{eff}}^4$$

1.1 Stellar photometry

- Photometry = technique to measure the brightness of an astronomical source.
- One distinguishes the apparent brightness (flux) and absolute brightness (luminosities).
- System of magnitudes. Bolometric magnitude:

$$M_{\rm bol} = -2.5\,\log\frac{L_{\rm bol}}{L_\odot} + 4.76$$

$$L_\odot = 3.845\;10^{33}\;{\rm erg\;s^{-1}}$$

- Observation through a filter with a limited bandwidth:

$$m_W = -2.5\,\log\int_0^\infty \mathcal{F}_\lambda\,W(\lambda)\,d\lambda + Cte$$

1.1 Stellar photometry

- Observation through a filter with a limited bandwidth:

$$m_W = -2.5\,\log \int_0^\infty \mathcal{F}_\lambda\, W(\lambda)\, d\lambda + Cte$$

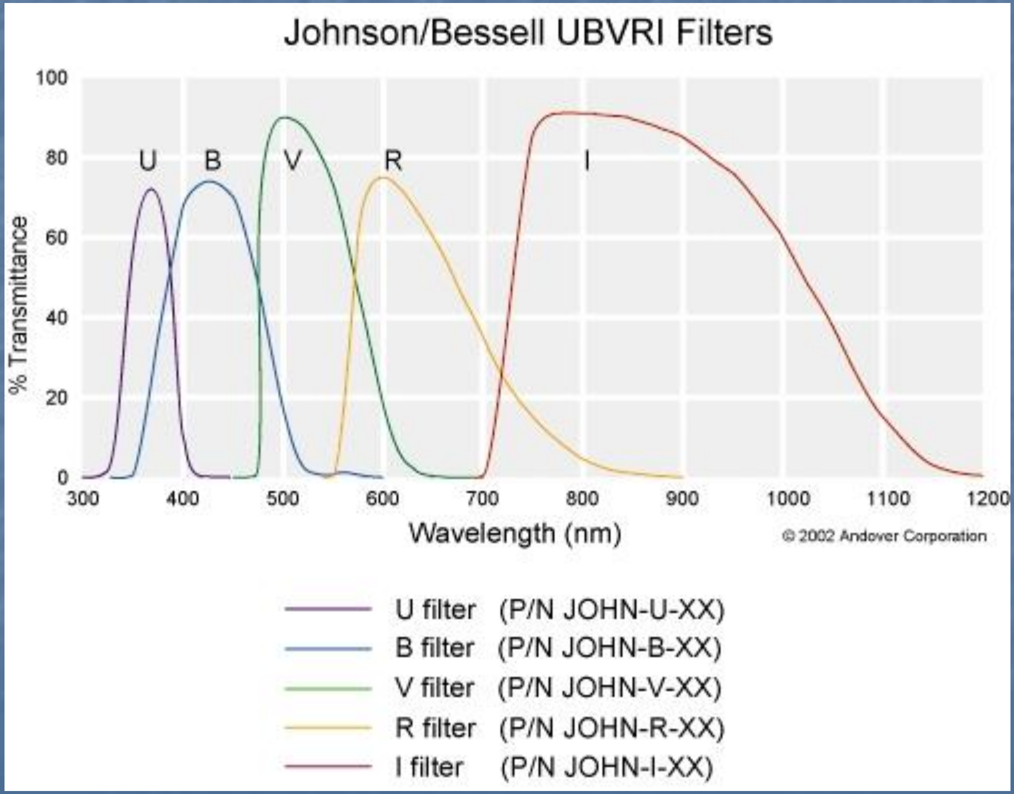

Filter	Effective wavelength (Å)	FWHM (Å)
U	3663	650
B	4361	890
V	5448	840
R	6407	1580
I	7980	1540
J	12200	2400
H	16300	4000
K	21900	6000

- Bolometric correction:

$$M_{\rm bol} = M_W + BC_W$$

1.1 Stellar photometry

- Observation through a filter with a limited bandwidth:

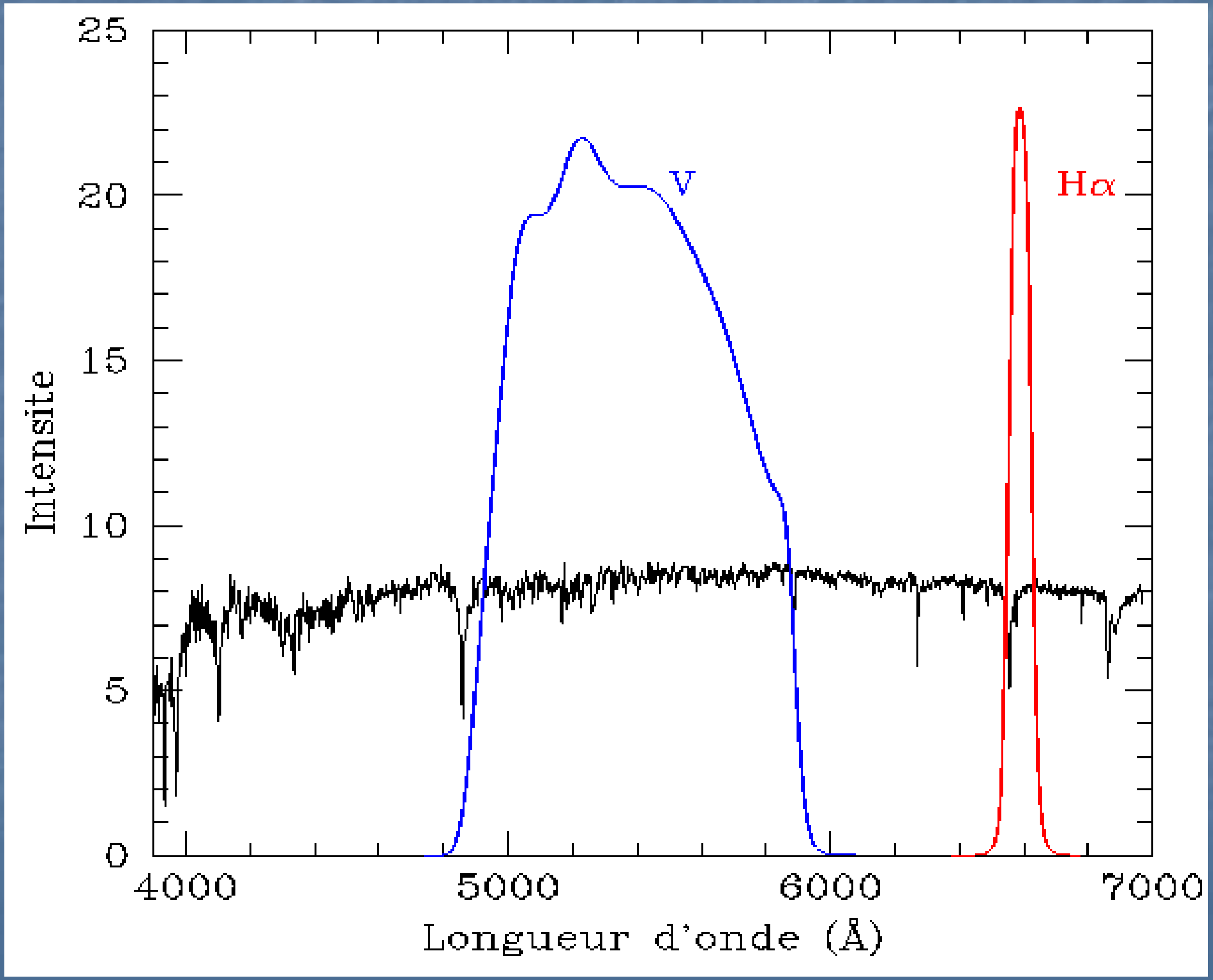

1.1 Stellar photometry

- Apparent magnitude depends on the distance and the interstellar absorption: $M_W = m_W + 5 - 5 \log d - A_W$

- Intrinsic colours (e.g. $(B\text{-}V)_0$ and $(U\text{-}B)_0$ see Table 1.2). Colour-magnitude and colour-colour diagrams:

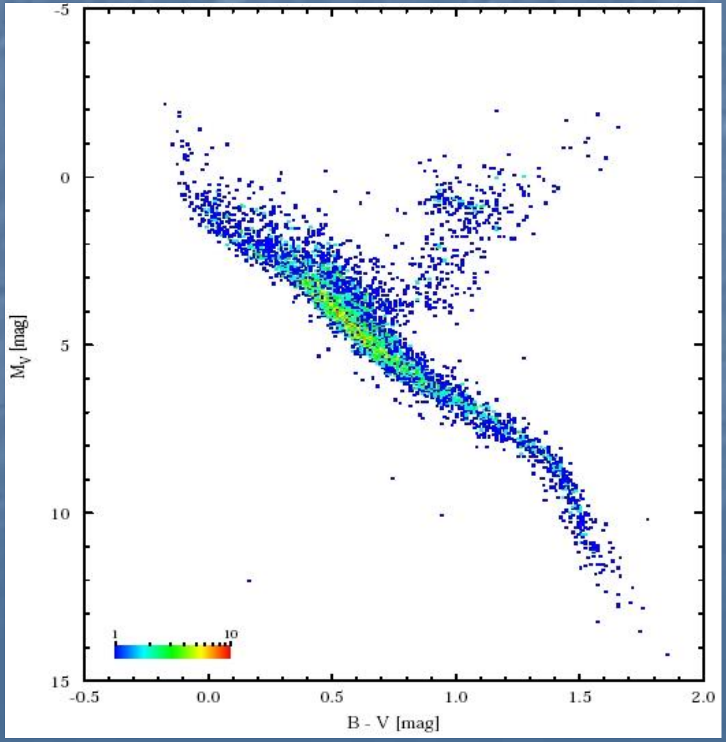

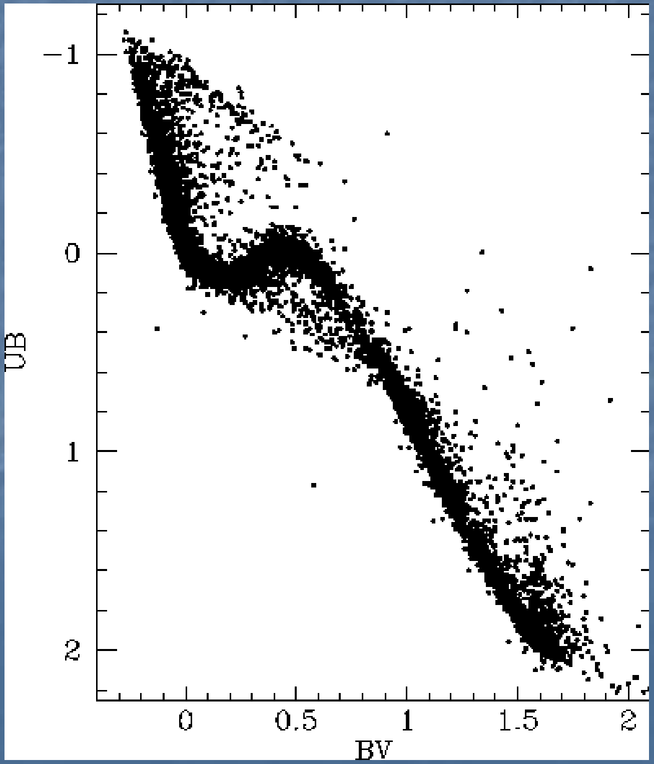

1.2 Stellar spectroscopy

- 1666: Newton discovers the diffraction of solar light into its colours with a prism.
- 1800 and 1801: Herschel and Ritter discover the infrared and ultraviolet light, respectively.
- 1802: Wollaston discovers the presence of dark lines in the Solar spectrum.
- 1814: Fraunhofer rediscovers the dark lines and names them with the letters from A to H. A & B = *telluric* lines; C = Hα, F = Hβ; D: Na I; H, K: Ca II; G = molecular bands.
- 1842: Becquerel obtains the first photograph of the Solar spectrum
- 1872: Draper obtains the first photograph of a stellar spectrum (Vega, α Lyrae)

1.2 Stellar spectroscopy

- Laws of Kirchhoff & Bunsen:
  - The spectrum of a source of white light is a continuum of colours.
  - White light that crosses a cool gas contains absorption lines (dark lines).
  - The light emitted by a hot and tenuous gas (e.g. a sodium vapour lamp) is made of narrow and intense emission lines (bright lines).

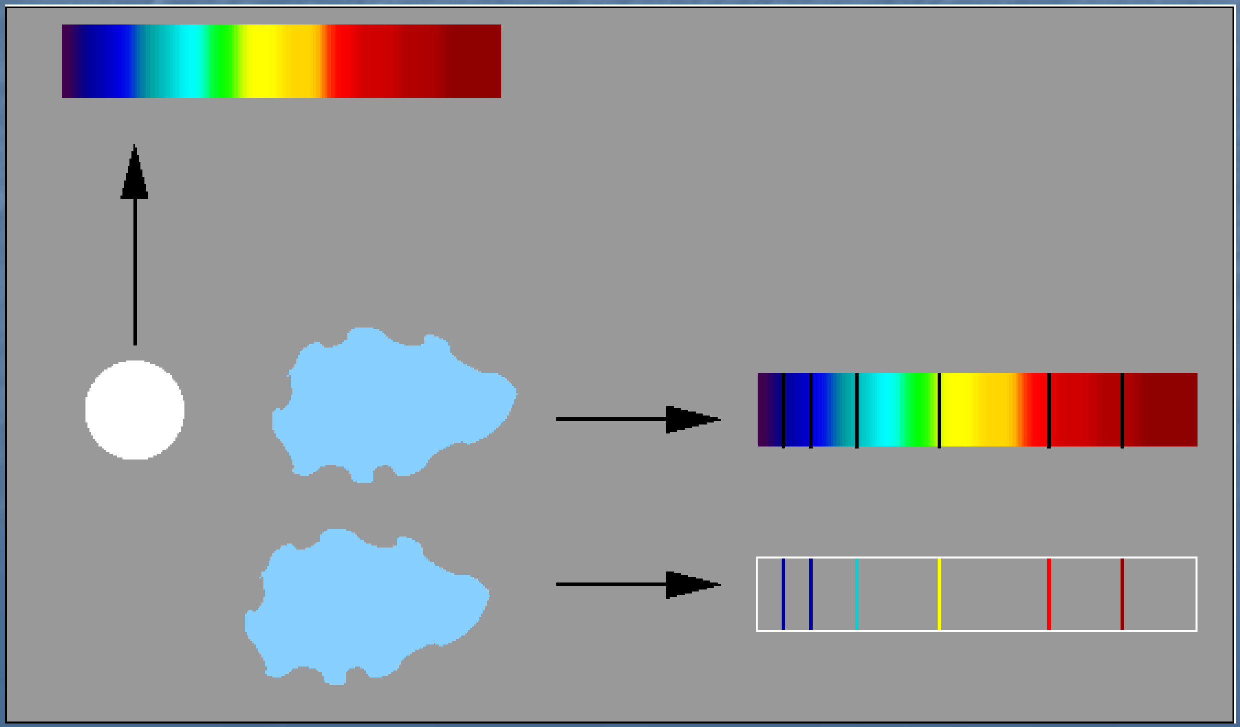

1.2 Stellar spectroscopy

- Decomposition of light into its different components:

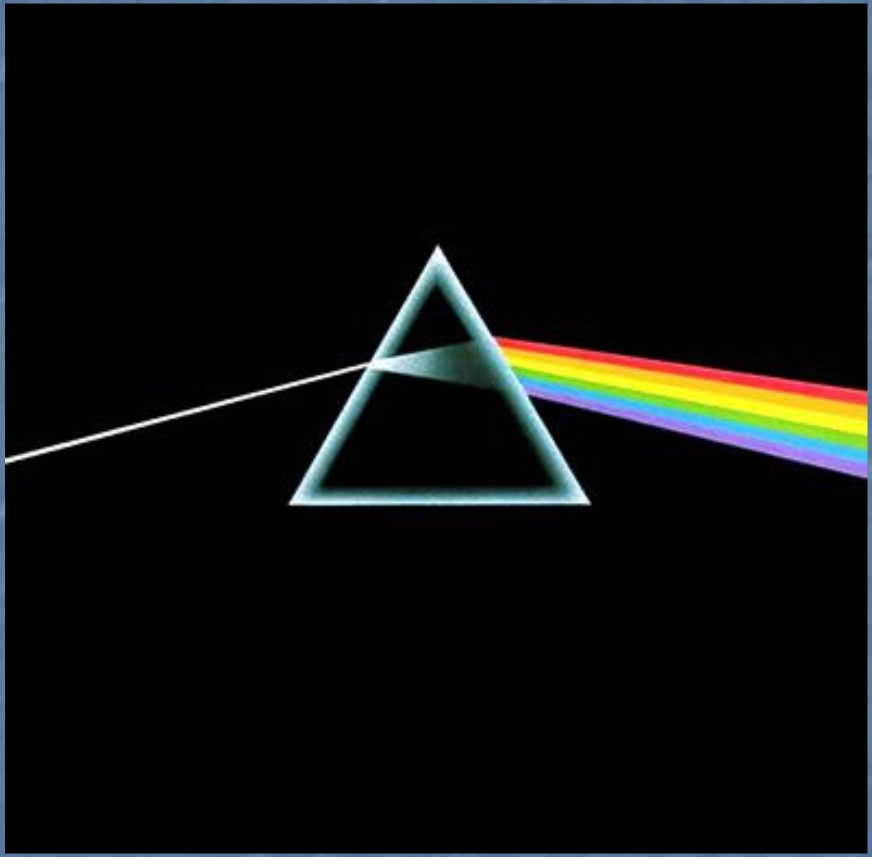

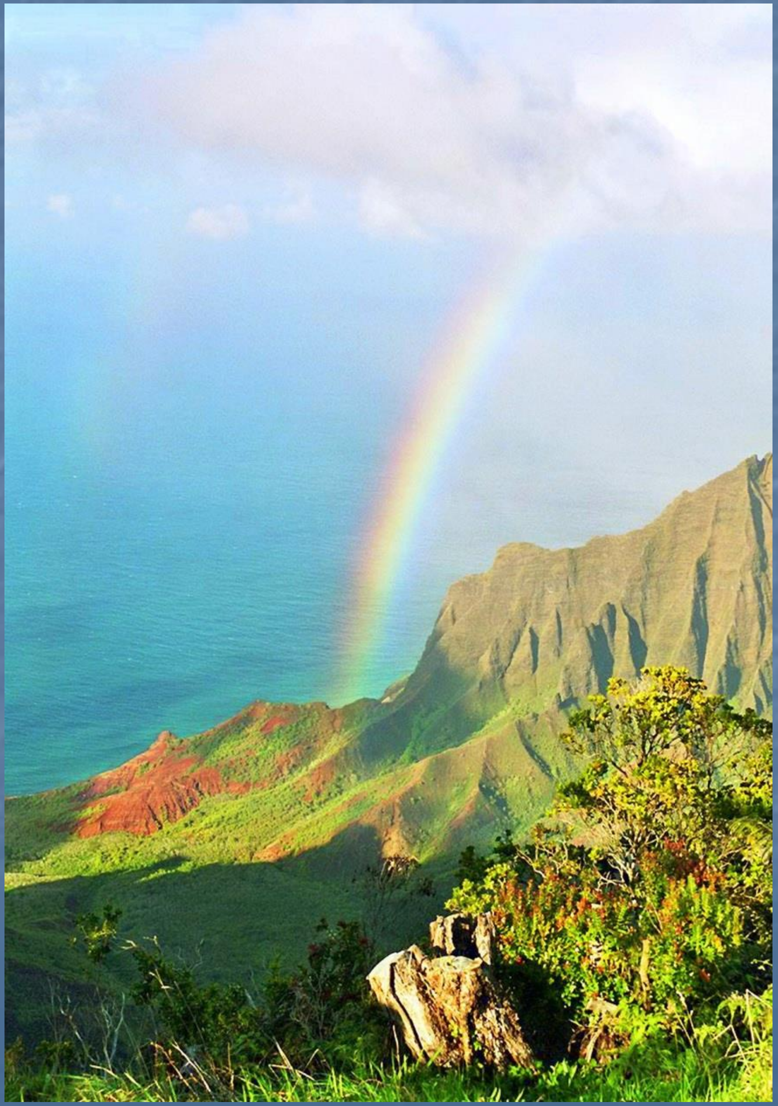

1.2 Stellar spectroscopy

- In a spectrograph, light is decomposed
  - using a prism

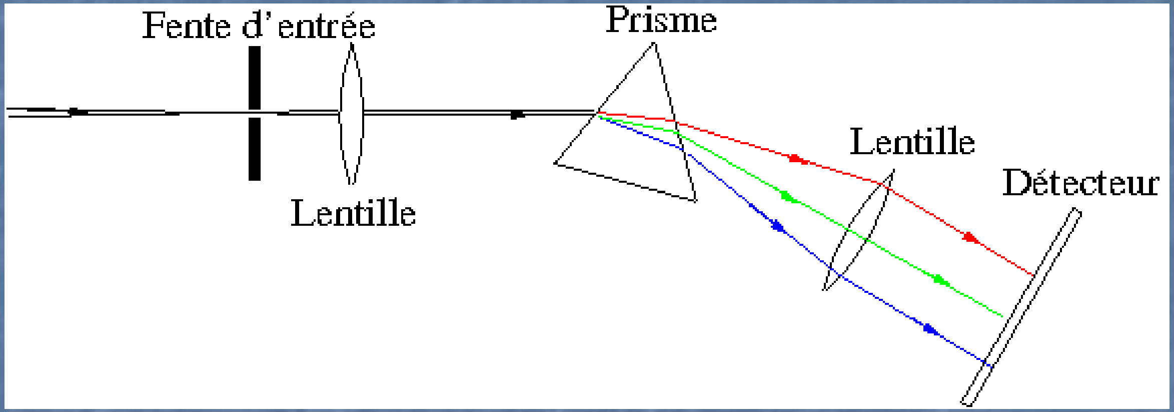

  - or using a diffraction grating (either via reflection or transmission)

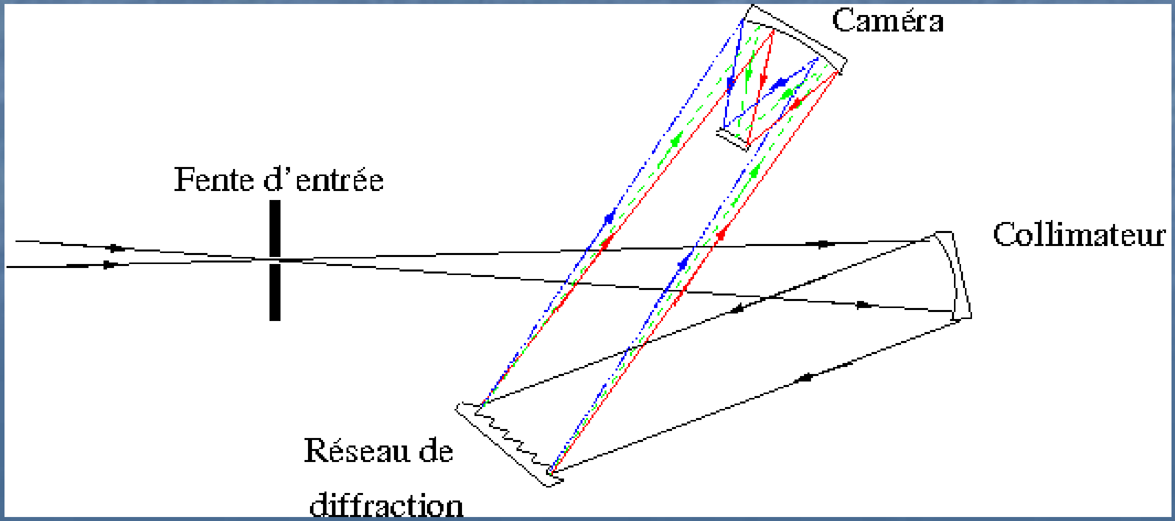

1.2 Stellar spectroscopy

- Light wave at a point of coordinate *x*:

$$F(x) = F_0 \exp \frac{2\,\pi\,i\,x\,\sin\alpha}{\lambda}$$

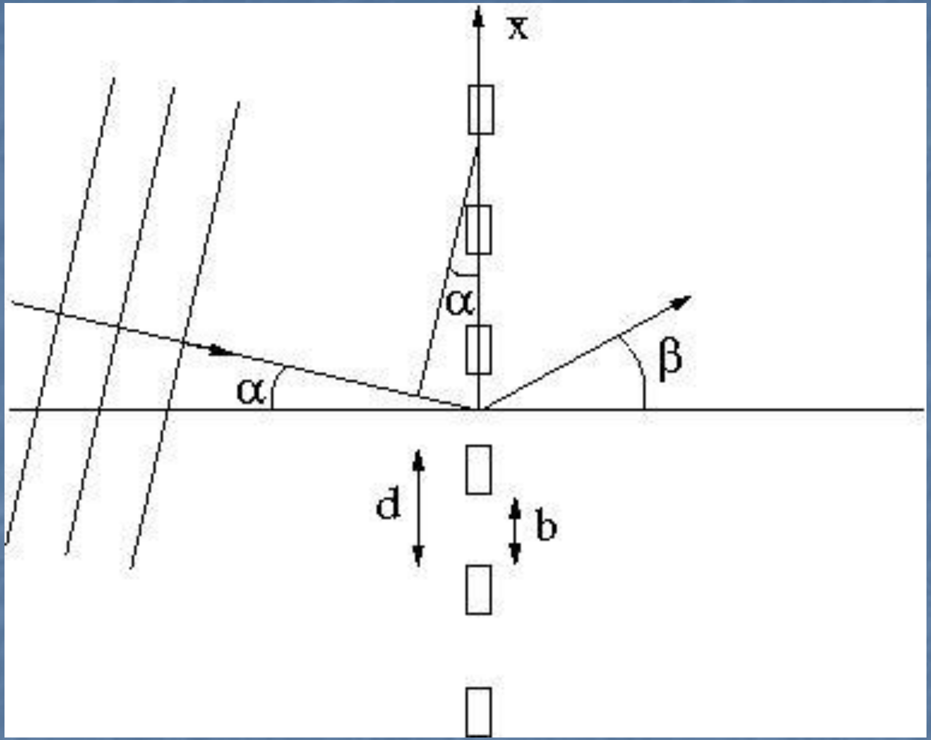

- Transmission function of the grating: *G(x) = 0* if *x* is outside the grooves of width *b*, *G(x) = 1* if *x* inside a groove.
- The diffracted wave becomes:

$$\begin{aligned} g(\beta) &= \int_{-\infty}^{+\infty} F(x)\,G(x)\,\exp \frac{2\,\pi\,i\,x\,\sin\beta}{\lambda}\,dx \\ &= F_0 \int_{-\infty}^{+\infty} G(x)\,\exp \frac{2\,\pi\,i\,x\,(\sin\beta + \sin\alpha)}{\lambda}\,dx \end{aligned}$$

1.2 Stellar spectroscopy

- Setting

$$\theta = \sin\alpha + \sin\beta$$

one obtains

$$g(\theta) \quad = \quad F_0 \int_{-\infty}^{+\infty} G(x)\,\exp\frac{2\,\pi\,i\,x\,\theta}{\lambda}\,dx$$

which is the Fourier transform of *G(x)*.

- Since

$$G(x) = B_1(x) * III(x)\;B_2(x)$$

with $III(x) = \sum_n \delta(x - n\,d)$

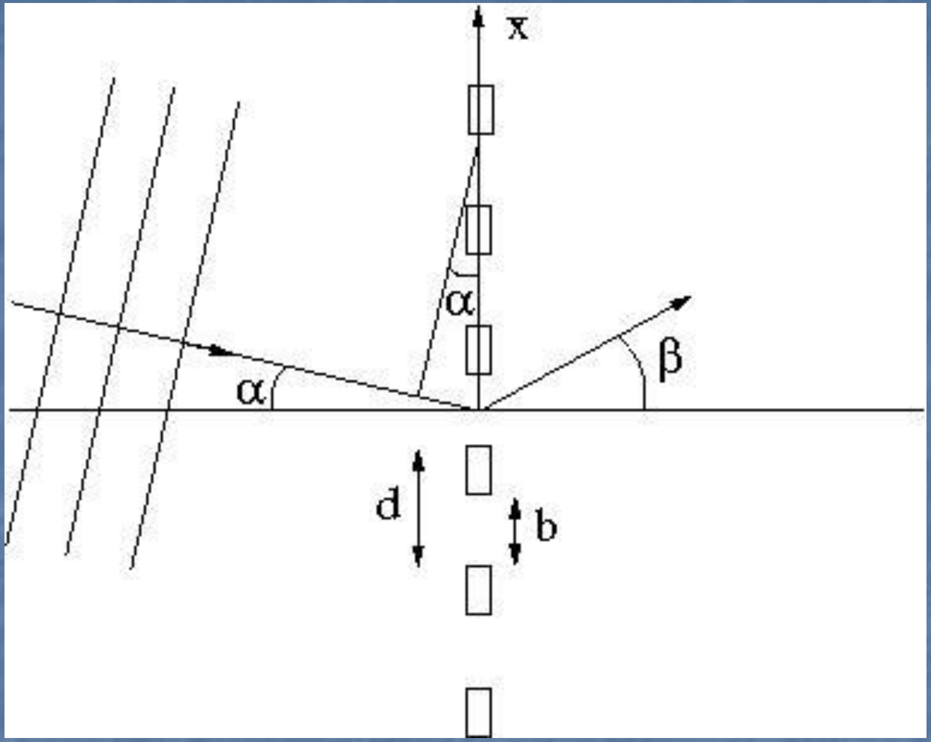

$$III(\theta) = \sum_n \delta(\theta/\lambda - n/d)$$

one finds

$$\boxed{\begin{aligned} g(\theta) &= III(\theta) * \frac{w\,\sin[\pi\,\theta\,w/\lambda]}{\pi\,\theta\,w/\lambda}\,\frac{b\,\sin[\pi\,\theta\,b/\lambda]}{\pi\,\theta\,b/\lambda} \\ &= \sum_n \frac{w\,\sin[\pi\,(\theta/\lambda - n/d)\,w]}{\pi\,(\theta/\lambda - n/d)\,w}\,\frac{b\,\sin[\pi\,\theta\,b/\lambda]}{\pi\,\theta\,b/\lambda} \end{aligned}}$$

1.2 Stellar spectroscopy

$$
\begin{aligned}
g(\theta) &= III(\theta) * \frac{w\ \sin\left[\pi\,\theta\,w/\lambda\right]}{\pi\,\theta\,w/\lambda}\ \frac{b\ \sin\left[\pi\,\theta\,b/\lambda\right]}{\pi\,\theta\,b/\lambda} \\
&= \sum_n \frac{w\ \sin\left[\pi\,(\theta/\lambda - n/d)\,w\right]}{\pi\,(\theta/\lambda - n/d)\,w}\ \frac{b\ \sin\left[\pi\,\theta\,b/\lambda\right]}{\pi\,\theta\,b/\lambda}
\end{aligned}
$$

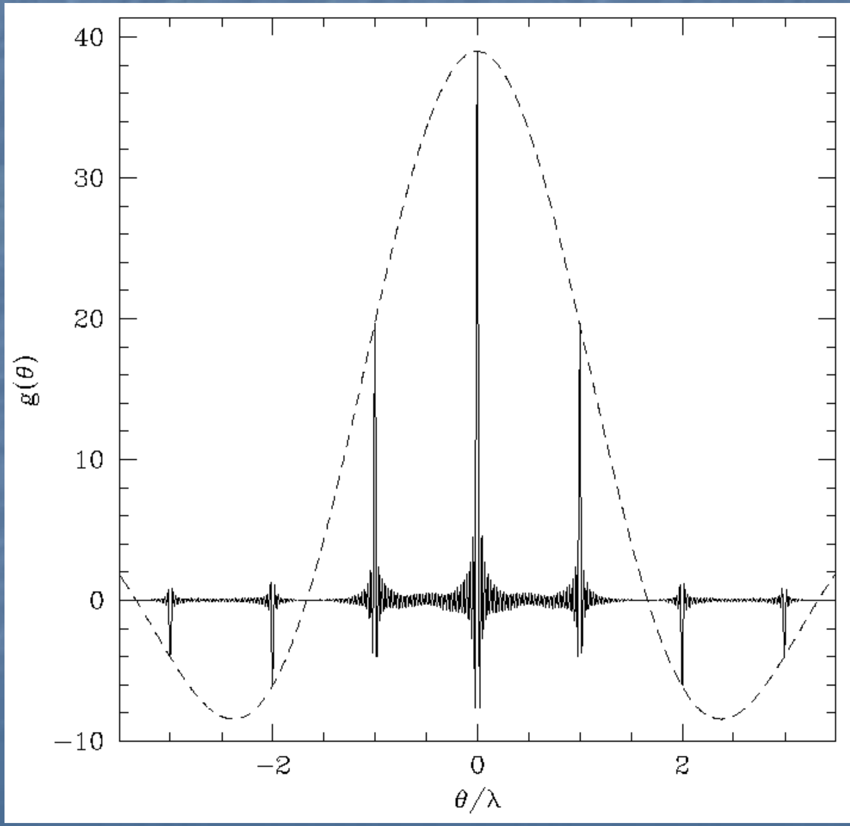

- The function $g(\theta)$ is maximum at $\theta/\lambda - n/d = 0$
  with n an integer number

1.2 Stellar spectroscopy

$$g(\theta) = III(\theta) * \frac{w \sin[\pi\,\theta\,w/\lambda]}{\pi\,\theta\,w/\lambda}\,\frac{b \sin[\pi\,\theta\,b/\lambda]}{\pi\,\theta\,b/\lambda}$$
$$= \sum_n \frac{w \sin[\pi\,(\theta/\lambda - n/d)\,w]}{\pi\,(\theta/\lambda - n/d)\,w}\,\frac{b \sin[\pi\,\theta\,b/\lambda]}{\pi\,\theta\,b/\lambda}$$

- The function g(θ) is maximum at $\theta/\lambda - n/d = 0$
- Equation of the grating: $\frac{n\,\lambda}{d} = \sin\alpha + \sin\beta$

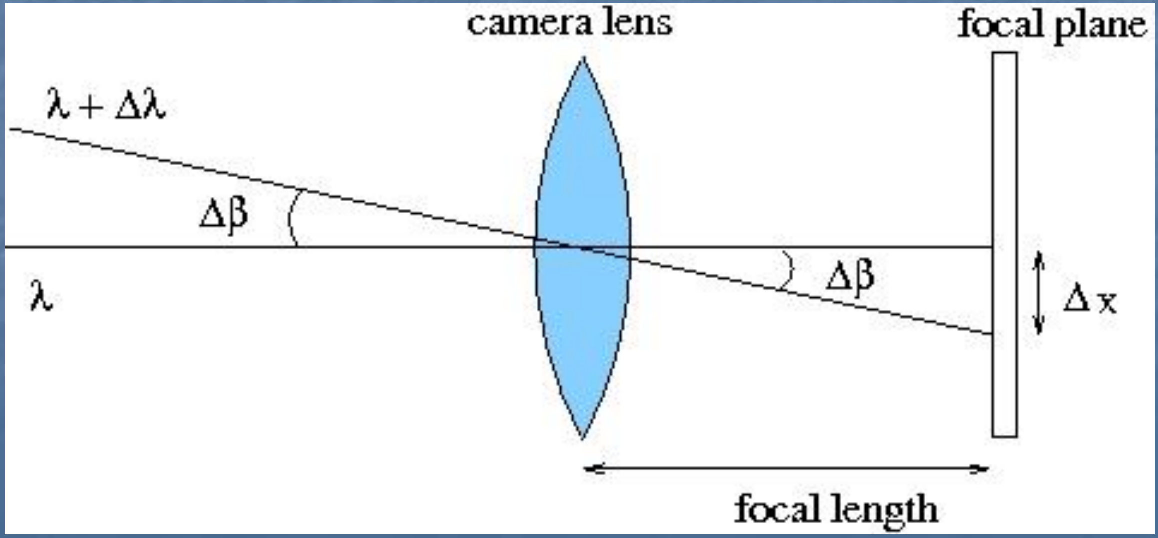

$$\frac{d\,\lambda}{dx} = \frac{\cos\beta\,d}{n\,f_{\mathrm{cam}}}$$

$$\Delta\,\lambda = -\frac{\cos\alpha\,w'\,d}{f_{\mathrm{coll}}\,n}$$

1.2 Stellar spectroscopy

- Echelle spectroscopy: highest spectral resolution

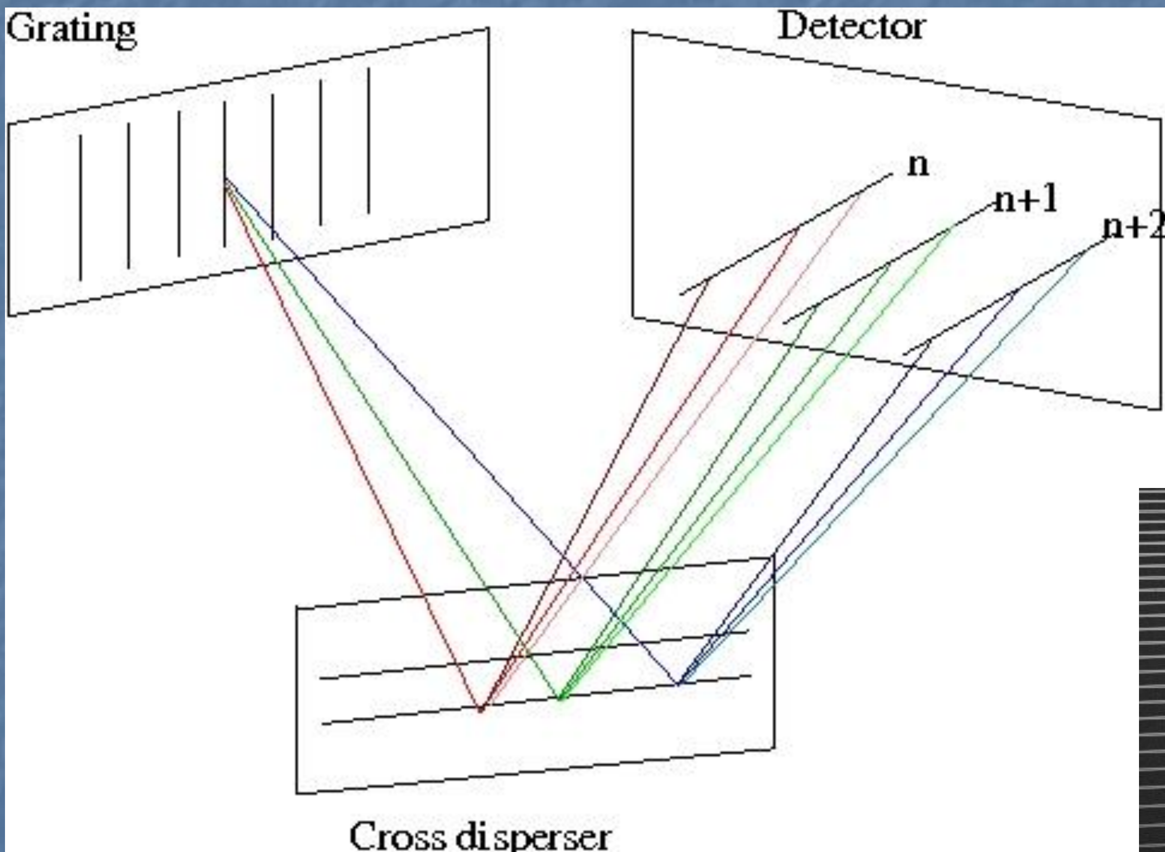

1.2 Stellar spectroscopy

- Long-slit spectroscopy. Raw data include:

1. Biases (offsets applied to the CCD).
2. Dark exposures (dark current of the CCD).
3. Flat fields (tungsten lamps, inter-pixel variations)
4. Hollow cathode (ThAr, HeAr, NeAr,… lamps)
5. Observations of the sky (stars…)
6. Possibly standard stars for flux or radial velocity calibrations…

- Data reduction:

1. Subtraction of the bias and the dark current
2. Division by the flat field
3. Wavelength calibration.

1.2 Stellar spectroscopy

- Flux calibration of the spectra: wide slit to ensure that all the flux enters the instrument (spectral resolution depends on the « seeing »).

$$\Delta\lambda = -\frac{\cos\alpha\, f_{\mathrm{eff}}\, d\, \Delta\phi}{f_{\mathrm{coll}}\, n}$$

- Absolute calibration based on absolute flux of Vega (challenging operation, subject to uncertainties of at least 1%).

1.3 Spectral classification

- Angelo Secchi (1818 – 1878) observed the spectra of about 4000 stars and discovered the existence of different spectral types.

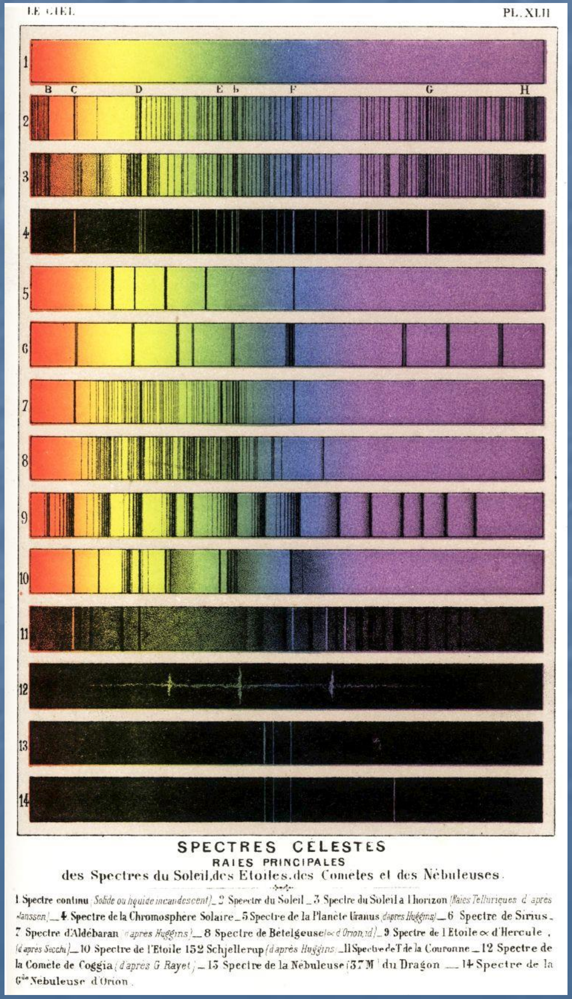

1.3 Spectral classification

- At Harvard observatory, Edward Pickering (1846 – 1919), initiated the study of a large sample of photographic stellar spectra. With the money from a donation from Henry Draper's widow, he hired women "because they are cheaper and more efficient than men".

1.3 Spectral classification

- 1890 – 1900: Williamina Fleming (1857 – 1911) introduced a classification based on the intensity of hydrogen lines.

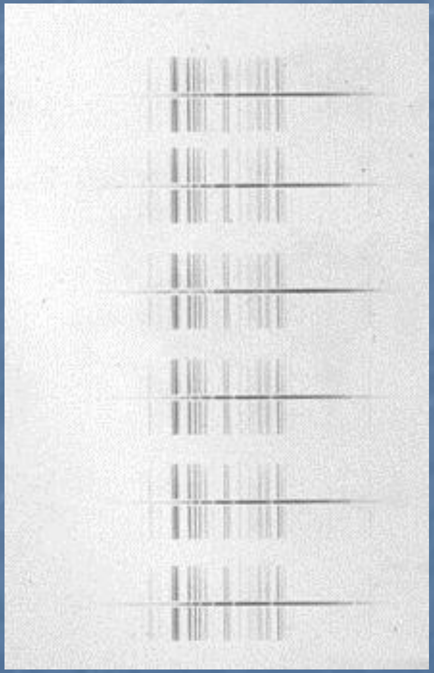

1.3 Spectral classification

- Annie Cannon (1863 – 1941) improved Fleming's method and proposed a sequence O B A F G K M
  and sub-classes (e.g. G2, A0,…)
- This classification is based on a series of criteria about the relative intensity of spectral lines.
- Mnemonic: « **Oh**, **Be** **A** **Fine** **Girl**/**Guy**, **Kiss** **Me**! »

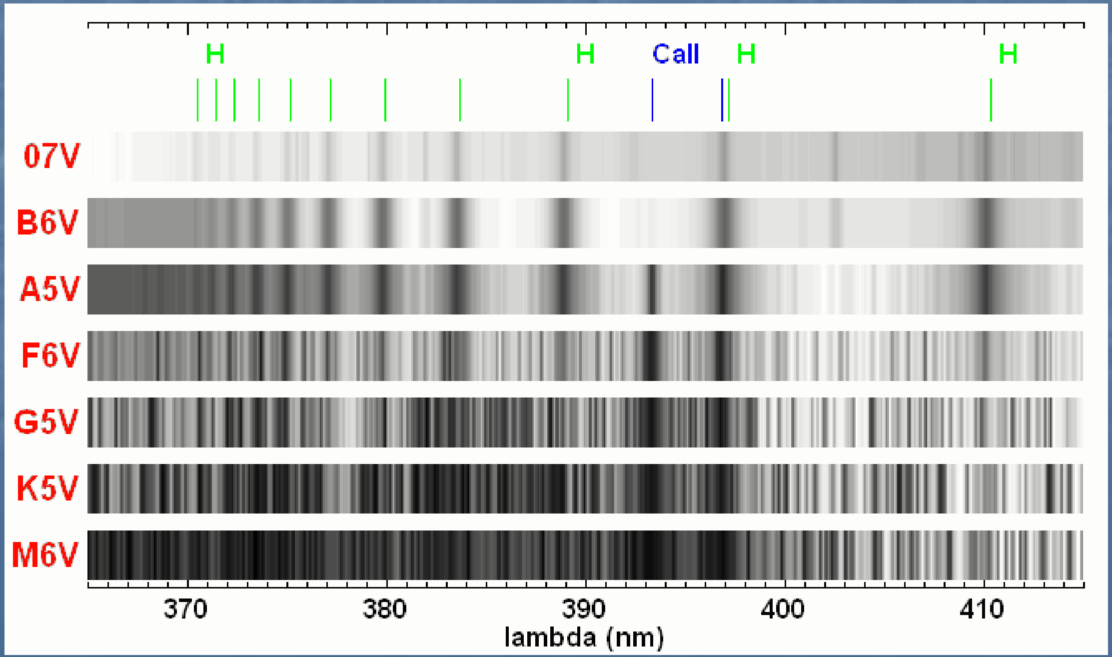

1.3 Spectral classification

- Antonia Maury (1866 – 1952), Ejnar Hertzsprung (1873 – 1967) and Henry Russell (1877 – 1957) introduced the concept of a bi-dimensional classification.
- In 1943, this gave rise to the concept of luminosity classes: 0 hypergiant, I, Ia, Ib, Iab supergiant, II luminous giants, III giants, IV sub-giants, V dwarfs, VI sub-dwarfs in the MKK classification (Morgan, Keenan & Kellman).

Fig. 51. Miss Antonia Caetano Maury, research associate, 1888–1933.

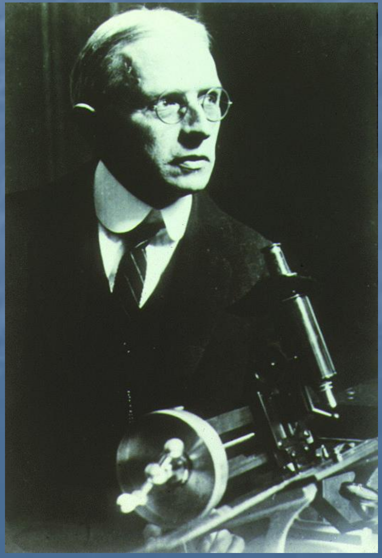

1.3 Spectral classification

- H-R diagram.
- At first it was thought that stars evolve along the main sequence from spectral type O (early) to M (late).

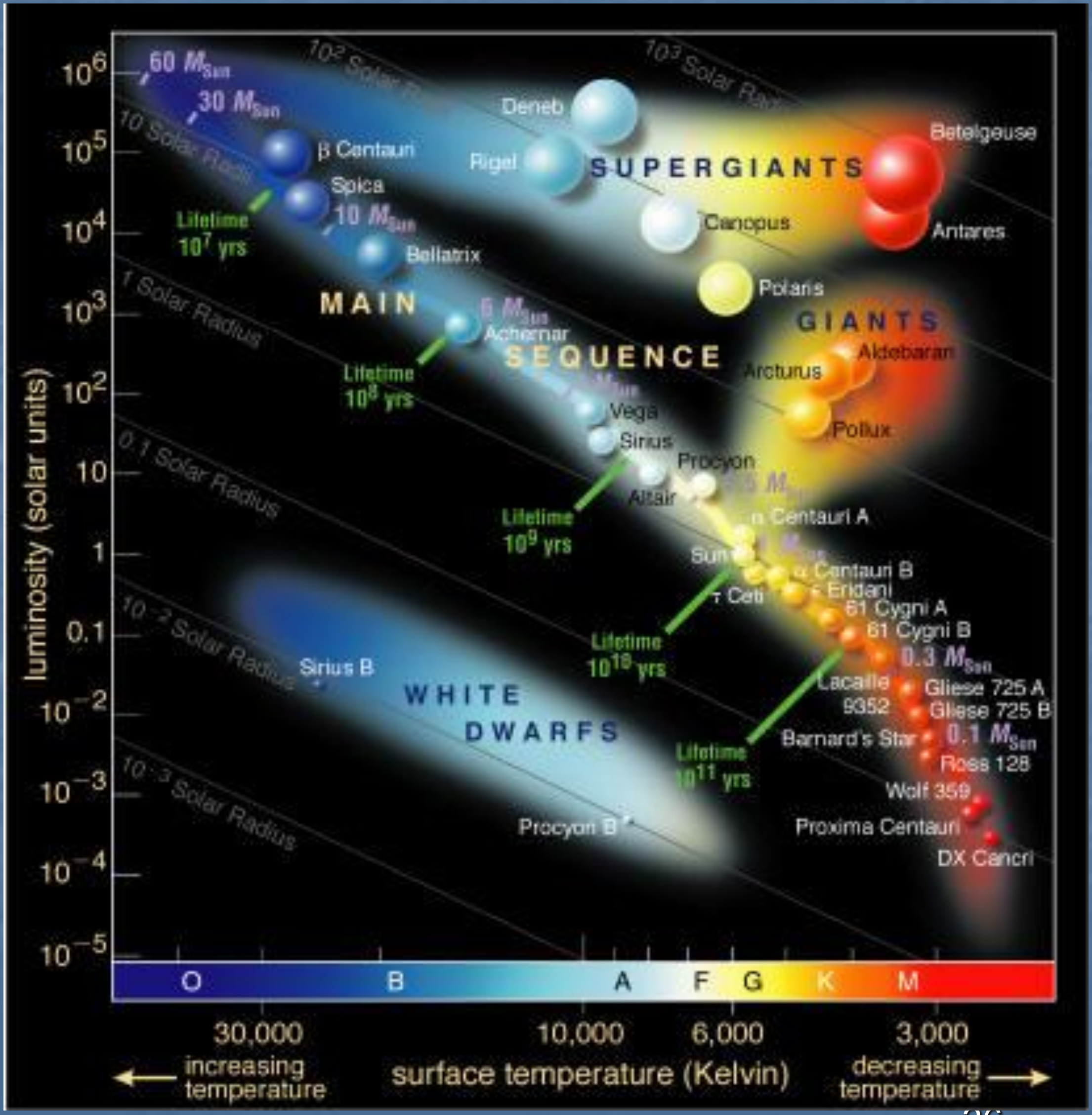

1.3 Spectral classification

- Until the years 1980, spectroscopy was done with photographic plates.
- To classify the spectra, one used observations of standards stars in the blue (maximum sensitivity of photographic plates) between Ca II K and Hβ.
- Today, one uses CCDs along with a series of digital spectral atlases and/or criteria based on ratios of spectral line intensities.

1.3 Spectral classification

- Balmer lines and Balmer discontinuity are strongest in spectra of A-type stars.

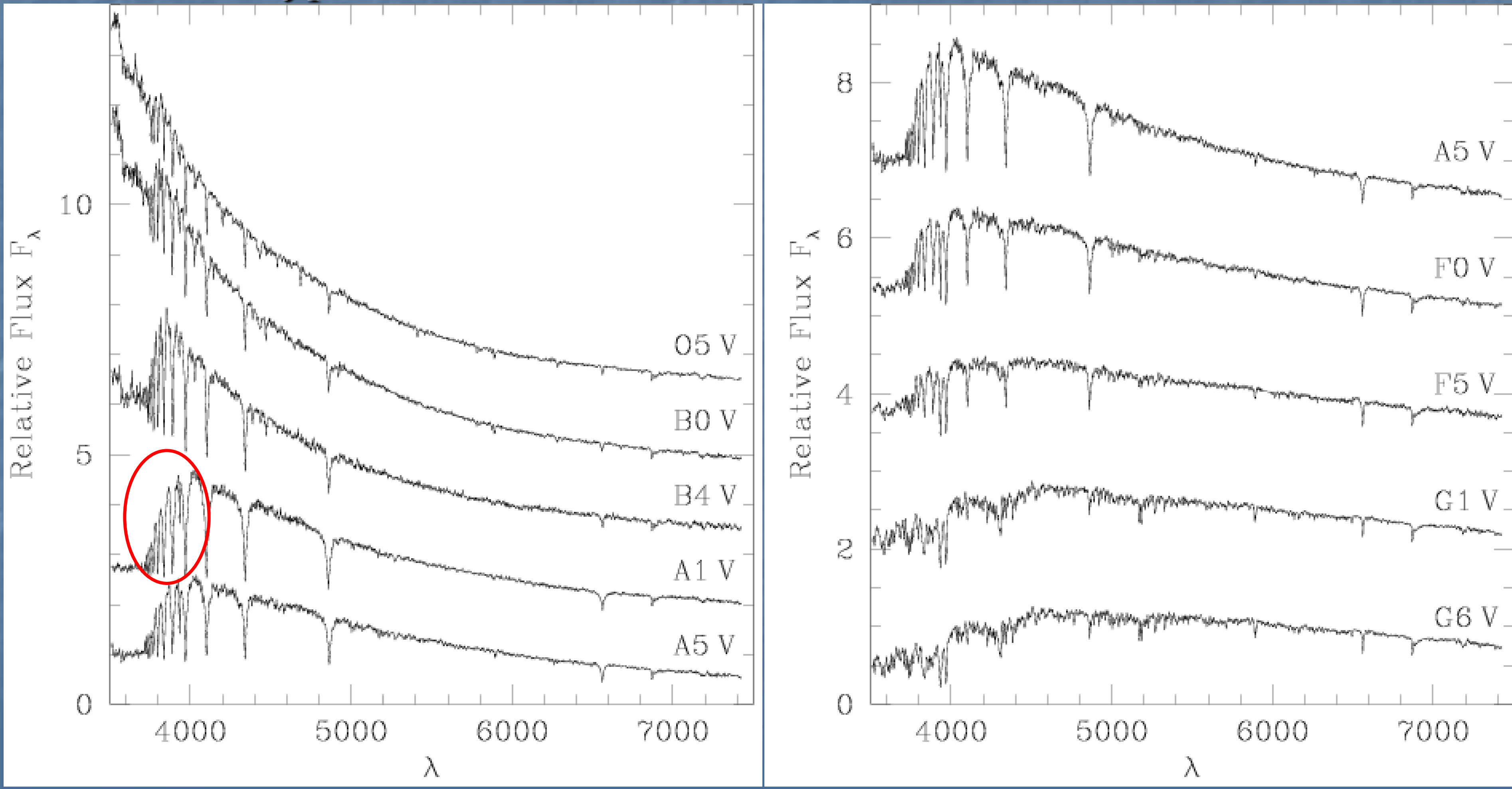

1.3 Spectral classification

- Lower number of lines (optical domain) in the spectra of O-type stars.

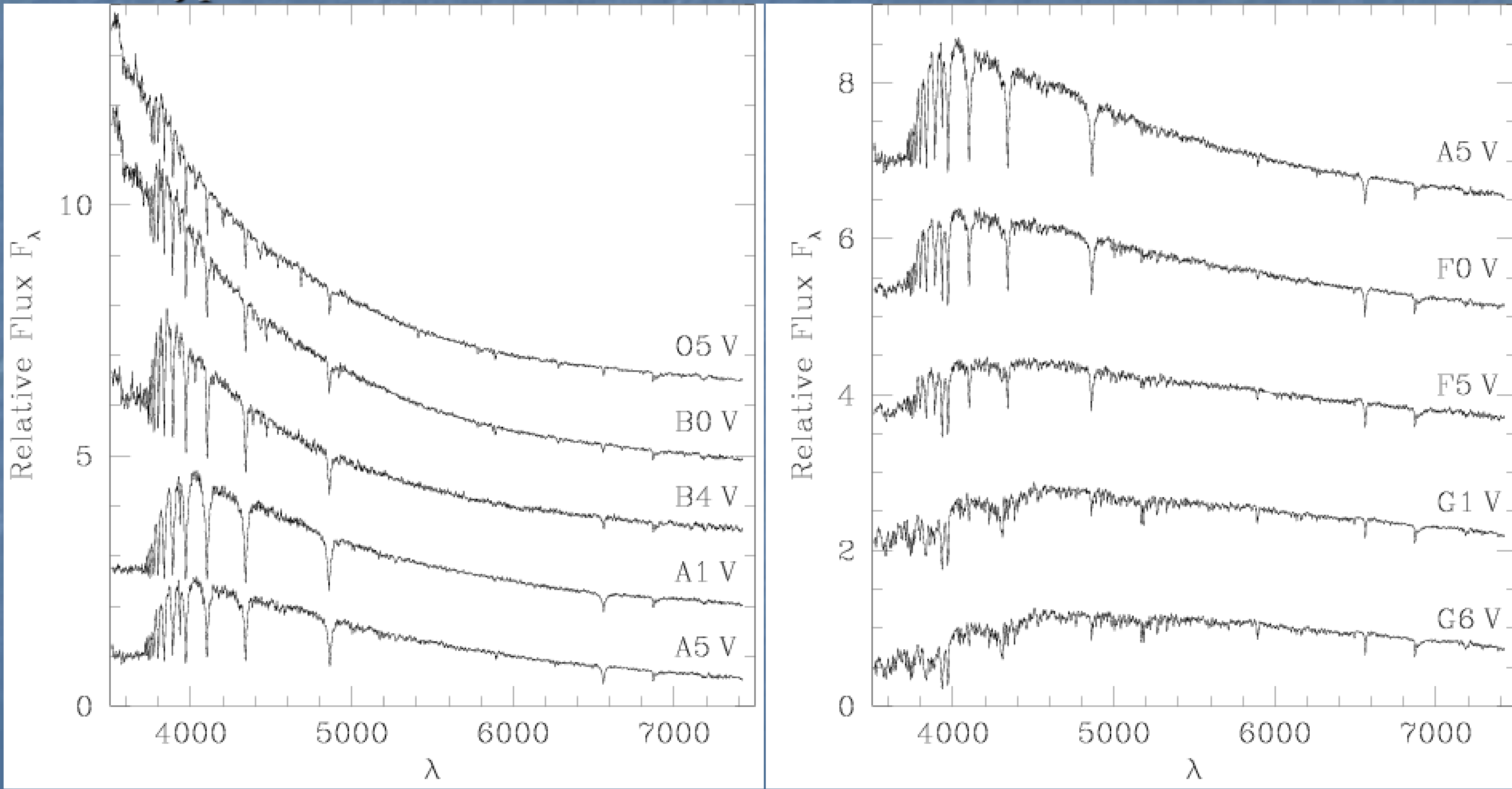

1.3 Spectral classification

- O-type stars: He I 4471 / He II 4542

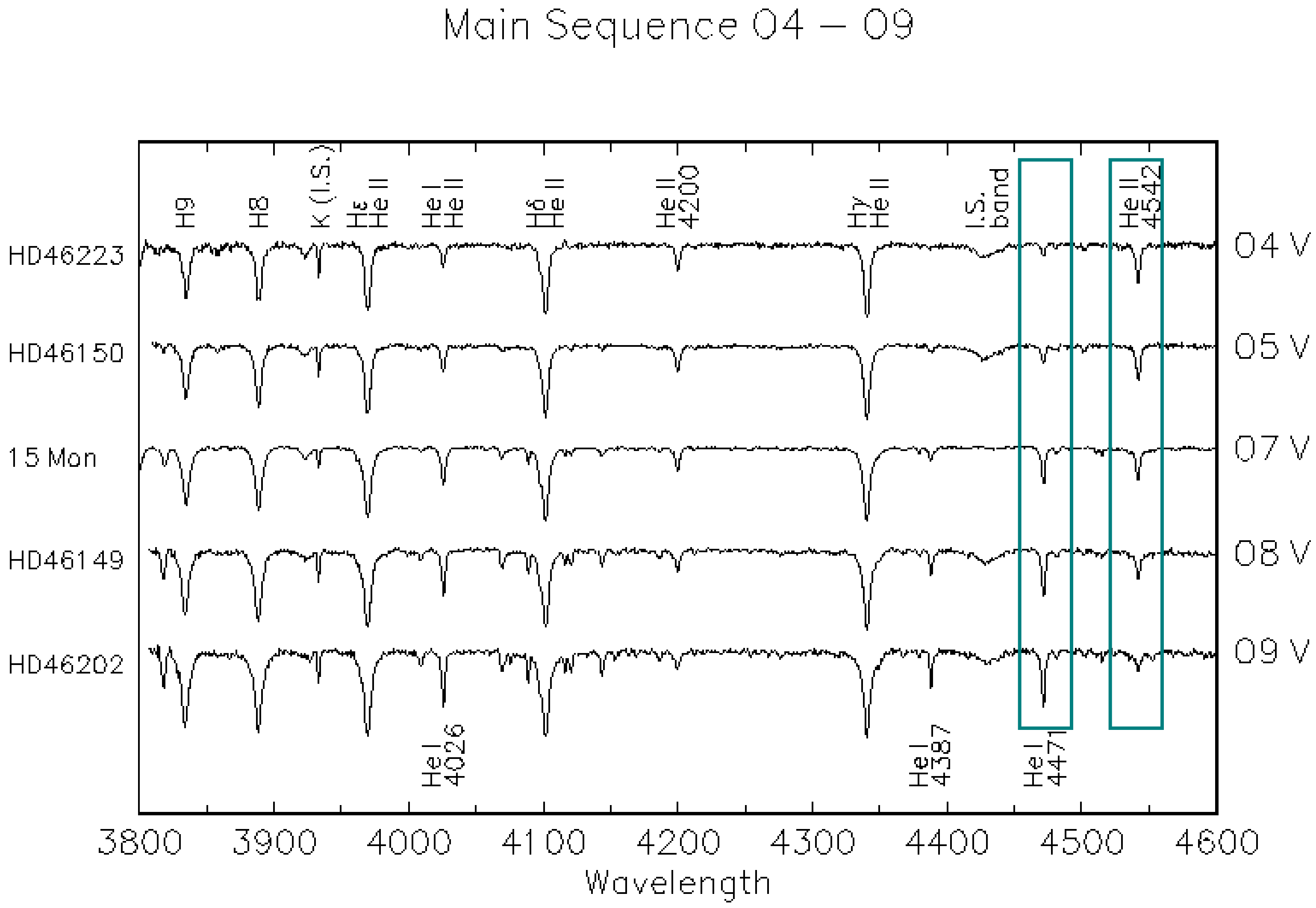

1.3 Spectral classification

- B-type stars: absence of He II, He I 4471 / Mg II 4481

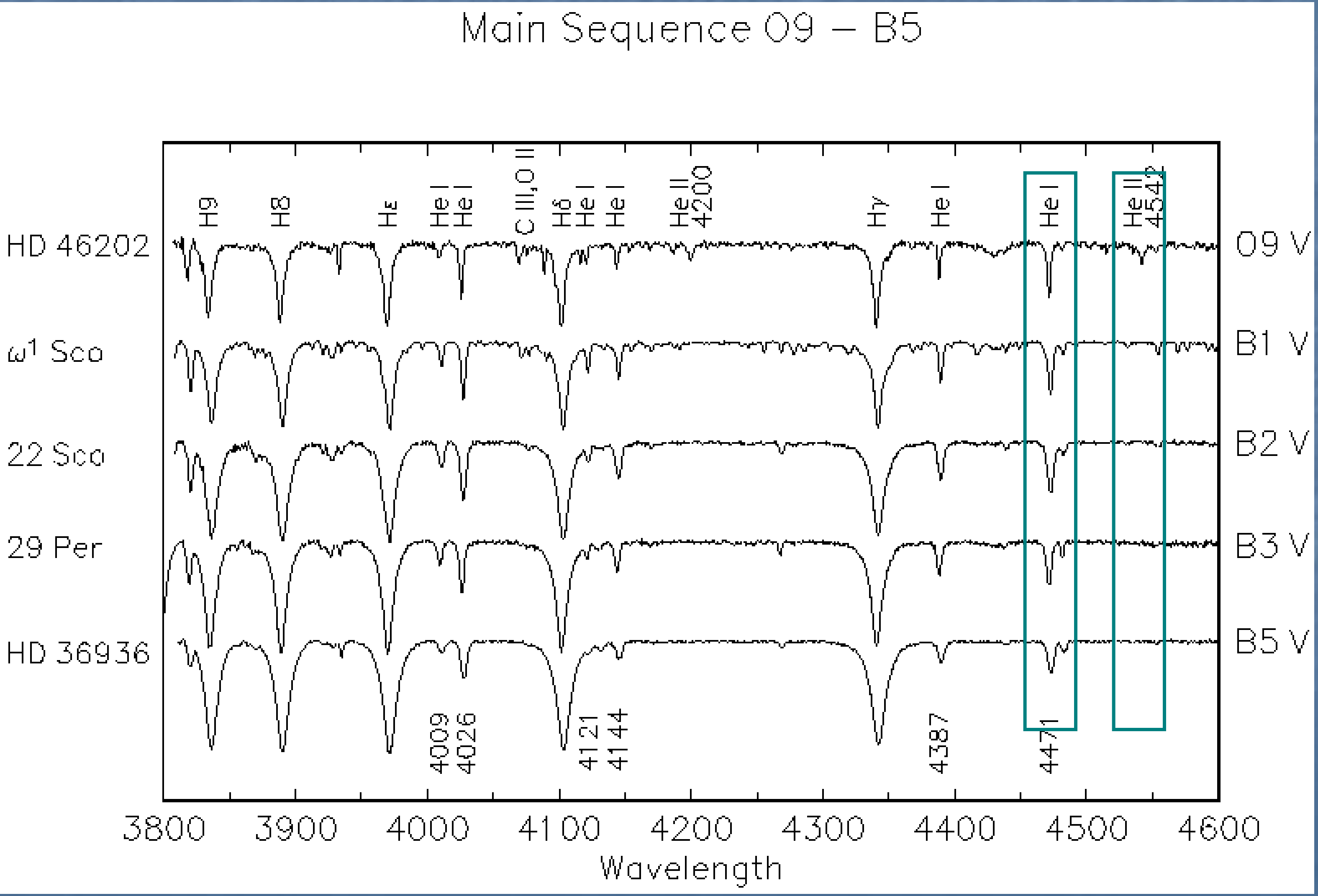

1.3 Spectral classification

- B-type stars: luminosities set by O II 4348/ H γ ratio.

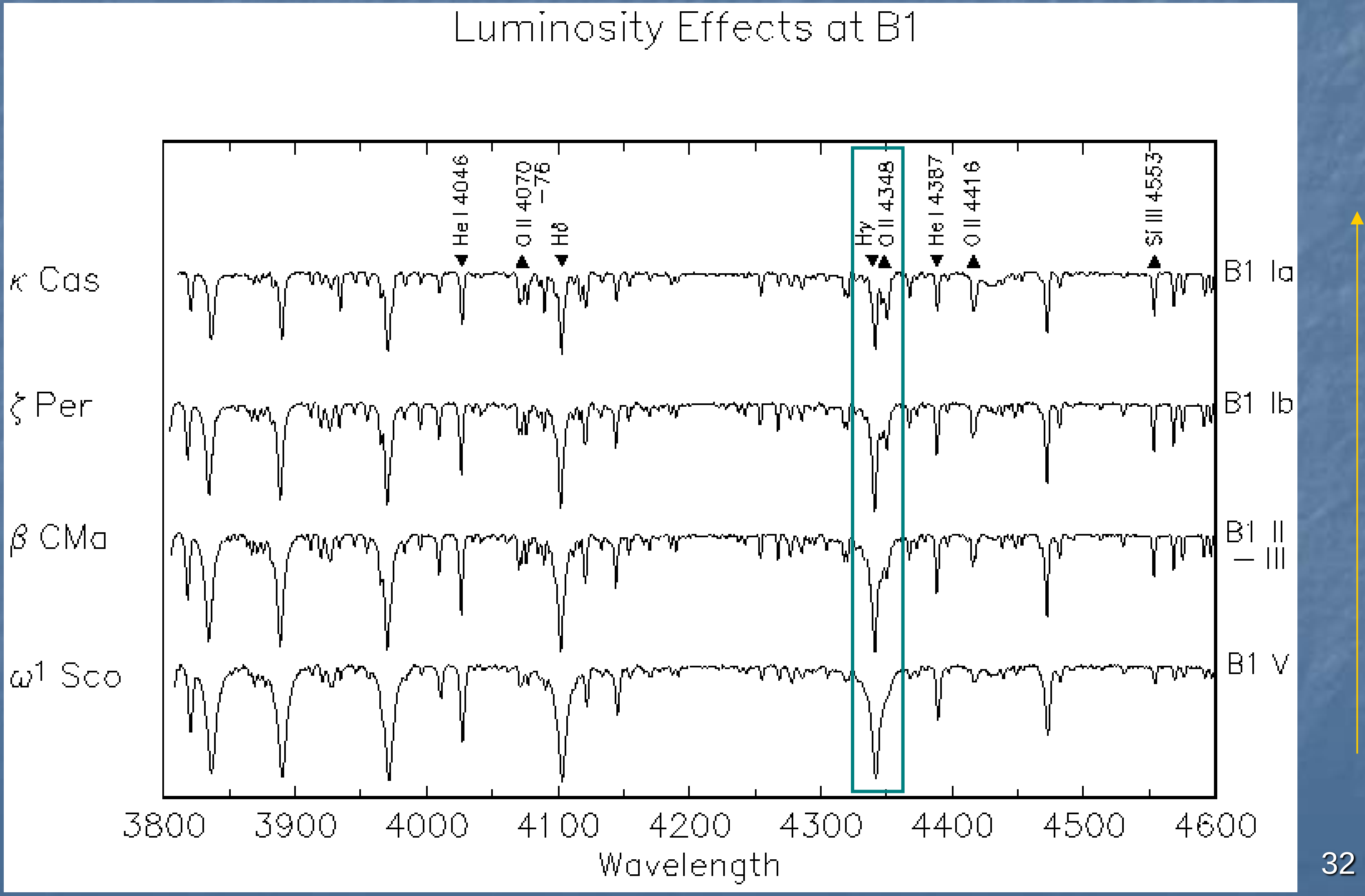

1.3 Spectral classification

- A-type stars: luminosity set by width of hydrogen lines

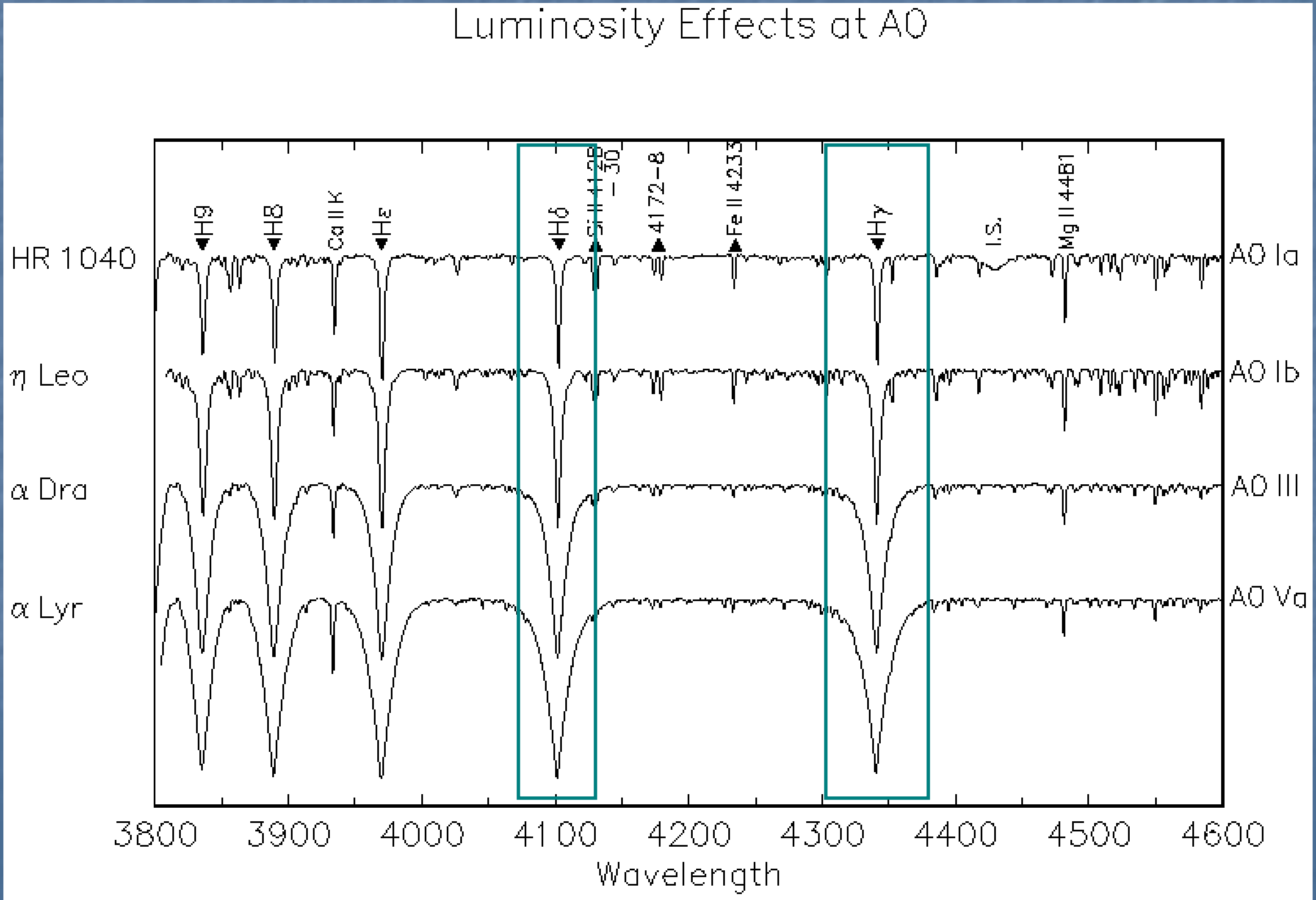

1.3 Spectral classification

- A-F-G stars: intensity of metal lines, G-band

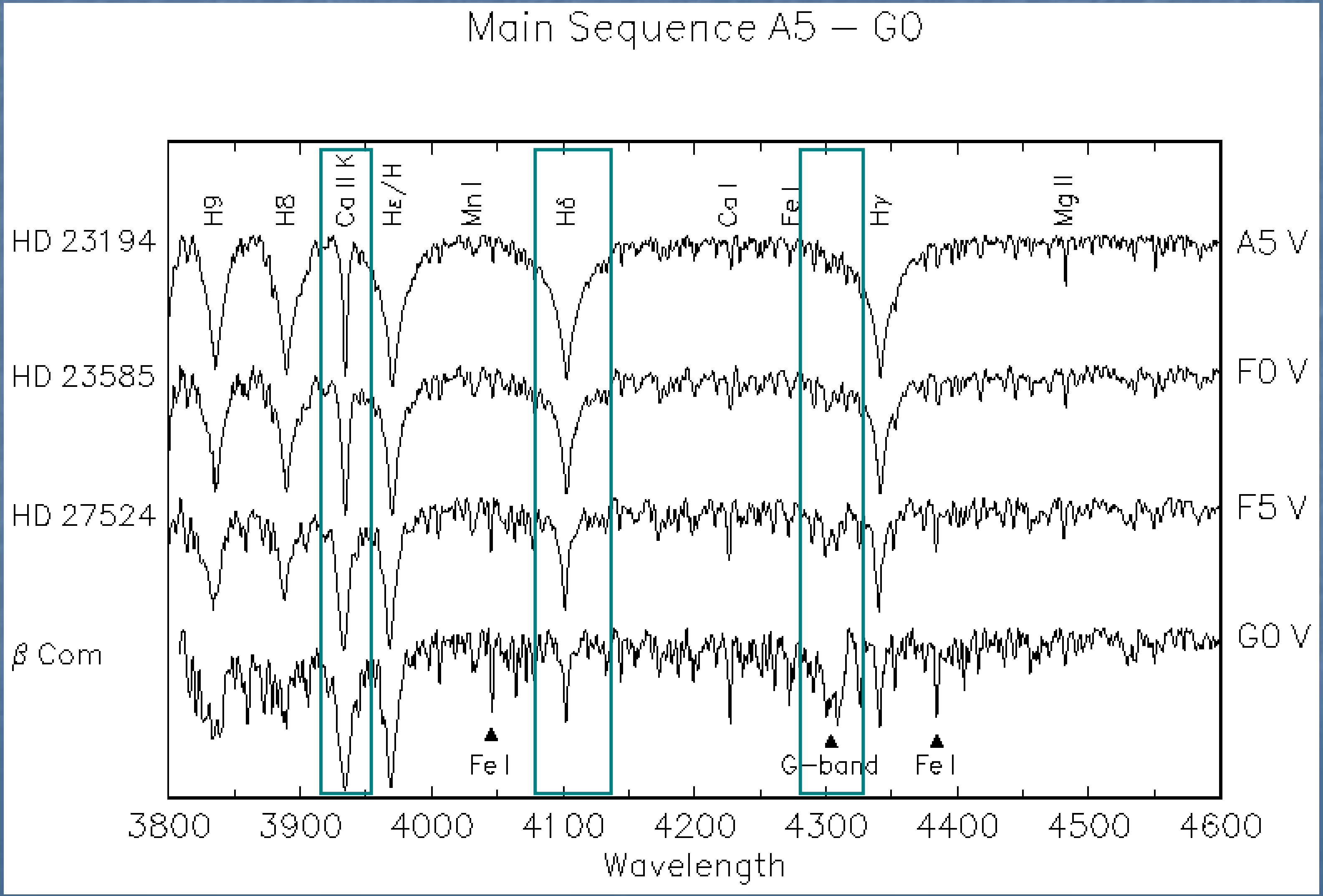

1.3 Spectral classification

- G-K type stars: intensity of the G band, Fe I 4325/Hγ ratio

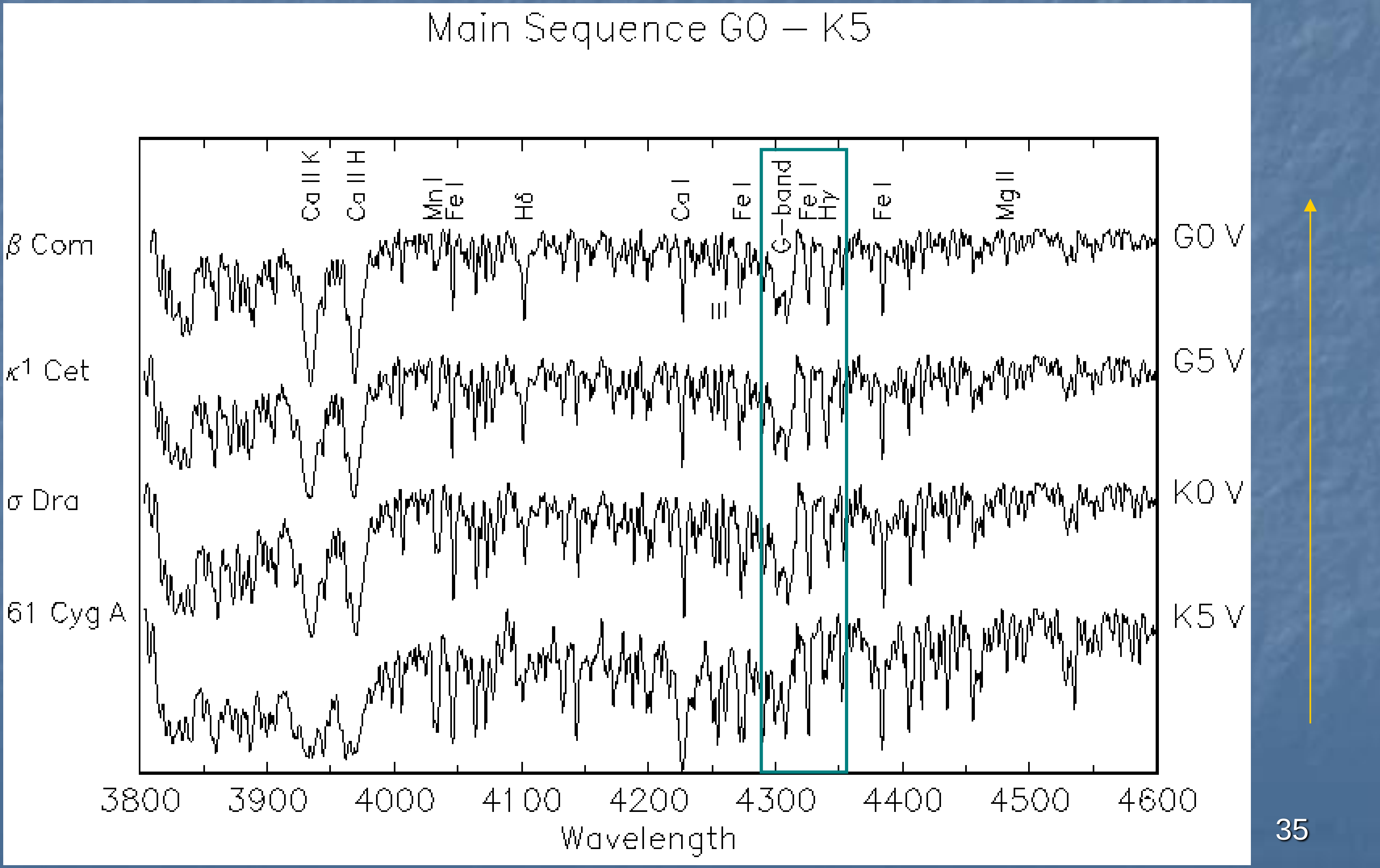

1.3 Spectral classification

- G-K type stars: luminosity set by intensities of CN bands and Y II 4376 / Fe I 4383 ratio

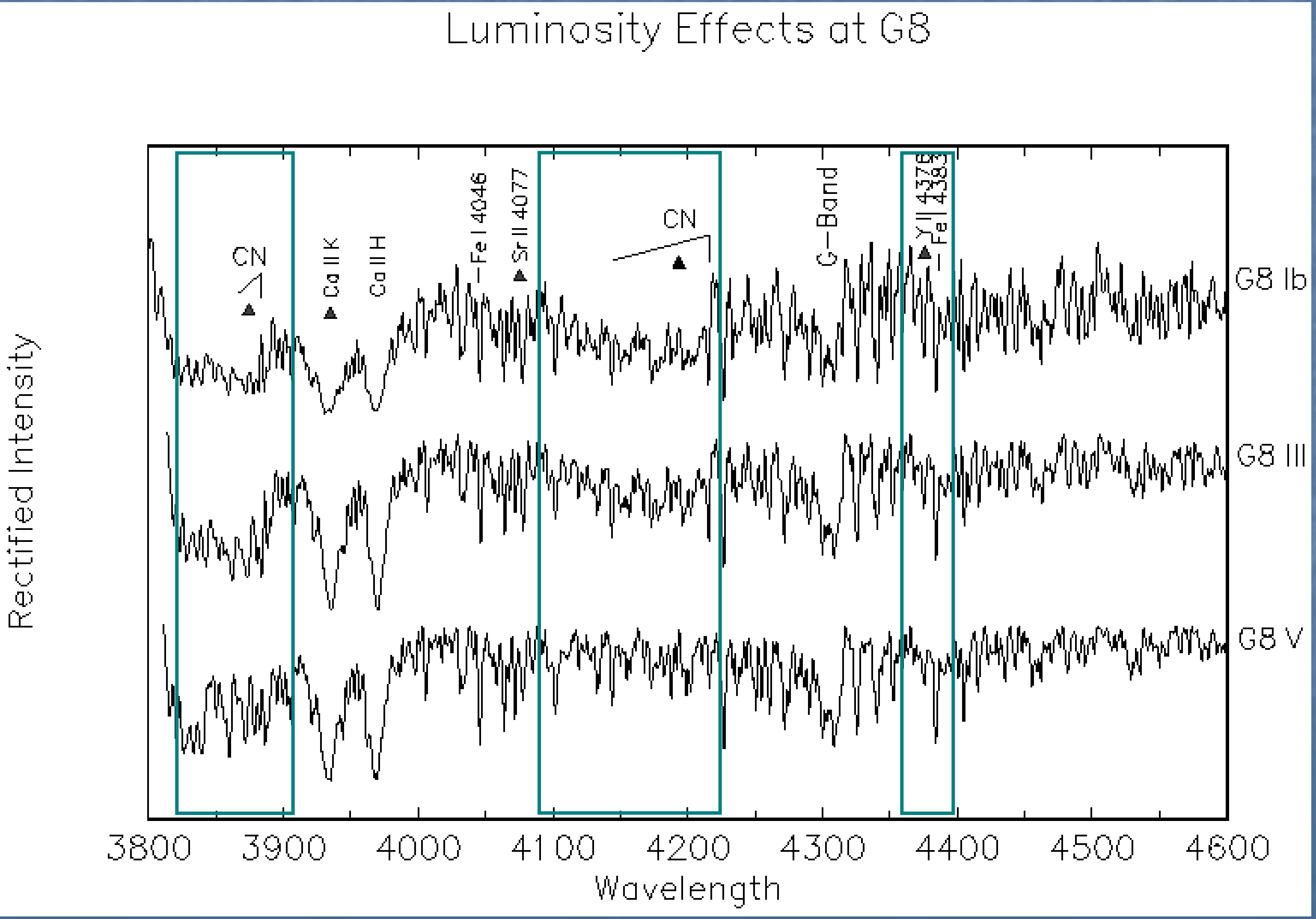

1.3 Spectral classification

- K-M type stars: TiO and CaOH bands

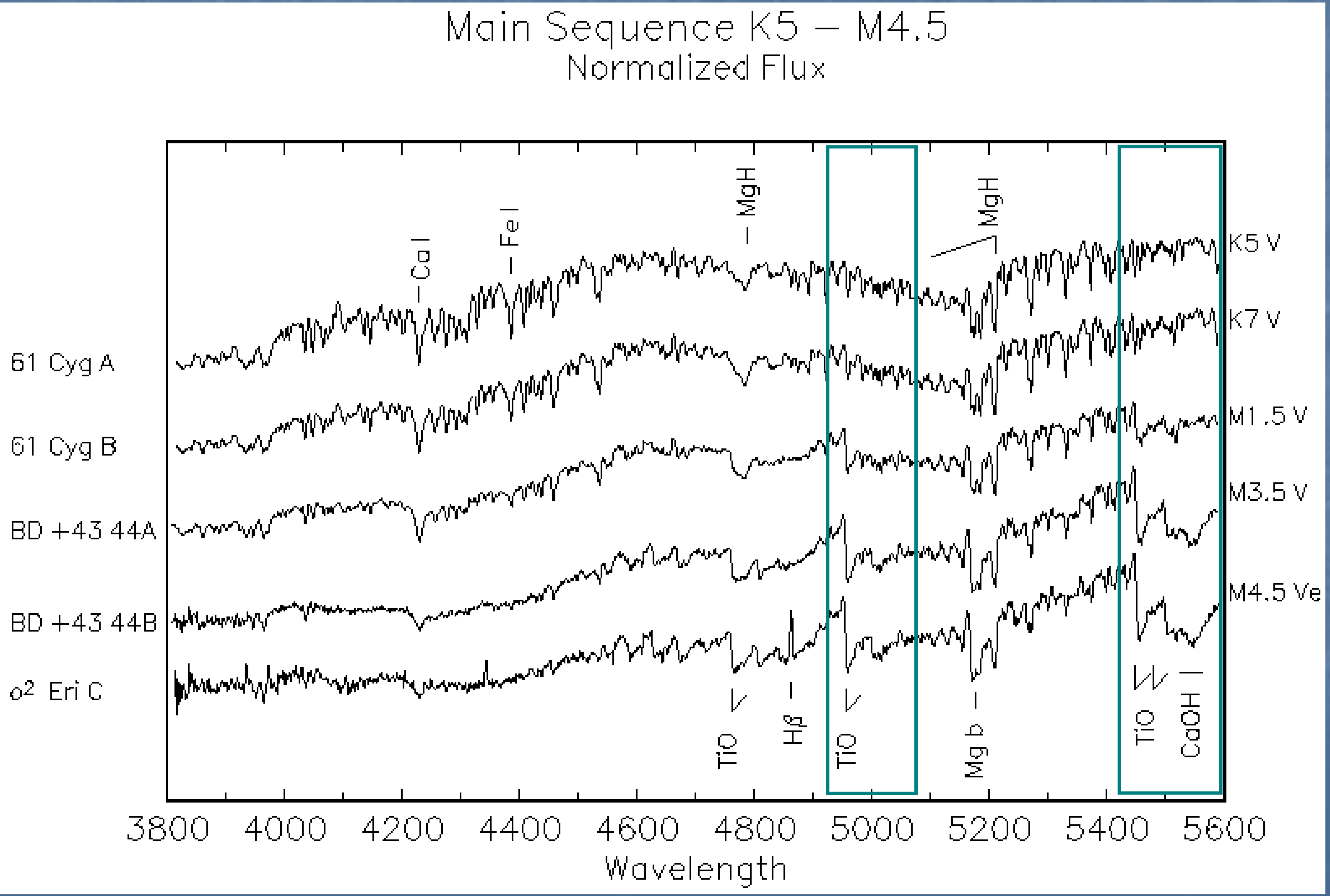

II. Interactions between matter and radiation

- The transport of energy in a stellar atmosphere is mainly done through radiation. Convection and conduction play only a very minor role and are usually neglected.
- Interactions between radiation and matter determine the shape of the spectrum of a star.
- The equations of radiative transfer are at the heart of this subject.

2.1 Basic concepts

- Specific intensity: I_ν quantity of energy dE_ν in the frequency range $[\nu,\nu+d\nu]$ that crosses a surface element dA during a time interval dt under an angle θ with respect to the surface and within an interval of solid angle $d\omega$.

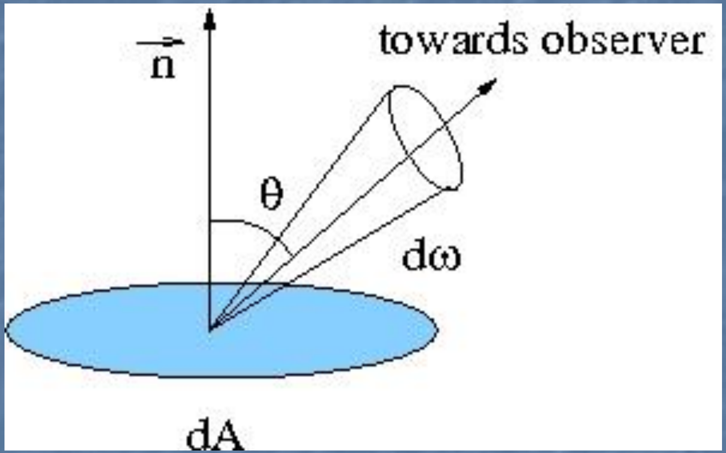

$$I_\nu = \frac{dE_\nu}{\cos\theta \, dA \, d\omega \, dt \, d\nu}$$

$$I_\nu \, d\nu = I_\lambda \, d\lambda$$

- Mean intensity: $$J_\nu = \frac{1}{4\pi} \oint I_\nu \, d\omega$$

2.1 Basic concepts

- Net radiative energy flux: $\mathcal{F}_\nu$ = first order moment of I_ν with respect to $cos\theta$ (zero for an isotropic radiation field):

$$\mathcal{F}_\nu = \frac{\oint dE_\nu}{dA\, dt\, d\nu} = \oint I_\nu \cos\theta \, d\omega$$

- Astrophysical flux: $$F_\nu = \frac{1}{\pi}\mathcal{F}_\nu$$

- At the boundary between the region that radiates and the interstellar space: $$\mathcal{F}_\nu = \mathcal{F}_\nu^{\mathrm{out}} + \mathcal{F}_\nu^{\mathrm{in}}$$

- Emerging flux: $$\mathcal{F}_\nu = 2\,\pi \int_0^{\pi/2} I_\nu \, \sin\theta \, \cos\theta \, d\theta$$

2.1 Basic concepts

- 2^{nd} order moment of I_ν with respect to $cos\theta$:

$$K_\nu = \frac{1}{4\,\pi} \oint I_\nu \, \cos^2\theta \, d\omega$$

- Quantity related to the radiation pressure:

$$dP_\nu = \frac{1}{c}\frac{d\,E_\nu \, \cos\theta}{dt\,dA} = \frac{I_\nu}{c} \, \cos^2\theta \, d\nu \, d\omega$$

- Total radiation pressure:

$$P_R = \frac{4\,\pi}{c} \int_0^\infty K_\nu \, d\nu$$

2.2 Radiative transfer

- Consider radiation that crosses a layer of material of width *dx*:

$$dI_\nu = -\kappa_\nu \, \rho \, I_\nu \, dx$$

- The absorption coefficient contains contributions from the true absorption and diffusion.
- Optical depth:

$$\tau_\nu = \int_0^L \kappa_\nu \, \rho \, dx \quad \Rightarrow \quad dI_\nu = -I_\nu \, d\tau_\nu$$

- If the matter does not emit any radiation:

$$I_\nu(x) = I_\nu^0 \, \exp\left(-\tau_\nu(x)\right)$$

2.2 Radiative transfer

- If the material does emit radiation: $$dI_\nu = j_\nu\,\rho\,dx$$

- Emission is made of true emission and scattered photons.
- Source function: $S_\nu = \frac{j_\nu}{\kappa_\nu}$
- If the emission is only due to scattering: $dj_\nu = \kappa_\nu\,I_\nu\,\frac{d\omega}{4\,\pi}$

$$\Rightarrow \qquad j_\nu = \frac{1}{4\,\pi}\oint \kappa_\nu\,I_\nu\,d\omega$$

- If the absorption coefficient is independent of the direction:

$$S_\nu = J_\nu$$

- For a local thermodynamic equilibrium (LTE; pure absorption and pure emission):

$$S_\nu = B_\nu(T) = \frac{2\,h\,\nu^3}{c^2}\,\frac{1}{\exp\left(h\,\nu/k\,T\right) - 1}$$

2.2 Radiative transfer

- Equation of radiative transfer: $$\frac{d\,I_\nu}{d\tau_\nu} = -I_\nu + S_\nu$$
- Look for formal solutions of the kind $$I_\nu(\tau_\nu) = f(\tau_\nu)\,\exp\,(b\,\tau_\nu)$$
- The equation now becomes:

$$b\,I_\nu(\tau_\nu) + \frac{d\,f}{d\tau_\nu}\,\exp\,(b\,\tau_\nu) = -I_\nu + S_\nu$$

- And the solution is

$$I_\nu(\tau_\nu) = \exp\,(-\tau_\nu)\,\int_0^{\tau_\nu} S_\nu(t_\nu)\,\exp\,(t_\nu)\,dt_\nu + I_\nu(0)\,\exp\,(-\tau_\nu)$$

2.3 Local thermodynamic equilibrium

- Consider an atom with a number of different energy levels.
- In thermodynamic equilibrium, the populations of the different levels are given by the Boltzmann law:

$$\frac{N_n}{N} = \frac{g_n}{u(T)} \exp\left(-\chi_n/kT\right)$$

$$u(T) = \sum_i g_i \exp -\chi_i/kT$$

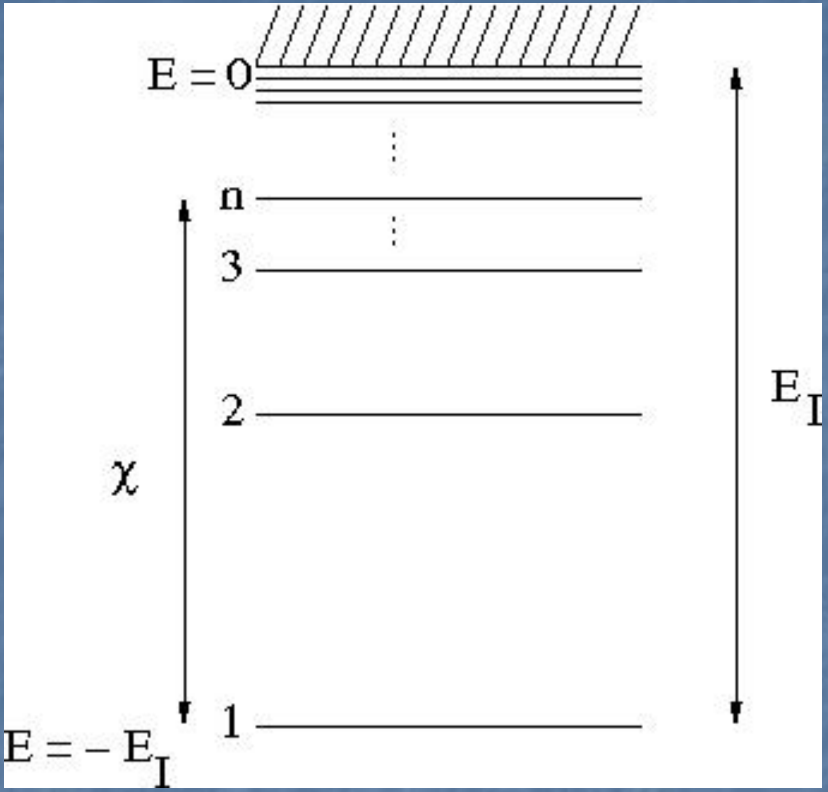

- Consider the simplified situation of a two-level (*u* and *l*) atom.

$$\frac{N_u}{N_l} = \frac{g_u}{g_l} \exp\left(-h\,\nu/kT\right)$$

2.3 Local thermodynamic equilibrium

- The probability of a spontaneous transition between u and l is $A_{u,l}\, dt\, d\omega$
- The probabilities of transition $u \rightarrow l$ and $l \rightarrow u$ induced by radiation are $B_{u,l}\, I_\nu\, dt\, d\omega$ and $B_{l,u}\, I_\nu\, dt\, d\omega$, respectively.
- The absorption coefficient corrected for stimulated emission thus becomes:

$$\kappa_\nu\, \rho\, I_\nu = N_l\, B_{l,u}\, I_\nu\, h\, \nu - N_u\, B_{u,l}\, I_\nu\, h\, \nu$$

- LTE implies:

$$N_u\, A_{u,l} + N_u\, B_{u,l}\, I_\nu = N_l\, B_{l,u}\, I_\nu$$

$$\Rightarrow \quad I_\nu = \frac{A_{u,l}}{B_{l,u}\, \frac{N_l}{N_u} - B_{u,l}} \qquad B_\nu(T) = \frac{2\, h\, \nu^3}{c^2}\, \frac{1}{\exp\,(h\, \nu / k\, T) - 1}$$

$$\Rightarrow \quad B_{u,l} = B_{l,u}\, \frac{g_l}{g_u} \quad \& \quad A_{u,l} = \frac{2\, h\, \nu^3}{c^2}\, B_{u,l}$$

Remain valid outside LTE.

2.4 Radiative transfer in different geometries

- Spherical atmosphere: $$\frac{d\,I_\nu}{d\tau_\nu} = -I_\nu + S_\nu$$

$$d\tau_\nu = \kappa_\nu\,\rho\,dz \qquad dr = \cos\theta\,dz \qquad r\,d\theta = -\sin\theta\,dz$$

$$\Rightarrow \quad \frac{d\,I_\nu}{dz} = \frac{\partial\,I_\nu}{\partial r}\frac{d\,r}{dz} + \frac{\partial\,I_\nu}{\partial\theta}\frac{d\,\theta}{dz} = \frac{\partial\,I_\nu}{\partial r}\cos\theta - \frac{\partial\,I_\nu}{\partial\theta}\frac{\sin\theta}{r}$$

$$\Rightarrow \quad \frac{\partial\,I_\nu}{\partial r}\frac{\cos\theta}{\kappa_\nu\,\rho} - \frac{\partial\,I_\nu}{\partial\theta}\frac{\sin\theta}{\kappa_\nu\,\rho\,r} = -I_\nu + S_\nu$$

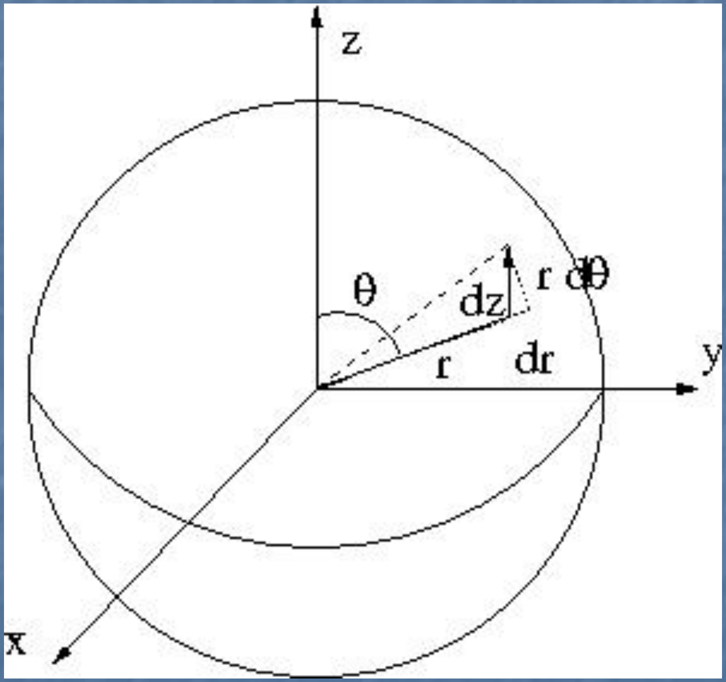

2.4 Radiative transfer in different geometries

- Plane parallel atmosphere:

$$\frac{d\,I_\nu}{d\tau_\nu} = -I_\nu + S_\nu$$

$$d\tau_\nu = \kappa_\nu\,\rho\,dz \qquad dr = \cos\theta\,dz \qquad \cancel{r\,d\theta = -\sin\theta\,dz}$$

$$\Rightarrow \quad \frac{d\,I_\nu}{dr}\,\frac{\cos\theta}{\kappa_\nu\,\rho} = -I_\nu + S_\nu \qquad d\tau_\nu = -\kappa_\nu\,\rho\,dr$$

$$\Rightarrow \quad \frac{d\,I_\nu}{d\tau_\nu}\,\cos\theta = I_\nu - S_\nu$$

Change in the definition of τ_ν.

$$I_\nu(\tau_\nu,\theta) = I_\nu^{\rm out}(\tau_\nu) \quad \text{if} \quad \theta \in [0,\pi/2[$$
$$I_\nu(\tau_\nu,\theta) = I_\nu^{\rm in}(\tau_\nu) \quad \text{if} \quad \theta \in]\pi/2,\pi]$$

2.4 Radiative transfer in different geometries

$$
\begin{aligned}
I_\nu(\tau_\nu, \theta) = I_\nu^{\mathrm{out}}(\tau_\nu) \quad \text{if} \quad \theta \in [0, \pi/2[\\
I_\nu(\tau_\nu, \theta) = I_\nu^{\mathrm{in}}(\tau_\nu) \quad \text{if} \quad \theta \in]\pi/2, \pi]
\end{aligned}
$$

- Integrated form of the equation of radiative transfer:

$$
I_\nu^{\mathrm{in/out}}(\tau_\nu) = -\int_{\tau_{\mathrm{start}}}^{\tau_\nu} S_\nu(t_\nu) \exp\left[-(t_\nu - \tau_\nu) \sec\theta\right] \sec\theta \, dt_\nu + I_\nu^{\mathrm{in/out}}(\tau_{\mathrm{start}}) \exp\left[(\tau_\nu - \tau_{\mathrm{start}}) \sec\theta\right]
$$

$\Rightarrow$

$$
\begin{aligned}
I_\nu^{\mathrm{out}}(\tau_\nu) &= \int_{\tau_\nu}^{\infty} S_\nu(t_\nu) \exp\left[(\tau_\nu - t_\nu) \sec\theta\right] \sec\theta \, dt_\nu \\
I_\nu^{\mathrm{in}}(\tau_\nu) &= -\int_{0}^{\tau_\nu} S_\nu(t_\nu) \exp\left[(\tau_\nu - t_\nu) \sec\theta\right] \sec\theta \, dt_\nu
\end{aligned}
$$

2.4 Radiative transfer in different geometries

- Resulting flux:

$$\begin{aligned}\mathcal{F}_\nu &= 2\,\pi \int_0^\pi I_\nu \,\cos\theta\,\sin\theta\,d\theta \\ &= 2\,\pi\left[\int_0^{\pi/2}\int_{\tau_\nu}^\infty S_\nu \,\exp\left[-(t_\nu-\tau_\nu)\,\sec\theta\right]\,\sin\theta\,dt_\nu\,d\theta - \int_{\pi/2}^{\pi}\int_0^{\tau_\nu} S_\nu\,\exp\left[-(t_\nu-\tau_\nu)\,\sec\theta\right]\,\sin\theta\,dt_\nu\,d\theta\right]\end{aligned}$$

$$\Rightarrow \quad \mathcal{F}_\nu = 2\,\pi\left[\int_{\tau_\nu}^\infty S_\nu\,E_2(t_\nu-\tau_\nu)\,dt_\nu - \int_0^{\tau_\nu} S_\nu\,E_2(\tau_\nu-t_\nu)\,dt_\nu\right]$$

- Exponential integral of degree *n*:

$$E_n(x) = \int_1^\infty \frac{\exp -x\,w}{w^n}\,dw$$

- Emerging flux:

$$\mathcal{F}_\nu(\tau_\nu=0) = 2\,\pi\int_0^\infty S_\nu\,E_2(t_\nu)\,dt_\nu$$

$$\begin{aligned}J_\nu &= \frac{1}{2}\left[\int_{\tau_\nu}^\infty S_\nu\,E_1(t_\nu-\tau_\nu)\,dt_\nu + \int_0^{\tau_\nu} S_\nu\,E_1(\tau_\nu-t_\nu)\,dt_\nu\right] \\ K_\nu &= \frac{1}{2}\left[\int_{\tau_\nu}^\infty S_\nu\,E_3(t_\nu-\tau_\nu)\,dt_\nu + \int_0^{\tau_\nu} S_\nu\,E_3(\tau_\nu-t_\nu)\,dt_\nu\right]\end{aligned}$$

2.5 Radiative equilibrium

- There is no production of energy inside the stellar atmosphere. Energy is only transported:

$$\frac{d}{dx}\int_0^\infty \mathcal{F}_\nu(\tau_\nu)\,d\nu = 0$$

$$\int_0^\infty \mathcal{F}_\nu(\tau_\nu)\,d\nu = \mathcal{F}_0 = Cte$$

- This situation yields the 3 Milne equations if S_ν does not depend on the direction.
- 1st Milne equation: consider the equation of radiative transfer

$$\frac{d\,I_\nu}{dx}\cos\theta = (I_\nu - S_\nu)\,\kappa_\nu\,\rho$$

$$\Rightarrow \quad \frac{d}{dx}\oint I_\nu\cos\theta\,d\omega = (\oint I_\nu\,d\omega - \oint S_\nu\,d\omega)\,\kappa_\nu\,\rho$$

$$\Rightarrow \quad \frac{d\,\mathcal{F}_\nu}{dx} = 4\,\pi\,\kappa_\nu\,\rho\,(J_\nu - S_\nu)$$

2.5 Radiative equilibrium

- Integrating over all frequencies, one obtains the first Milne equation:

$$\frac{d\,\mathcal{F}_0}{dx} = 0 = 4\,\pi\,\rho\left[\int_0^\infty \kappa_\nu\,J_\nu\,d\nu - \int_0^\infty \kappa_\nu\,S_\nu\,d\nu\right]$$

$$\boxed{\int_0^\infty \kappa_\nu\left[\frac{1}{2}\int_{\tau_\nu}^\infty S_\nu\,E_1(t_\nu-\tau_\nu)\,dt_\nu + \frac{1}{2}\int_0^{\tau_\nu} S_\nu\,E_1(\tau_\nu-t_\nu)\,dt_\nu - S_\nu\right]d\nu = 0}$$

- Second Milne equation:

$$\int_0^\infty \mathcal{F}_\nu(\tau_\nu)\,d\nu = \mathcal{F}_0 = Cte$$

$$\boxed{2\,\pi\int_0^\infty\left[\int_{\tau_\nu}^\infty S_\nu\,E_2(t_\nu-\tau_\nu)\,dt_\nu - \int_0^{\tau_\nu} S_\nu\,E_2(\tau_\nu-t_\nu)\,dt_\nu\right]d\nu = \mathcal{F}_0}$$

2.5 Radiative equilibrium

- Third Milne equation: multiply the transfer equation by *cosθ* and integrate over solid angle.

$$\frac{d}{dx} \oint I_\nu \cos^2\theta \, d\omega = \left(\oint I_\nu \cos\theta \, d\omega - \oint S_\nu \cos\theta \, d\omega \right) \kappa_\nu \, \rho$$

$$\int_0^\infty \frac{d\,K_\nu}{d\tau_\nu} \, d\nu = \frac{\mathcal{F}_0}{4\,\pi}$$

$$\boxed{\int_0^\infty \frac{d}{d\tau_\nu} \left[\frac{1}{2} \int_{\tau_\nu}^\infty S_\nu \, E_3(t_\nu - \tau_\nu) \, dt_\nu + \frac{1}{2} \int_0^{\tau_\nu} S_\nu \, E_3(\tau_\nu - t_\nu) \, dt_\nu \right] d\nu = \frac{\mathcal{F}_0}{4\,\pi}}$$

- Grey atmosphere:

$$\frac{d\,I}{d\tau} \cos\theta = I - S$$

2.5 Radiative equilibrium

- Milne equations for a grey atmosphere:

$$\begin{aligned} J &= S \\ \mathcal{F} &= \mathcal{F}_0 \\ \frac{d\,K}{d\tau} &= \frac{\mathcal{F}_0}{4\,\pi} \end{aligned}$$

- Solution found by Eddington:
  $I(\tau) = I^{out}(\tau)$ for $0 \leq \theta < \pi/2$ and
  $I(\tau) = I^{in}(\tau)$ for $\pi/2 \leq \theta \leq \pi$

$$J(\tau) = \frac{1}{2}\left[I^{\text{out}}(\tau) + I^{\text{in}}(\tau)\right]$$

$$\mathcal{F}(\tau) = \pi\left[I^{\text{out}}(\tau) - I^{\text{in}}(\tau)\right]$$

$$K(\tau) = \frac{1}{6}\left[I^{\text{out}}(\tau) + I^{\text{in}}(\tau)\right]$$

2.5 Radiative equilibrium

- Integration of Milne's 3rd equation:

$$\frac{dK}{d\tau} = \frac{\mathcal{F}_0}{4\pi} \Rightarrow K(\tau) = \frac{\mathcal{F}_0}{4\pi}\tau + Cte$$

- Boundary conditions at the top of the atmosphere:

$$\Rightarrow K(\tau) = \frac{\mathcal{F}_0}{4\pi}(\tau + \frac{2}{3})$$

$J = S$ & J = 3 K $\Rightarrow$ $S(\tau) = \frac{3\mathcal{F}_0}{4\pi}(\tau + \frac{2}{3})$

$$\Rightarrow T(\tau) = \left[\frac{3}{4}(\tau + \frac{2}{3})\right]^{1/4} T_{\text{eff}}$$

2.6 The absorption coefficient

- The absorption coefficient in the continuum depends on the temperature stratification of the atmosphere.
- It reflects the bound – free and free – free processes.
- The absorption coefficients must be corrected for the effect of stimulated emission (e.g. in LTE):

$$\kappa_\nu \, \rho = N_l \, B_{l,u} \, h \, \nu - N_u \, B_{u,l} \, h \, \nu = N_l \, B_{l,u} \, h \, \nu (1 - \exp(-h \, \nu / k \, T))$$

- The opacity of the continuum: mainly due to hydrogen (most abundant chemical element in "normal" stars).
- Bound – free absorption from energy level *n*

$$E = -\frac{\mathcal{R} \, h \, c}{n^2}$$

$$\alpha_{bf} = 1.0449 \, 10^{-26} \, g_{bf} \, \frac{\lambda^3}{n^5}$$

with

$$g_{bf} = 1 + \frac{0.3456}{(\lambda \, \mathcal{R})^{1/3}} \left[\frac{\lambda \, k \, T}{h \, c} - \frac{1}{2} \right]$$

2.6 The absorption coefficient

- Bound – free absorption from energy level *n*

$$\alpha_{bf} = 1.0449\,10^{-26}\, g_{bf}\, \frac{\lambda^3}{n^5}$$

$$\Rightarrow \quad \begin{aligned} \kappa(H_{bf})\,\rho &= N \sum_{n=n_0}^{\infty} \frac{\alpha_{bf}\, N_n}{N} \\ &= 1.0449\,10^{-26}\, N \sum_{n=n_0}^{\infty} \frac{\lambda^3}{n^3}\, g_{bf}\, \exp\left(-\chi_n/k\,T\right) \end{aligned}$$

in LTE with

$$\frac{N_n}{N} = \frac{g_n}{u(T)}\, \exp\left(-\chi_n/kT\right)$$

2.6 The absorption coefficient

- Hydrogen bound – free absorption from energy level *n*

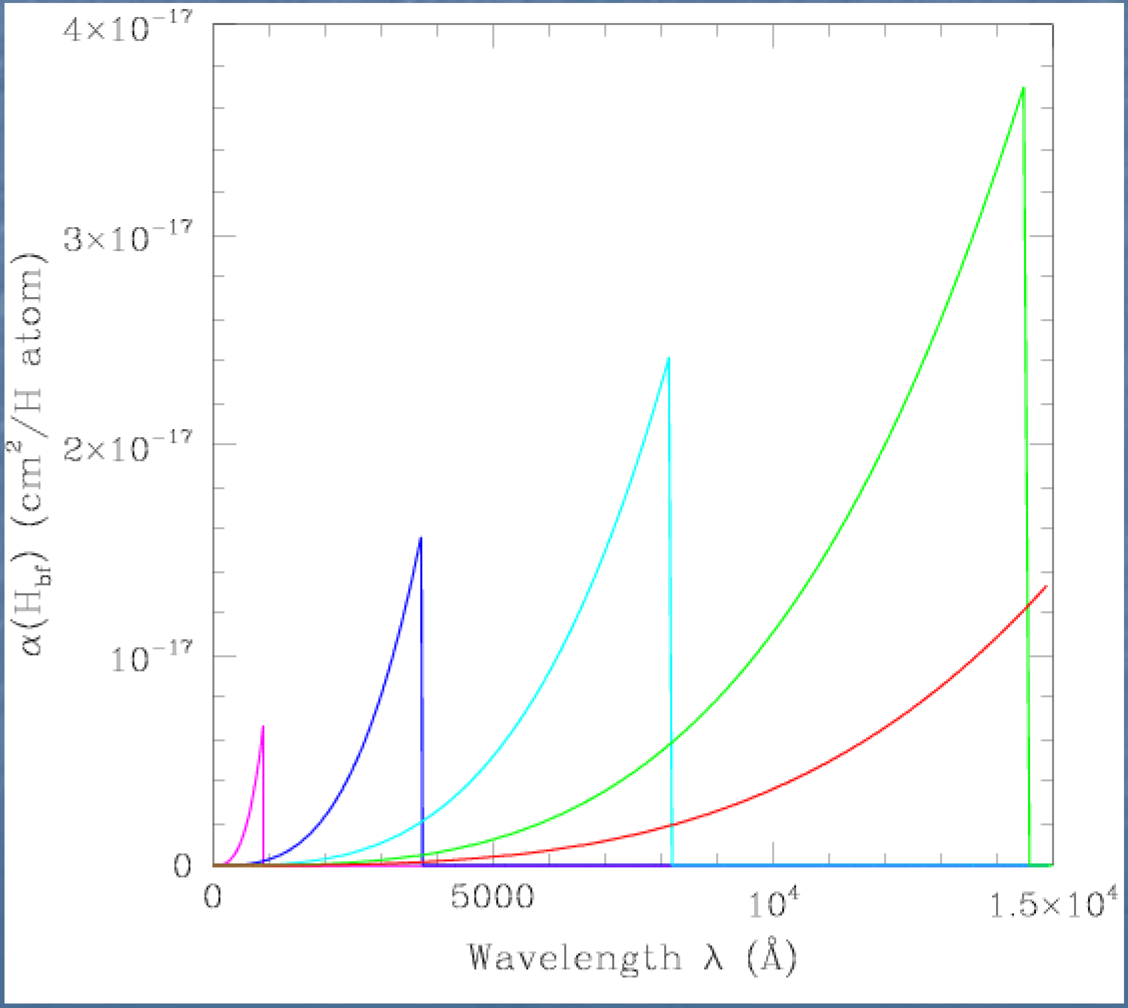

2.6 The absorption coefficient

- Hydrogen bound – free absorption from energy level *n*

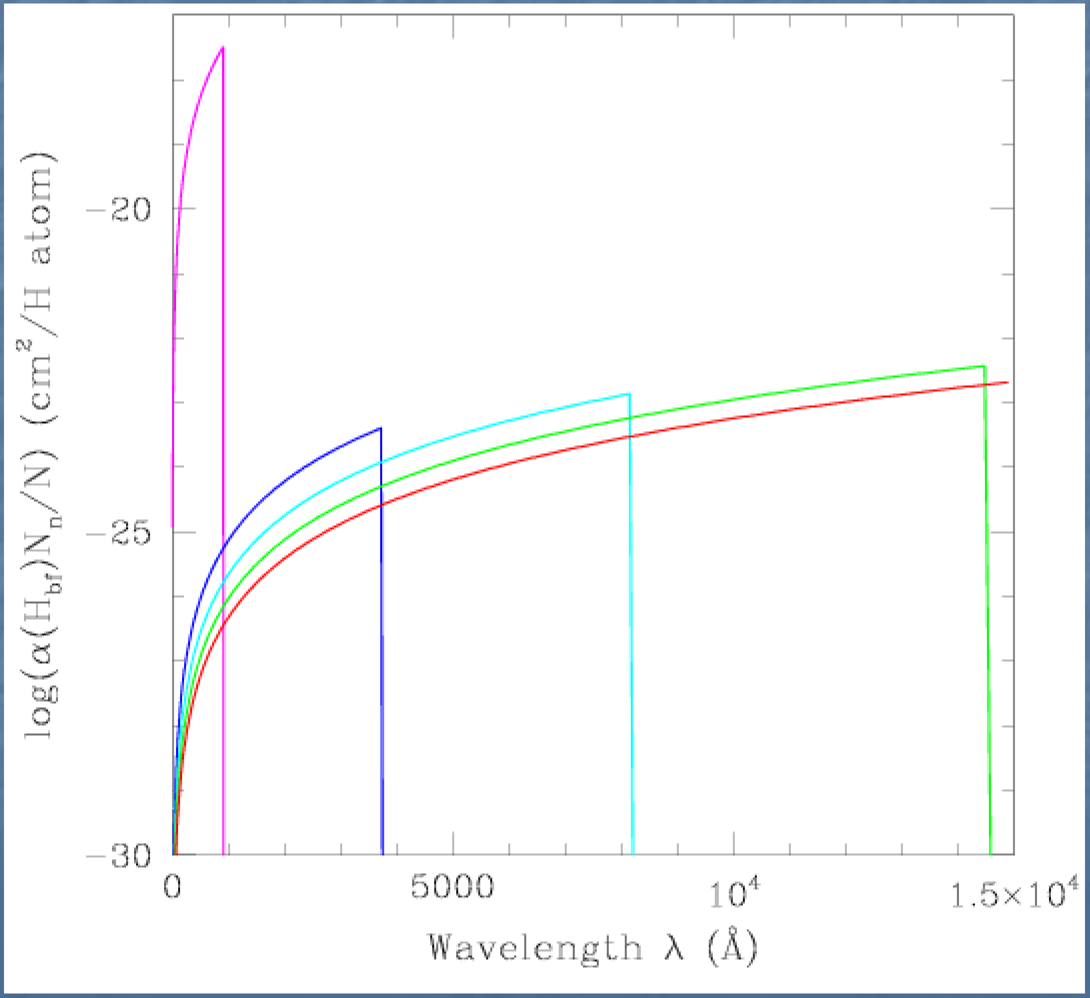

2.6 The absorption coefficient

- The Balmer discontinuity (3646 Å) across the Hertzsprung-Russell diagram:

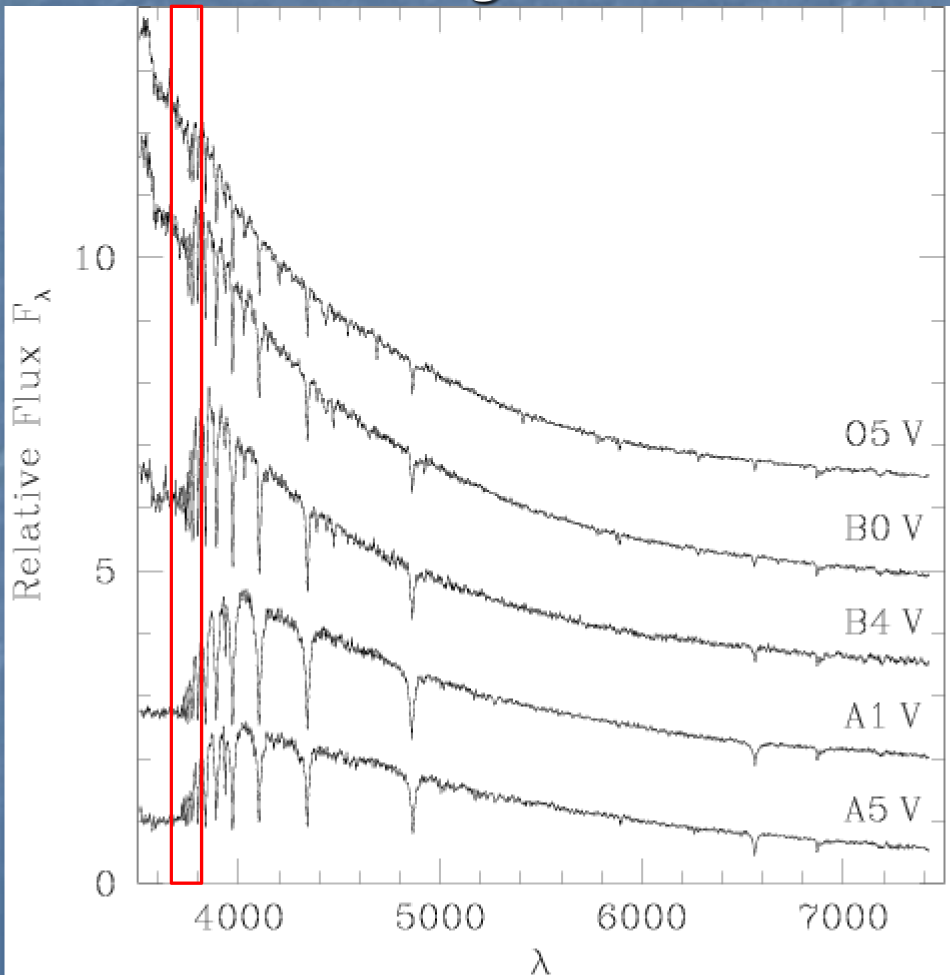

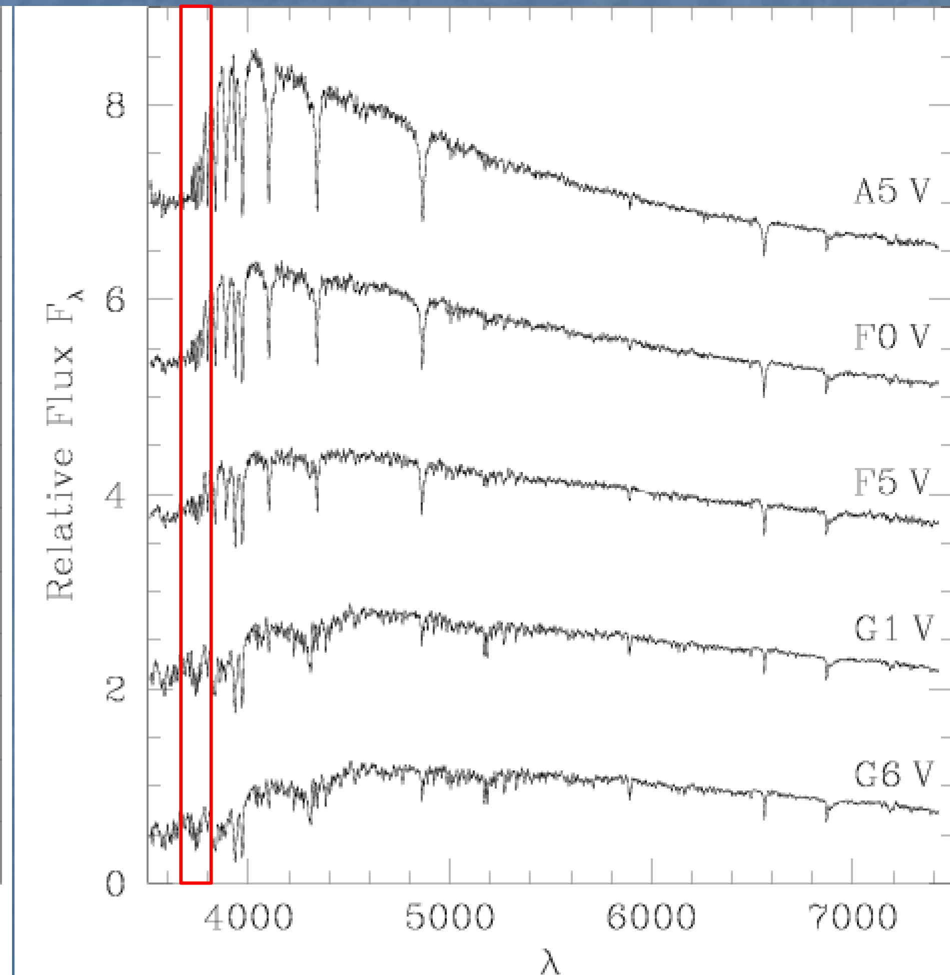

2.6 The absorption coefficient

- Free – free absorption of hydrogen

$$\alpha_{ff} = \frac{2\, g_{ff}}{3\sqrt{3}} \frac{h^2\, e^2\, \mathcal{R}}{\pi\, m^3\, \nu^3} \left(\frac{2\, m}{\pi\, k\, T}\right)^{1/2}$$

$$\Rightarrow \quad \begin{aligned} \kappa(H_{ff}) &= \frac{\alpha_{ff}\, N_i\, N_e}{N_0} \\ &= 1.0449\, 10^{-26}\, g_{ff}\, \lambda^3 \frac{k\, T}{2\, E_I} \exp\left(\frac{-E_I}{k\, T}\right) \end{aligned}$$

in LTE with $\frac{N_i}{N_0} P_e = \frac{(2\,\pi\, m_e)^{3/2}\, (k\, T)^{5/2}}{h^3} \frac{2\, u_1(T)}{u_0(T)} \exp\left(-E_I/kT\right)$

$$g_{ff} = 1 + \frac{0.3456}{(\lambda\, \mathcal{R})^{1/3}} \left[\frac{\lambda\, k\, T}{h\, c} + \frac{1}{2}\right]$$

- Neutral hydrogen is the main source of opacity in the atmospheres of B, A and F-type stars.

2.6 The absorption coefficient

- Bound – free absorption of the negative hydrogen ion: H^- formed by the capture of a free electron coming from the ionization of metals. The binding energy is 0.755 eV.
- Main source of opacity in the Sun between 4000 and 15000Å!

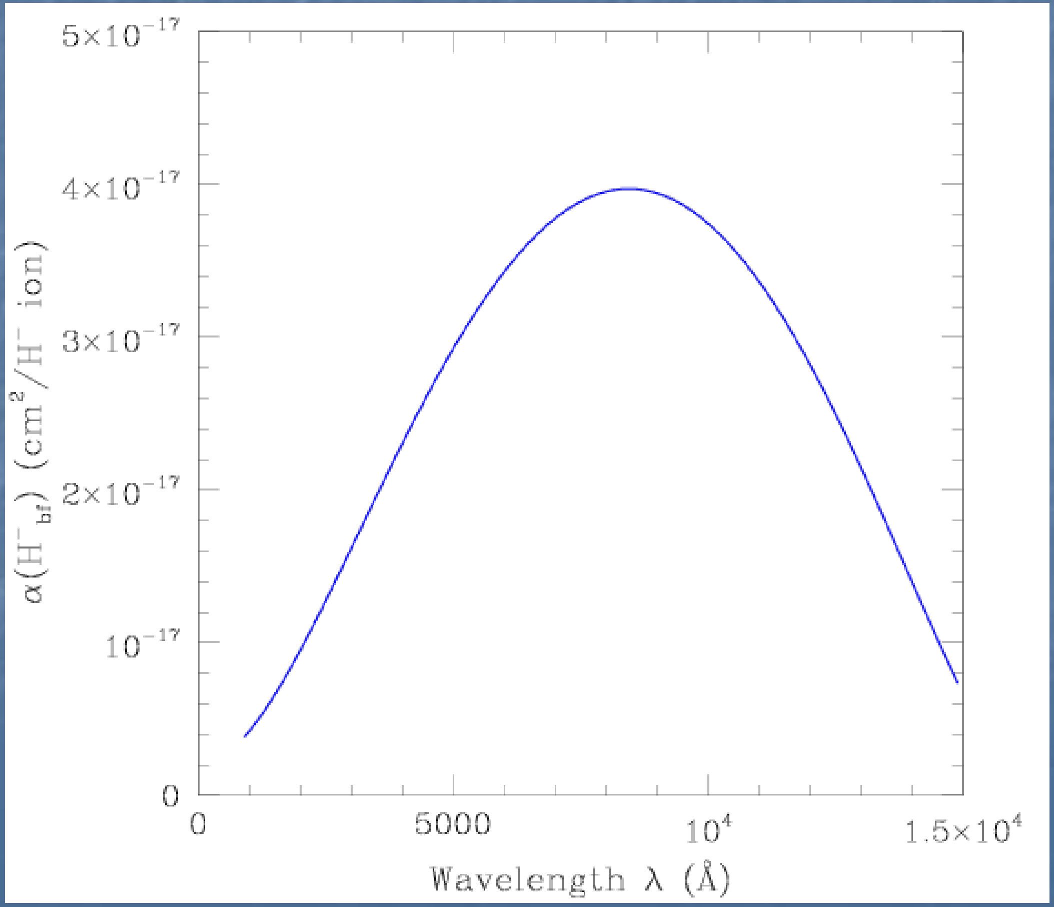

2.6 The absorption coefficient

- At first sight, the importance of the H^- ion is not obvious: for a solar-type star, compared to neutral hydrogen, the H^- ion only accounts for a relative abundance of 3×10^{-8}
- However, since we are interested in the opacity in the optical domain, it is not the full population of neutral hydrogen that matters, but only those H atoms that have their electron on the $n=3$ energy level.
- Hence $N(\mathrm{H}, n=3)/N(\mathrm{H}^-) = 0.02$.

2.6 The absorption coefficient

- Other sources of opacity in the continuum: hydrogen molecules (cool stars), helium (neutral or ionized in OB-stars), free electrons (Thomson scattering, hot stars)

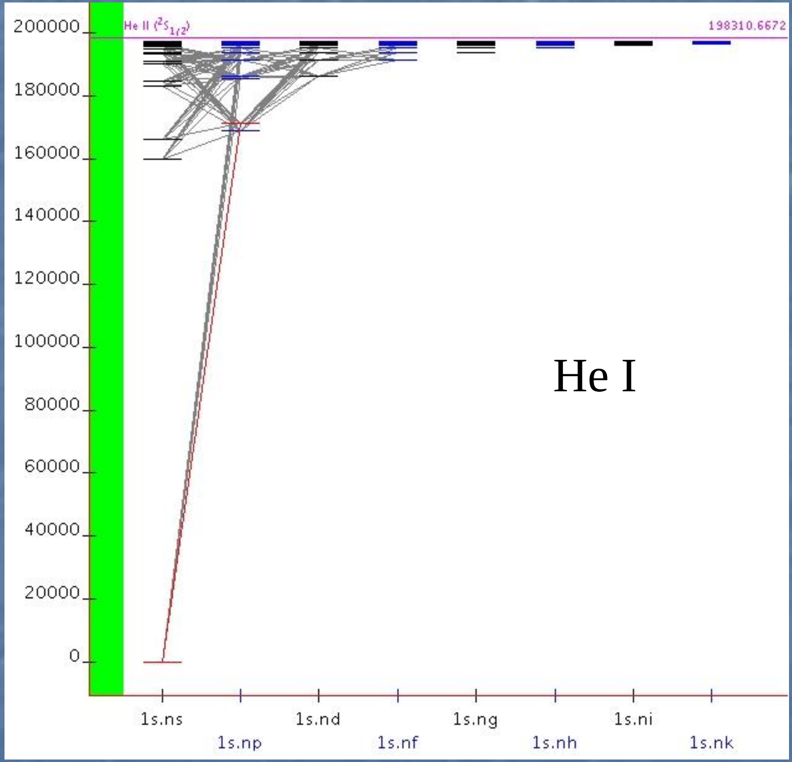

$$\sigma(e^-) = 6.648\,10^{-25}\ \mathrm{cm}^2$$

- Metal ions and atoms (mostly in the UV).
- Molecules (TiO,…) in cool stars…

2.7 The line absorption coefficient

- Consider the electric field of an electromagnetic wave moving along the *x* axis in a medium of permittivity ε:

$$E = E_0 \exp\left[-i\,\omega\,(x/v - t)\right]$$

- The wave moves at a velocity

$$v/c = (\epsilon_0/\epsilon)^{1/2}$$

- where we have $$\frac{\epsilon}{\epsilon_0} = 1 + \frac{4\pi N e z}{E}$$

- *z* is the separation of the charges of the dipole.
- In quantum mechanics, the interaction between the electron and the photon triggers oscillations of the electron density (the electron's probability of being present at a specific location): [..\Quantum\index.html](..\Quantum\index.html)

2.7 The line absorption coefficient

- In classical mechanics, the electron behaves as a forced and damped oscillator (emission of light induces a loss of energy):

$$\frac{d^2 z}{dt^2} + \gamma \frac{d z}{dt} + \omega_0^2 z = \frac{e}{m_e} E_0 \exp(i \omega t)$$

- We search solutions of the kind: $z = z_0 \exp(i \omega t)$

- Hence: $-\omega^2 z_0 + i \gamma \omega z_0 + \omega_0^2 z_0 = \frac{e}{m_e} E_0$

$$\Rightarrow \quad z = \frac{\frac{e}{m_e} E}{(\omega_0^2 - \omega^2) + i \gamma \omega}$$

- We thus obtain: $c/v \simeq 1 + \frac{2 \pi N e^2}{m_e [(\omega_0^2 - \omega^2) + i \gamma \omega]} = n - i k$

$$E = E_0 \exp[-i \omega (x/v - t)] = E_0 \exp[-i \omega (n x/c - t)] \exp[-k \omega x/c]$$

2.7 The line absorption coefficient

$$E = E_0 \exp\left[-i\,\omega\,(x/v - t)\right] = E_0 \exp\left[-i\,\omega\,(n\,x/c - t)\right] \exp\left[-k\,\omega\,x/c\right]$$

$$\Rightarrow I \propto E\,E^* = I_0 \exp\left[-2\,k\,\omega\,x/c\right] = I_0 \exp\left[-l_\nu\,\rho\,x\right] = I_0 \exp\left[-N\,\alpha\,x\right]$$

- The intrinsic absorption coefficient can thus be written as a Lorentzian profile:

$$\begin{aligned}\alpha &= \frac{4\,\pi\,e^2}{m_e\,c}\,\frac{\gamma}{4\,(\Delta\,\omega)^2 + \gamma^2}\\ &= \frac{e^2}{m_e\,c}\,\frac{\gamma/(4\,\pi)}{(\Delta\,\nu)^2 + (\gamma/(4\,\pi))^2}\end{aligned}$$

- If true, this result implies that all lines should have identical integrated strength!

$$\int_0^\infty \alpha\,d\nu = \frac{\pi\,e^2}{m\,c}$$

- Quantum mechanical treatment $\int_0^\infty \alpha\,d\nu = \frac{\pi\,e^2}{m\,c}\,f_{l,u} = B_{l,u}\,h\,\nu$

2.7 The line absorption coefficient

- Oscillator strength: $$f_{u,l} = \frac{g_l}{g_u} f_{l,u}$$
- Building a model atmosphere requires a huge number of atomic parameters.
- A recent database of such parameters is the Atomic Spectra Database of the National Institute of Standards & Technology (NIST): http://www.nist.gov/pml/data/asd.cfm
- A compilation of atomic lines may be found on the website http://www.pa.uky.edu/~peter/atomic

2.7 The line absorption coefficient

- Collisional broadening (pressure broadening): the interaction between an atom and its neighbours alters the energy levels of the atom.

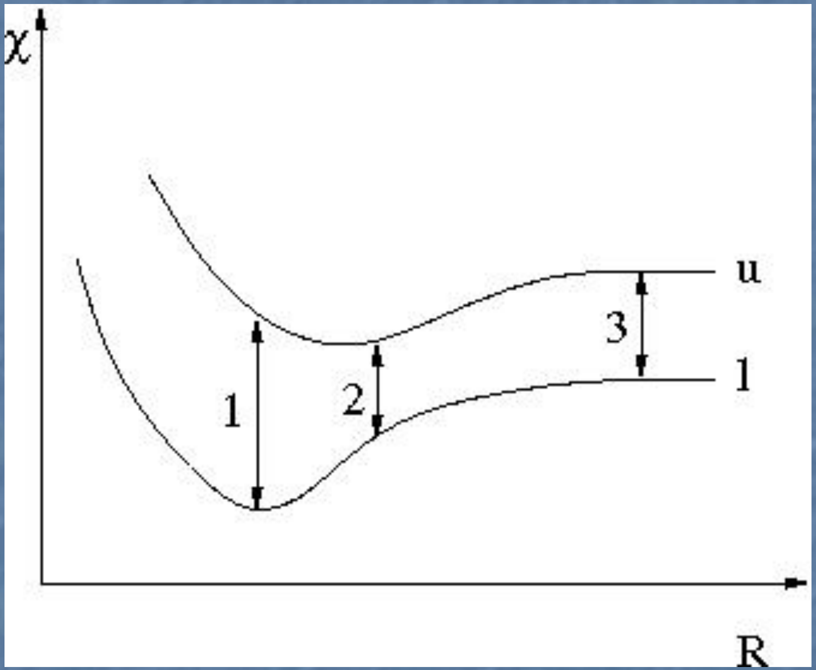

$$\Rightarrow \quad \Delta \nu = C_p(l, u) / R^p$$

2.7 The line absorption coefficient

- Pressure broadening yields an absorption coefficient:

$$\alpha \propto \frac{\gamma_p/4\,\pi}{(\nu-\nu_0)^2+(\gamma_p/4\,\pi)^2}$$

  where the damping coefficient depends on the average time between two collisions.

$$\gamma_p = 2/\Delta\,t$$

- One distinguishes different types of broadening:

1. Linear Stark effect (p = 2) due to protons and free electrons. Important for hydrogen.
2. Quadratic Stark effect (p = 4). Important in atmospheres of hot stars (ions and free electrons).
3. van der Waals interaction (p = 6) in the atmospheres of cooler stars (action of neutral hydrogen).

$$\gamma_4 \simeq 39\,C_4(l,u)^{2/3}\left[\frac{8\,k\,T}{\pi}\left(\frac{1}{m_A}+\frac{1}{m_e}\right)\right]^{1/6} N_e + 39\,C_4(l,u)^{2/3}\left[\frac{8\,k\,T}{\pi}\left(\frac{1}{m_A}+\frac{1}{m_{ion}}\right)\right]^{1/6} N_{ion}$$

2.7 The line absorption coefficient

- The impact of the linear Stark effect on the lines of hydrogen in A-type stars:

Increasing gravity → increasing Stark effect

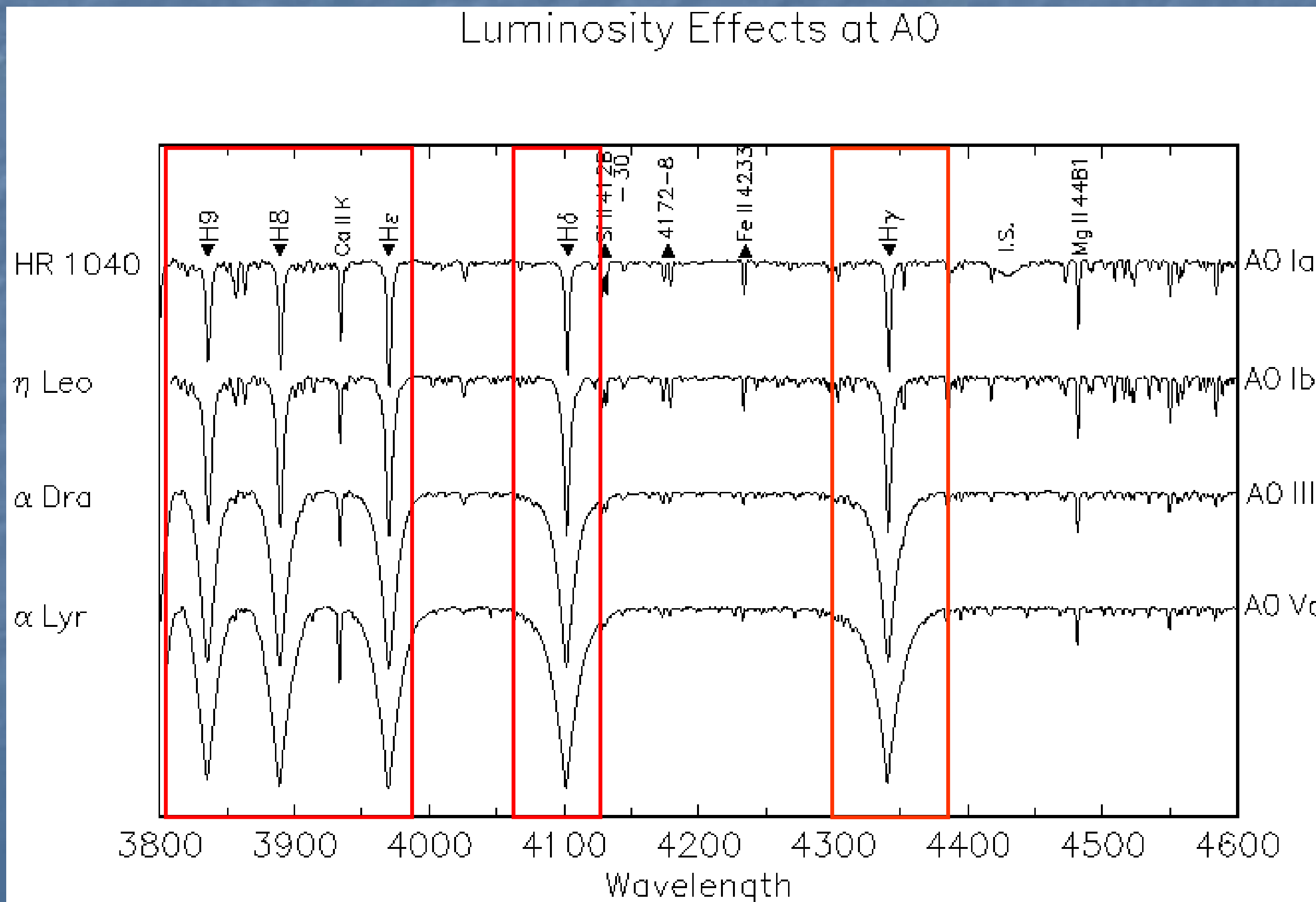

Increasing luminosity

2.7 The line absorption coefficient

- Linear Stark effect: the electric field lifts the degeneracy of the energy levels of same principal quantum number:

$$\Delta\lambda_j = C_j\, E$$

- Approximation of the nearest neighbour: it's the nearest disturber that has the largest effect.
- Probability that the nearest disturber be located in a shell of inner radius R and outer radius $R + dR$ = product of the probability that a disturber be located in this shell and the probability $s(R)$ that no other disturber lies within a sphere of radius R:

$$p(R)\, dR = s(R)\, 4\,\pi\, R^2\, dR\, N$$

where $$s(R + dR) = s(R)\,(1 - 4\,\pi\, R^2\, dR\, N) = s(R) + \frac{d\,s}{dR}\, dR$$

$$\Rightarrow \quad s(R) = \exp\left[-(R/R_0)^3\right]$$

2.7 The line absorption coefficient

$$p(R)\,dR = s(R)\,4\,\pi\,R^2\,dR\,N$$

- Let R_0 be the average distance between particles:

$$R_0 \;=\; (4\,\pi\,N/3)^{-1/3} \qquad E_0 = \frac{q}{R_0^2}$$

$$\Rightarrow \quad p(R)\,dR = \frac{3\,R^2}{R_0^3}\,\exp\left[-(R/R_0)^3\right]dR$$

since $\dfrac{R}{R_0} = \sqrt{\dfrac{E_0}{E}}, \Rightarrow \quad \dfrac{dR}{R_0} = -\dfrac{1}{2}\left(\dfrac{E_0}{E}\right)^{3/2}\dfrac{dE}{E_0}$

- We can thus express the probability in terms of the electric field produced by the nearest neighbour:

$$p(E)\,dE = \frac{3}{2}\left(\frac{E_0}{E}\right)^{5/2}\exp\left[-(E_0/E)^{3/2}\right]\frac{dE}{E_0}$$

2.7 The line absorption coefficient

$$p(E)\,dE = \frac{3}{2}\left(\frac{E_0}{E}\right)^{5/2} \exp\left[-(E_0/E)^{3/2}\right]\frac{dE}{E_0}$$

since $\Delta\lambda_j = C_j\,E$

$$\Rightarrow \quad p(E/E_0)\,\frac{dE}{E_0} = p\left(\frac{\Delta\lambda}{C_j\,E_0}\right)\frac{d\,\Delta\lambda}{C_j\,E_0}$$

Each transition between sublevels has its own oscillator strength and the resulting absorption coefficient is the weighted (by p(E)) average of the different Stark components:

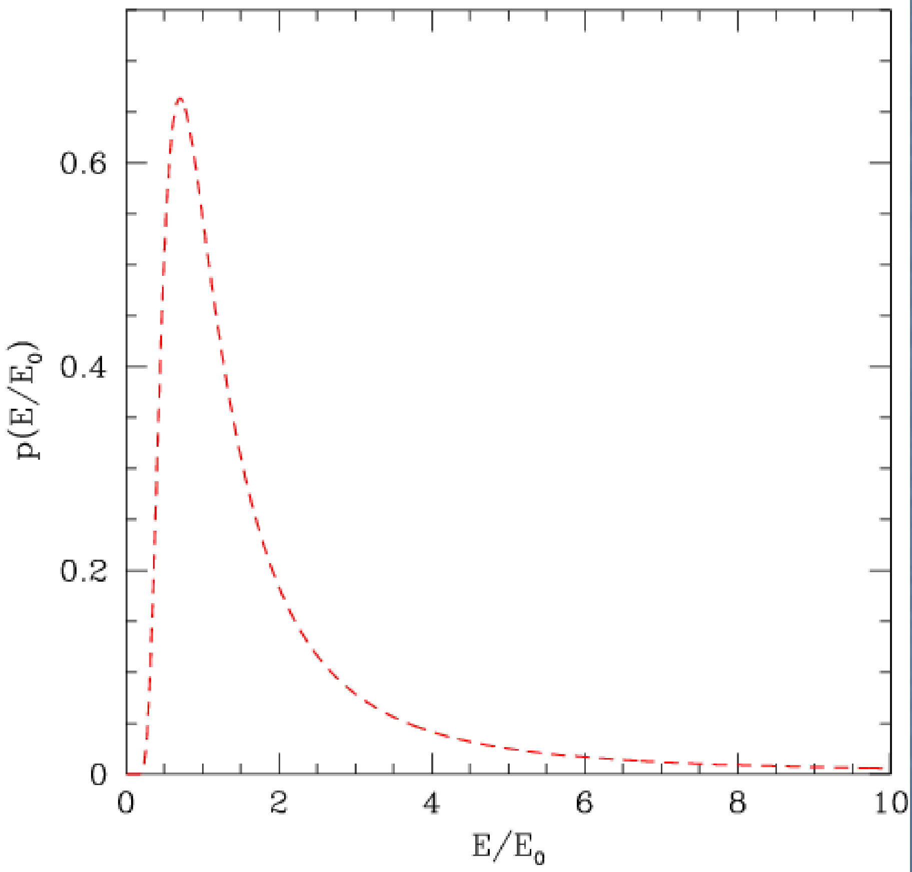

$$\alpha\,d\Delta\lambda = \frac{\pi\,e^2}{m\,c}\,\frac{\lambda^2}{c}\left[\sum_j \frac{p\left(\frac{\Delta\lambda}{C_j\,E_0}\right) f_j}{n_l^2\,C_j\,E_0} + f_0\,\delta(\Delta\,\lambda)\right] d\,\Delta\lambda$$

2.7 The line absorption coefficient

- Thermal broadening: thermal agitation of the absorber creates a Brownian motion with a radial velocity component (hence Doppler effect):

$$\frac{\Delta\,\lambda}{\lambda_0} = \frac{\lambda - \lambda_0}{\lambda_0} = \frac{v_r}{c}$$

M-B distribution: $$\frac{dN}{N} = \left(\frac{m}{2\,\pi\,k\,T}\right)^{1/2} \exp\left[-\frac{m\,v_r^2}{2\,k\,T}\right] dv_r$$

- The Doppler velocity is defined as: $$v_D^2 = \frac{2\,k\,T}{m}$$
- This corresponds to a Doppler wavelength shift of:

$$\Delta\lambda_D = \frac{v_D\,\lambda_0}{c}$$

$$\Rightarrow \quad \frac{dN}{N} = \frac{1}{\pi^{1/2}\,\Delta\lambda_D} \exp\left[-\left(\frac{\Delta\lambda}{\Delta\lambda_D}\right)^2\right] d\Delta\lambda$$

2.7 The line absorption coefficient

- Absorption coefficient broadened by thermal agitation:

$$\alpha = \frac{\pi^{1/2}\, e^2\, \lambda_0^2}{m_e\, c^2} \frac{f}{\Delta\lambda_D} \exp\left[-\left(\frac{\Delta\lambda}{\Delta\lambda_D}\right)^2\right]$$

- This is a Gaussian profile.
- There exist other motions of the material which arise from non-thermal processes (micro-turbulence):

$$\Rightarrow \quad \Delta\lambda_D = \frac{\lambda_0}{c}\left(\frac{2\,k\,T}{m} + \xi^2\right)^{1/2}$$

2.7 The line absorption coefficient

Comparison Lorentzian and Gaussian:

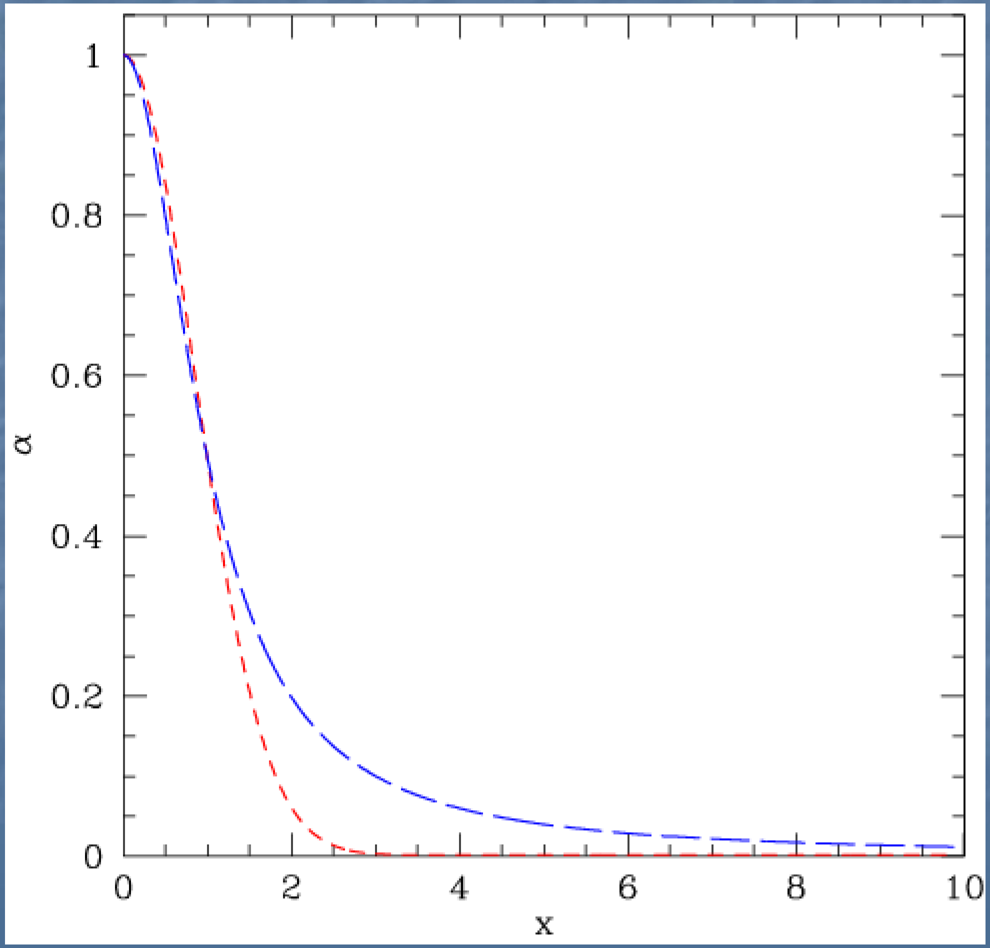

2.7 The line absorption coefficient

- Combination of different broadening effects:

α = α(intrinsic) * α (collisional) * α(thermal) * α(microturbulence)

convolution of 2 Lorentzians — convolution of 2 Gaussians

$$\Gamma = \gamma + \gamma_p$$

$$\Delta\lambda_D = \frac{\lambda_0}{c}\left(\frac{2\,k\,T}{m} + \xi^2\right)^{1/2}$$

$$\Rightarrow \boxed{\alpha = \frac{\pi^{1/2}\,e^2\,\lambda_0^2}{m\,c^2}\,\frac{f}{\Delta\lambda_D}\int_{-\infty}^{+\infty}\frac{\frac{\Gamma\,\lambda_0^2}{4\,\pi\,c}}{(\lambda_0+\Delta\lambda-\lambda)^2+(\frac{\Gamma\,\lambda_0^2}{4\,\pi\,c})^2}\,\exp\,[-(\frac{\Delta\lambda}{\Delta\lambda_D})^2]\,d\Delta\lambda}$$

- Voigt-Hjerting function:

$$H(a,u) = \frac{a}{\pi}\int_{-\infty}^{+\infty}\frac{\exp\,(-y^2)\,dy}{(y-u)^2+a^2}$$

2.7 The line absorption coefficient

Voigt-Hjerting function:

$$H(a,u) = \frac{a}{\pi}\int_{-\infty}^{+\infty} \frac{\exp(-y^2)\,dy}{(y-u)^2 + a^2}$$

Gaussian in the core, wings due to Lorentzian

$$a = \frac{\Gamma\,\lambda_0^2}{4\,\pi\,c\,\Delta\lambda_D}$$

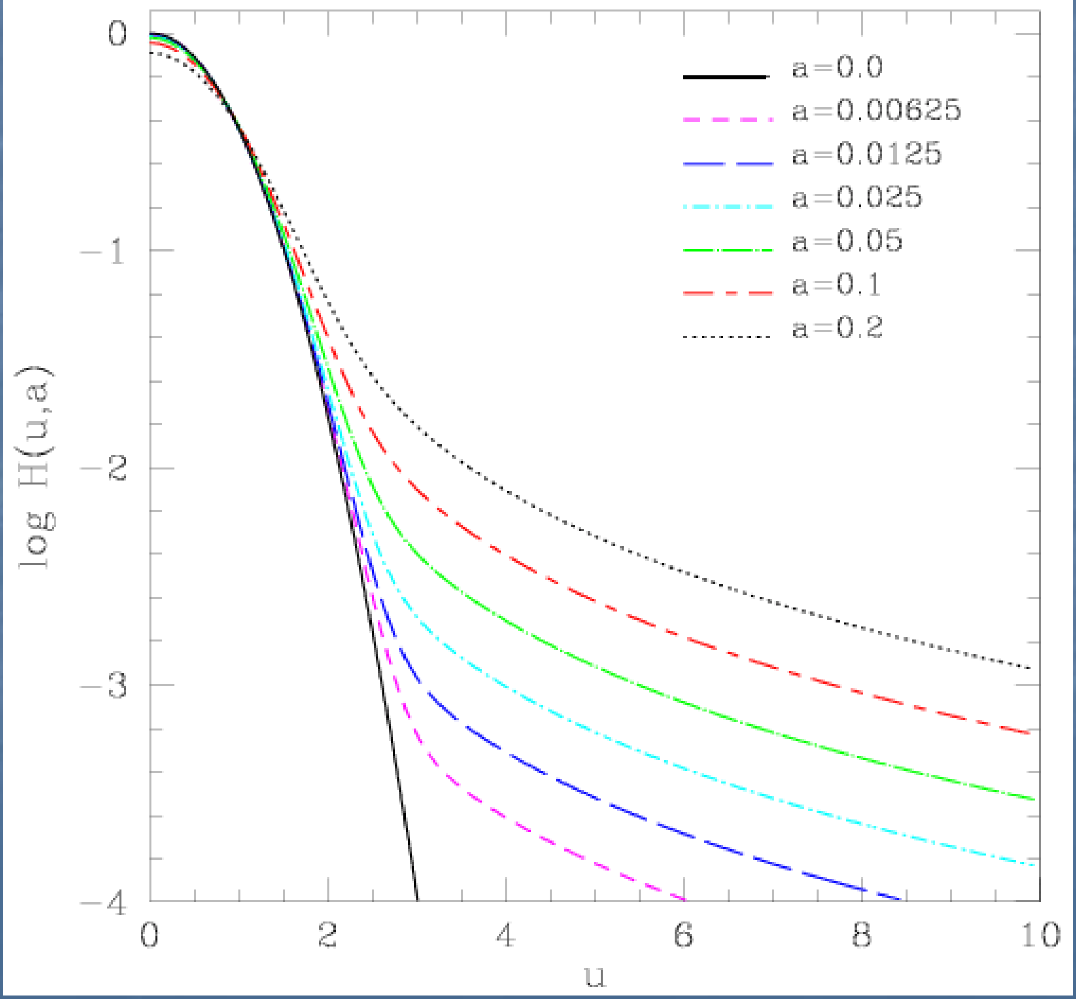

III. LTE plane-parallel stellar atmospheres

- Model atmosphere = table giving the physical parameters of the gas as a function of optical depth.
- One takes a number of simplifying assumptions:

1. Plane-parallel geometry
2. Hydrostatic equilibrium: $\frac{d\,P_g}{dx} = \rho\, g \quad \Rightarrow \quad \frac{d\,P_g}{d\tau_\nu} = \frac{g}{\kappa_\nu}$

for an isothermal atmosphere, one defines the pressure scale height

$$H_P = \frac{\mathcal{R}\,T}{\mu\, g}$$

The equation of hydrostatic equilibrium yields:

$$\frac{d\,P_g}{dx} = \frac{P_g}{H_P} \quad \Rightarrow \quad P_g(x) = P_g(0)\ \exp\left[x/H_P\right]$$

A star with a large value of g will have a more compact atmosphere. The plane-parallel approximation is thus better justified for dwarfs than for giants or supergiants.

III. LTE plane-parallel stellar atmospheres

- One takes a number of simplifying assumptions:

3. There are neither star spots, nor granulation.
4. There is no magnetic field.
5. Atmosphere in LTE: the populations of the energy levels are given by the Boltzmann and Saha equations:

$$\frac{N_n}{N} = \frac{g_n}{u(T)} \exp\left(-\chi_n/kT\right)$$

$$\frac{N_{Z,i+1}}{N_{Z,i}} = \frac{2\,u_{Z,i+1}(T)}{N_e\,u_{Z,i}(T)} \left(\frac{2\,\pi\,m_e\,k\,T}{h^2}\right)^{3/2} \exp\left(-\chi_i/kT\right)$$

Non-LTE conditions are strongest in the atmospheres of hot stars with very intense radiation fields.

3.1 The source function

- The source function *S(τ)* plays a fundamental role. It is crucial for the computation of specific intensities, fluxes,…

$$
\begin{aligned}
I_\nu^{\mathrm{out}}(\tau_\nu) &= \int_{\tau_\nu}^{\infty} S_\nu(t_\nu)\,\exp\left[(\tau_\nu - t_\nu)\,\sec\theta\right]\,\sec\theta\,dt_\nu \\
I_\nu^{\mathrm{in}}(\tau_\nu) &= -\int_{0}^{\tau_\nu} S_\nu(t_\nu)\,\exp\left[(\tau_\nu - t_\nu)\,\sec\theta\right]\,\sec\theta\,dt_\nu
\end{aligned}
$$

$$
\mathcal{F}_\nu = 2\,\pi\left[\int_{\tau_\nu}^{\infty} S_\nu\,E_2(t_\nu - \tau_\nu)\,dt_\nu - \int_0^{\tau_\nu} S_\nu\,E_2(\tau_\nu - t_\nu)\,dt_\nu\right]
$$

$$
\begin{aligned}
J_\nu &= \frac{1}{2}\left[\int_{\tau_\nu}^{\infty} S_\nu\,E_1(t_\nu - \tau_\nu)\,dt_\nu + \int_0^{\tau_\nu} S_\nu\,E_1(\tau_\nu - t_\nu)\,dt_\nu\right] \\
K_\nu &= \frac{1}{2}\left[\int_{\tau_\nu}^{\infty} S_\nu\,E_3(t_\nu - \tau_\nu)\,dt_\nu + \int_0^{\tau_\nu} S_\nu\,E_3(\tau_\nu - t_\nu)\,dt_\nu\right]
\end{aligned}
$$

3.1 The source function

- One way to deal with the source function is to expand it into a series:

$$S_\nu(t_\nu) = \sum_{n=0}^{n_{max}} Q_n \, t_\nu^n$$

- If we set $\mu = \cos\theta$

$$\Rightarrow \quad \begin{aligned} I_\nu(\tau_\nu = 0) &= \int_0^\infty S_\nu(t_\nu)\, \exp\left(-t_\nu/\mu\right) \mu^{-1}\, dt_\nu \\ &= \sum_{n=0}^{n_{max}} Q_n \int_0^\infty t_\nu^n \, \exp\left(-t_\nu/\mu\right) \frac{dt_\nu}{\mu} \\ &= \sum_{n=0}^{n_{max}} Q_n \, \mu^n \, n! \end{aligned}$$

- From this relation we see that the limb darkening actually reflects the behaviour of the source function. Determining the limb darkening observationally hence allows to derive the source function.

3.1 The source function

- Example: limb darkening of a grey atmosphere with the Eddington solution.

$$S(\tau) = \frac{3\,\mathcal{F}_0}{4\,\pi}\,(\tau + \frac{2}{3})$$

$$\Rightarrow \quad I_\nu(\tau_\nu = 0, \mu) = I_\nu(0,1)\,\frac{2}{5}\,\left(1 + \frac{3}{2}\,\mu\right)$$

- Labs formulation: $S(\tau) = \frac{3\,\mathcal{F}_0}{4\,\pi}\,(a + \tau - A\,\exp\,(-\alpha\,\tau))$

$$\Rightarrow \quad I_\nu(\tau_\nu = 0, \mu) = I_\nu(0,1)\,\frac{a + \mu - A/(1 + \alpha\,\mu)}{a + 1 - A/(1 + \alpha)}$$

3.1 The source function

Limb darkening of a grey atmosphere (comparison Eddington vs. Labs):

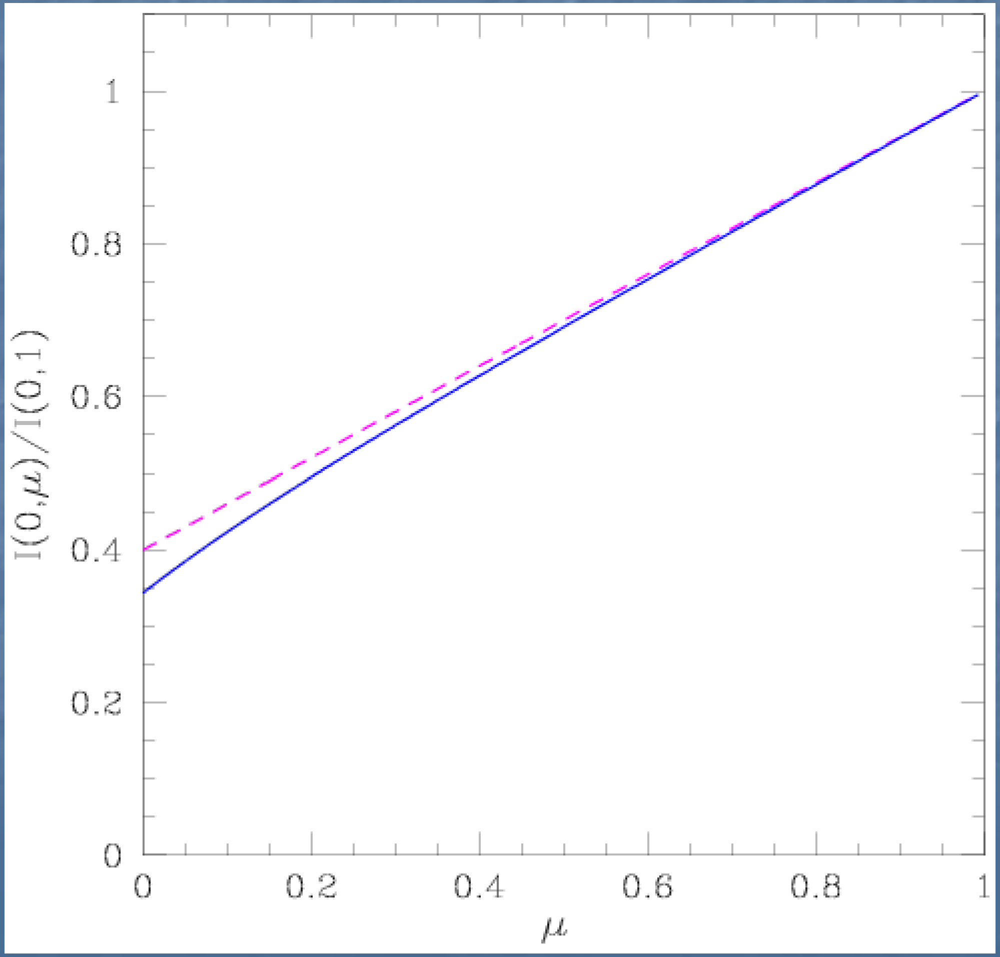

3.1 The source function

- The opacity depends on the electron density.
- Consider a chemical element Z with abundance (relative to H):

$$A_Z = N_Z / N_H$$

- Ionization equilibrium $Z^0 \rightleftharpoons Z^{1+} + e^-$
  is described via the Saha equation:

$$\frac{N_i}{N_0} P_e = \frac{(2\,\pi\, m_e)^{3/2}\,(k\,T)^{5/2}}{h^3} \frac{2\,u_1(T)}{u_0(T)} \exp\left(-E_I/kT\right)$$

$$\Rightarrow \quad \frac{N_{Z^{1+}}}{N_{Z^0}} = \frac{\Phi_Z(T)}{P_e} = \frac{N_{e,Z}}{N_{Z^0}}$$

$$P_e = \sum_Z N_{e,Z}\, k\,T \quad \Rightarrow \quad N_{e,Z} = \frac{\Phi_Z(T)\,N_Z}{P_e + \Phi_Z(T)}$$

$$\& \quad P_g = \sum_Z (N_{e,Z} + N_Z)\, k\,T$$

$$\frac{d\,P_g}{d\tau_\nu} = \frac{g}{\kappa_\nu}$$

$$\Rightarrow \quad P_e = P_g \frac{\sum_Z A_Z \frac{\Phi_Z(T)}{P_e + \Phi_Z(T)}}{\sum_Z A_Z \left(1 + \frac{\Phi_Z(T)}{P_e + \Phi_Z(T)}\right)}$$

These equations are solved iteratively.

3.2 The diffusion approximation

- For large optical depths, LTE is a good approximation.
- However, the atmosphere cannot be isothermal, otherwise there would be no transport of radiative flux.
- Consider a Taylor expansion of the source function as a function of optical depth:

$$S_\nu(t_\nu) = \sum_{n=0}^{\infty} \frac{(t_\nu - \tau_\nu)^n}{n!} \left[\frac{d^n B_\nu[T(t_\nu)]}{dt_\nu^n}\right]_{\tau_\nu}$$

- Here, we restrict ourselves to the first 2 terms of the expansion:

$$S_\nu(t_\nu) = B_\nu(\tau_\nu) + (t_\nu - \tau_\nu) \left[\frac{d\,B_\nu[T(t_\nu)]}{dt_\nu}\right]_{\tau_\nu}$$

- The specific intensity hence becomes

$$I_\nu(\tau_\nu) = B_\nu(\tau_\nu) + \mu \left[\frac{d\,B_\nu[T(t_\nu)]}{dt_\nu}\right]_{\tau_\nu}$$

3.2 The diffusion approximation

$$I_\nu(\tau_\nu) = B_\nu(\tau_\nu) + \mu \left[\frac{d\,B_\nu[T(t_\nu)]}{dt_\nu}\right]_{\tau_\nu}$$

- We deduce: $$J_\nu = 3\,K_\nu = B_\nu$$

$$H_\nu = \frac{1}{3}\,\frac{d\,B_\nu}{d\tau_\nu} = \frac{1}{3\,\kappa_\nu\,\rho}\,\frac{d\,B_\nu}{dT}\,\frac{d\,T}{dx}$$

- Radiative energy is transported owing to the temperature gradient.
- Rosseland opacity: weighted by the flux.

$$\overline{\kappa}_R = \frac{\int \frac{d\,B_\nu}{dT}\,d\nu}{\int \frac{1}{\kappa_\nu}\,\frac{d\,B_\nu}{dT}\,d\nu}$$

- Temperature profile:

$$\frac{d\,T}{dx} = \frac{3}{16}\,\overline{\kappa}_R\,\rho\,\left(\frac{R_*}{r}\right)^2\,\left(\frac{T_{\rm eff}}{T}\right)^4\,T$$

3.3 Line blanketing

- Opacity is larger in the lines than in the continuum.
- The opacity of the lines partially blocks the radiative flux.
- Therefore, the available "bandwidth" for the radiative flux becomes narrower.
- To evacuate the radiative flux, the temperature in the part of the atmosphere where the lines form (T'_{eff}) must thus increase.

$$T_{\mathrm{eff}}^4/T'^{4}_{\mathrm{eff}} = 1 - f$$

- In the case of the Sun, "line blanketing" yields f = 0.014 which results in a difference in effective temperature of 200K compared to a hypothetic case of an identical star without spectral lines.

IV. Diagnostics from line and continuum spectra

- Use of spectral lines and properties of the continuum to infer the physical properties of the stellar atmosphere and of the star.
- Measurements of spectral lines (and their limitations).
- Link between line flux and line opacity.
- Intensity of spectral lines as a function of

1. Populations of energy levels (statistical equilibrium)
2. Temperature and pressure
3. Chemical abundances

- The influence of photospheric velocity fields on the line profiles

1. Micro and macro-turbulence
2. Stellar rotation

- Observational determination of the stellar properties

4.1 Measurements of spectral lines

- Observed spectrum = convolution of real spectrum and instrumental response:

$$D(\lambda) = \mathcal{F}(\lambda) * G(\lambda)$$

- In Fourier space:

$$d(\sigma) = f(\sigma)\, g(\sigma)$$

- The instrumental profile is determined by observing lines that are intrinsically very narrow.
- If the instrumental response is sufficiently well known, one can attempt a deconvolution (difficult in practice).

4.1 Measurements of spectral lines

- Strength of a spectral line: concept of equivalent width:

$$EW = \int_{\lambda_1}^{\lambda_2} (1 - N(\lambda))\, d\lambda = \int_{\lambda_1}^{\lambda_2} \frac{D_c(\lambda) - D(\lambda)}{D_c(\lambda)}\, d\lambda$$

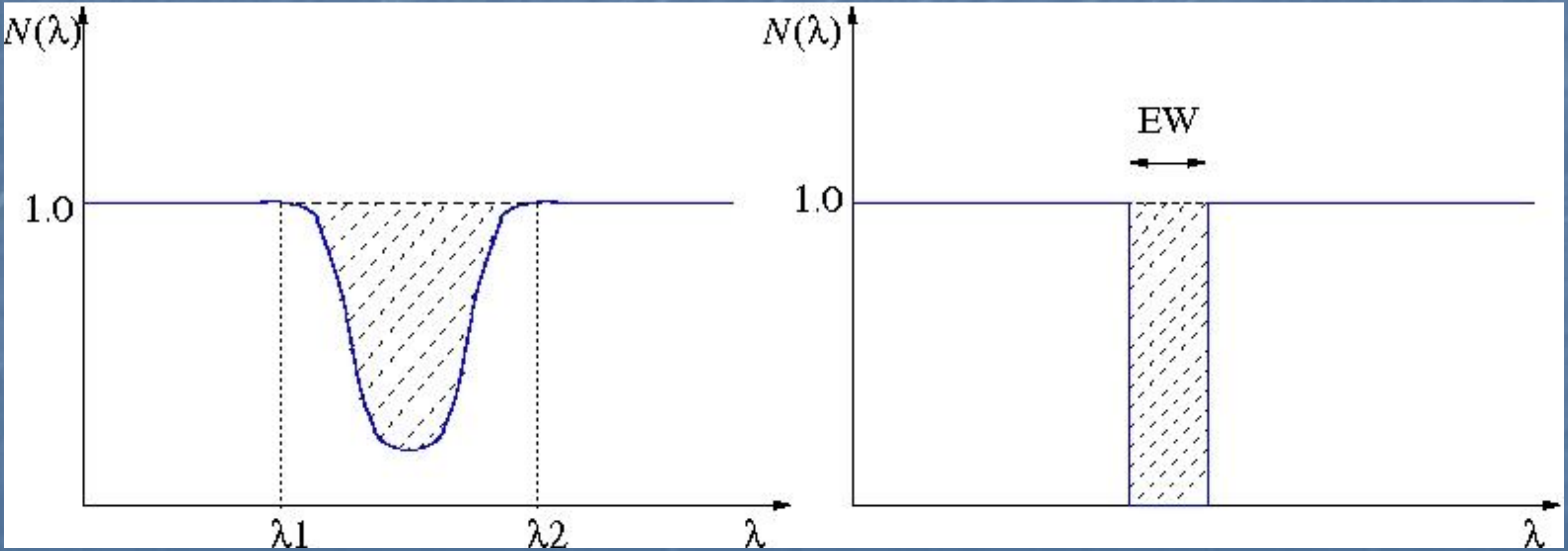

4.1 Measurements of spectral lines

- Measurement of the line position, various methods:

1. Cross-correlation with synthetic profile or spectrum of a standard star.
2. Bisector method.
3. Fit of a Gaussian.

- Measures in the air or in a vacuum: speed of light in the air $v = c/n$ where $n_0 = 1.0003$ under normal conditions of temperature and pressure.

$$\lambda_a = \frac{\lambda_v}{n} \quad \Rightarrow \quad \Delta\lambda = \lambda_a\,(n-1)$$

$$n - 1 = (n_0 - 1)\,\frac{P\,T_0}{T\,P_0}$$

4.2 Link between line flux and opacity

- Consider l_ν and κ_ν the opacities in the line and in the continuum. Consider j^l_ν and j^c_ν the emissivities of the line and continuum.
- The total optical depth becomes: $$d\tau_\nu = (l_\nu + \kappa_\nu)\,\rho\,dx$$
- The total source function writes

$$S_\nu = \frac{j^l_\nu + j^c_\nu}{l_\nu + \kappa_\nu} = \frac{\frac{l_\nu}{\kappa_\nu} S_l + S_c}{1 + \frac{l_\nu}{\kappa_\nu}} = \frac{\eta_\nu\, S_l + S_c}{1 + \eta_\nu}$$

where $$\eta_\nu = \frac{l_\nu}{\kappa_\nu}$$

- The emerging flux of a plane-parallel atmosphere becomes:

$$\mathcal{F}_\nu(\tau_\nu = 0) = 2\,\pi \int_0^\infty S_\nu\, E_2(t_\nu)\, dt_\nu$$

$$\tau_\nu = \int_0^{\tau_0} \frac{l_\nu + \kappa_\nu}{\kappa_0}\, dt_0 = \tau_l + \tau_c$$

$$\begin{aligned}\mathcal{F}_\nu &= 2\,\pi \int_0^\infty B_\nu(T)\, E_2(\tau_\nu)\, d\tau_\nu \\ &= 2\,\pi \int_0^\infty B_\nu(T)\, E_2(\tau_\nu)\, \frac{l_\nu + \kappa_\nu}{\kappa_0}\, d\tau_0\end{aligned}$$

4.2 Link between line flux and opacity

- If the source function can be described by the Eddington solution:

$$S(\tau) = \frac{3\,\mathcal{F}_\nu(0)}{4\,\pi}\left(\tau + \frac{2}{3}\right)$$

- Hence, $S(\tau_1) = \mathcal{F}_\nu(0)/\pi$ provided that $\tau_1 = 2/3$ (Eddington-Barbier relation)

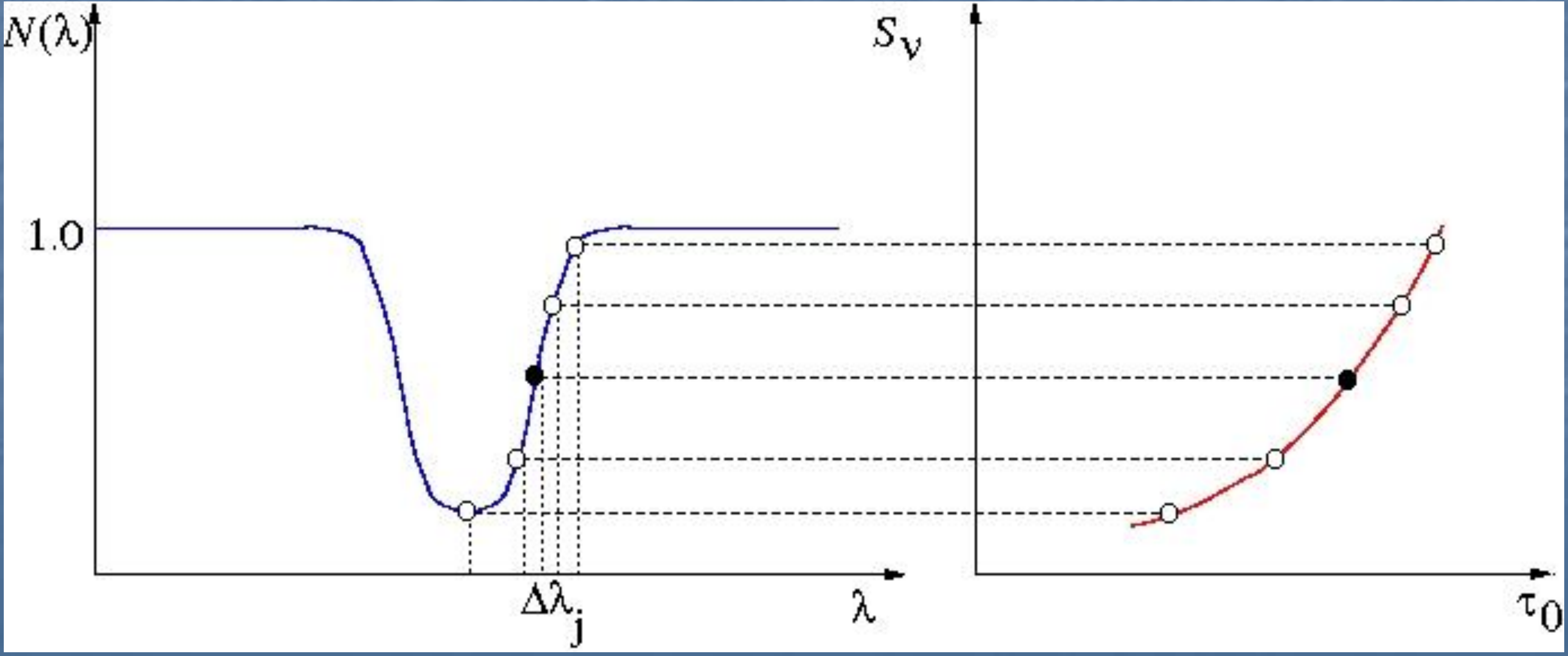

4.2 Link between line flux and opacity

$S(\tau_1) = \mathcal{F}_\nu(0)/\pi$ & $\tau_1 = 2/3$

- For a weak line, we get

$$\frac{\mathcal{F}_c - \mathcal{F}_\nu}{\mathcal{F}_c} \simeq \frac{S_\nu(\tau_c = \tau_1) - S_\nu(\tau_\nu = \tau_1)}{S_\nu(\tau_c = \tau_1)}$$

- Expanding the source function to 1st order:

$$S_\nu(\tau_\nu = \tau_1) = S_\nu(\tau_l + \tau_c = \tau_1) = S_\nu(\tau_c = \tau_1 - \tau_l) = S_\nu(\tau_c = \tau_1) - \frac{d\,S_\nu}{d\tau_c}\,\tau_l$$

- Thus,

$$\frac{\mathcal{F}_c - \mathcal{F}_\nu}{\mathcal{F}_c} \simeq \frac{\tau_l}{S_\nu(\tau_c = \tau_1)}\,\frac{d\,S_\nu}{d\tau_c} \simeq \frac{\tau_1}{S_\nu(\tau_c = \tau_1)}\,\frac{d\,S_\nu}{d\tau_c}\,\frac{l_\nu}{\kappa_\nu}$$

4.2 Link between line flux and opacity

- For very opaque lines, τ_1 is not reached inside the photosphere, but only inside the chromosphere. Temperature increases inside the chromosphere. If there is enough material in the chromosphere, one observes chromospheric emission lines:

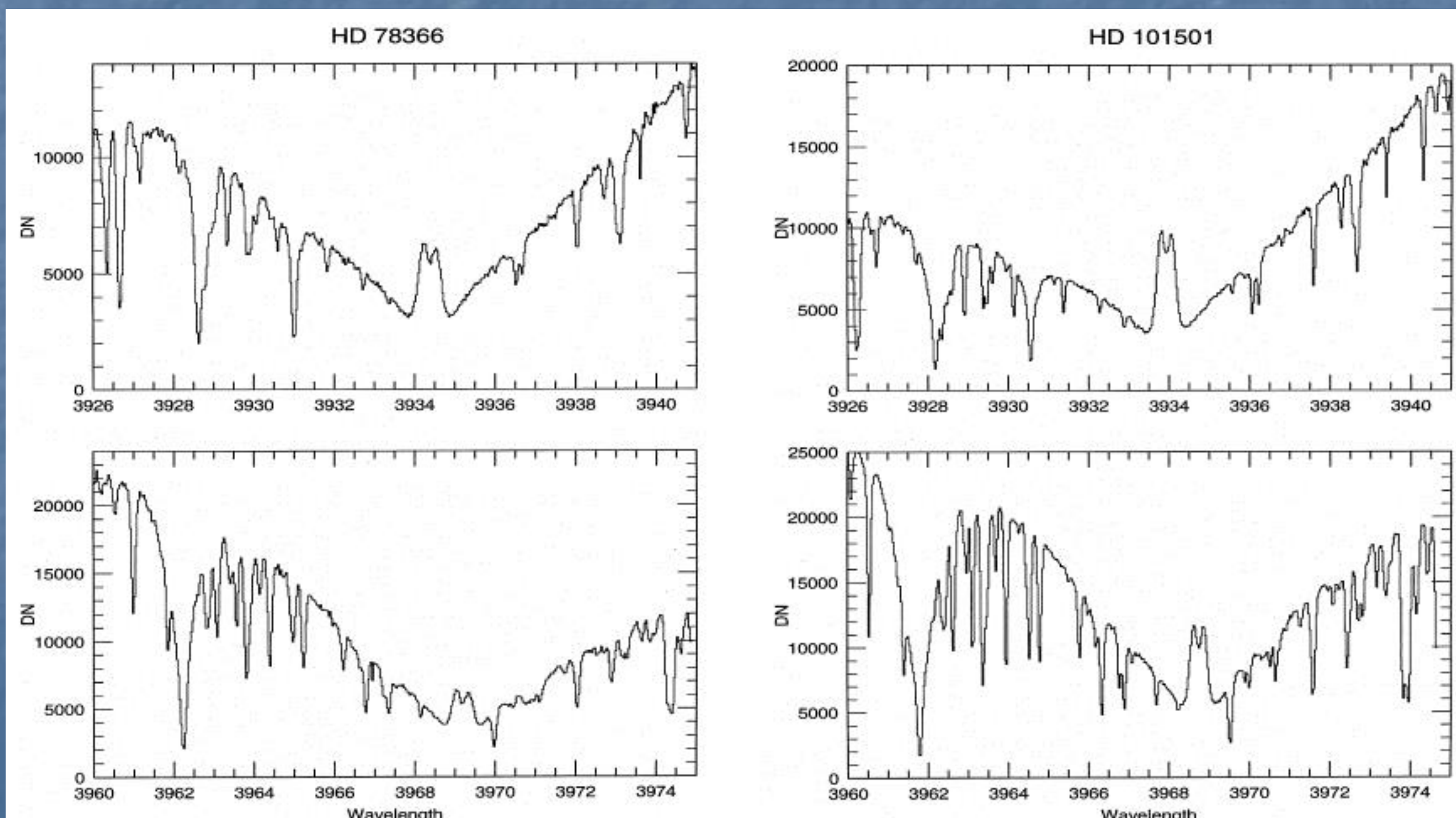

4.3 Line strength

- The strength of a line increases when the number of absorbers increases. One needs to know the populations of the atomic energy levels.
- Outside LTE conditions, we make the assumption of statistical equilibrium.
- Emission: $j^l_\nu\,\rho = N_u\,A_{u,l}\,\phi(\nu)\,h\,\nu$
- Net absorption: $l_\nu\,\rho = N_l\,B_{l,u}\,\phi(\nu)\,h\,\nu - N_u\,B_{u,l}\,\phi(\nu)\,h\,\nu$
- Source function of the line:

$$S_l = \frac{j^l_\nu}{l_\nu} = \frac{N_u\,A_{u,l}\,\phi(\nu)}{N_l\,B_{l,u}\,\phi(\nu) - N_u\,B_{u,l}\,\phi(\nu)} = \frac{2\,h\,\nu^3}{c^2}\,\frac{1}{\frac{N_l\,g_u}{N_u\,g_l} - 1}$$

- Statistical equilibrium:

$$\frac{d\,N_j}{dt} = \sum_{i=1}^{M}(N_i\,P_{i,j} - N_j\,P_{j,i}) = 0 \qquad i \neq j, j = 1, \ldots, M$$

4.3 Line strength

- Statistical equilibrium: *M* linearly dependent equations, underdetermined system.

$$\frac{d\,N_j}{dt} = \sum_{i=1}^{M}(N_i\,P_{i,j} - N_j\,P_{j,i}) = 0 \qquad i \neq j, j = 1, \ldots, M$$

- Transition rates:

$$\begin{aligned}
P_{i,j} &= 4\,\pi\,A_{i,j} + 4\,\pi\,B_{i,j}\int_0^\infty J_\nu\,\phi(\nu)\,d\nu + c_{i,j} && \text{for} \quad i > j \\
P_{i,j} &= 4\,\pi\,B_{i,j}\int_0^\infty J_\nu\,\phi(\nu)\,d\nu + c_{i,j} && \text{for} \quad i < j \\
P_{j,i} &= 4\,\pi\,A_{j,i} + 4\,\pi\,B_{j,i}\int_0^\infty J_\nu\,\phi(\nu)\,d\nu + c_{j,i} && \text{for} \quad i < j \\
P_{j,i} &= 4\,\pi\,B_{j,i}\int_0^\infty J_\nu\,\phi(\nu)\,d\nu + c_{j,i} && \text{for} \quad i > j
\end{aligned}$$

- Closure condition:

$$\sum_j N_j = N_{\text{total}}$$

- One usually suppresses the equation relative to the ground level.

4.3 Line strength

- I_ν depends on S_ν which depends on the populations N_u, N_l which in turn are set by the equations of statistical equilibrium that involve J_ν
- This problem must be solved in an iterative way.
- Λ operator

$$J_\nu = \frac{1}{2}\left[\int_{\tau_\nu}^{\infty} S_\nu\, E_1(t_\nu - \tau_\nu)\, dt_\nu + \int_0^{\tau_\nu} S_\nu\, E_1(\tau_\nu - t_\nu)\, dt_\nu\right] = \Lambda_{\tau_\nu}(S_\nu)$$

- Λ iterations
- Simplifications such as grouping some energy levels into "superlevels" and linearization of the Λ operator.

4.3 Line strength

- Numerical implementation of Λ iterations: the Feautrier method
- The equations of radiative transfer are discretized on a grid of nodes in optical depth τ (index i) and $\mu = \cos\theta$ (index j): for instance

$$J_\nu = \frac{1}{2} \sum_{j=1}^{m} w_j \, I_j$$

- The transfer equation is split into two parts

$$\mu \, \frac{d\, I_\nu}{d\tau_\nu} = I_\nu - S_\nu \quad \Rightarrow \quad \begin{aligned} \mu \, \frac{d\, I_\nu^{\mathrm{out}}}{d\tau_\nu} &= I_\nu^{\mathrm{out}} - S_\nu \\ -\mu \, \frac{d\, I_\nu^{\mathrm{in}}}{d\tau_\nu} &= I_\nu^{\mathrm{in}} - S_\nu \end{aligned}$$

- With $\mu \geq 0$ and the boundary conditions: $I_\nu^{\mathrm{in}}(\tau = 0) = 0$

$$I_\nu^{\mathrm{out}}(\tau = +\infty) = 0$$

4.3 Line strength

- One introduces new variables:

$$
\begin{aligned}
P_\nu(\mu) &= \frac{1}{2}\left[I_\nu^{\mathrm{out}}(\mu) + I_\nu^{\mathrm{in}}(\mu)\right] \\
R_\nu(\mu) &= \frac{1}{2}\left[I_\nu^{\mathrm{out}}(\mu) - I_\nu^{\mathrm{in}}(\mu)\right]
\end{aligned}
$$

- The transfer equation yields

$$
\begin{aligned}
\mu \frac{d\, I_\nu^{\mathrm{out}}}{d\tau_\nu} &= I_\nu^{\mathrm{out}} - S_\nu \\
-\mu \frac{d\, I_\nu^{\mathrm{in}}}{d\tau_\nu} &= I_\nu^{\mathrm{in}} - S_\nu
\end{aligned}
\quad \Rightarrow \quad
\begin{aligned}
\mu \frac{d\, R_\nu}{d\tau_\nu} &= P_\nu - S_\nu \\
\mu \frac{d\, P_\nu}{d\tau_\nu} &= R_\nu
\end{aligned}
$$

- Hence the 2nd degree equation in P_ν:

$$
\mu^2 \frac{d^2\, P_\nu}{d\tau_\nu^2} = P_\nu - S_\nu
$$

$$
\begin{aligned}
\mu \frac{d\, P_\nu}{d\tau_\nu}(\tau = 0) &= P_\nu(\tau = 0) \\
\mu \frac{d\, P_\nu}{d\tau_\nu}(\tau = \infty) &= -P_\nu(\tau = \infty)
\end{aligned}
$$

4.3 Line strength

$$\mu^2 \frac{d^2 P_\nu}{d\tau_\nu^2} = P_\nu - S_\nu$$

- This equation is discretized as

$$W(i,i-1)^j \, P_{i-1}^j + W(i,i)^j \, P_i^j + W(i,i+1)^j \, P_{i+1}^j = S_i$$

$$\underline{\underline{\mathbf{W}}}^{\mathbf{j}} \, \vec{\mathbf{P}}^{\mathbf{j}} = \vec{\mathbf{S}}$$

- Tri-diagonal matrix equation, resolution straightforward.
- Numerical Λ iteration:

1. Start with an initial estimate of the source function $S_\nu^{(0)} = B_\nu(T)$
2. At each iteration, compute $J_\nu^{(k)}(\tau_\nu) = \Lambda_{\tau_\nu}[S_\nu^{(k)}]$
3. Use the mean intensity to solve the equations of statistical equilibrium and compute a new approximation of the source function.

4.3 Line strength

- The temperature is a key parameter for the strength of a line.
- If continuum absorption is dominated by the negative hydrogen ion:

$$\kappa_{bf}(\mathrm{H}^-) \propto \alpha_{bf}(\mathrm{H}^-)\, P_e\, T^{-5/2}\, \exp\left[\frac{0.754}{k\,T}\right]$$

- Consider a line of an ion Z^y where Z^y is the dominating ionization state of the species Z. $N_l \propto \exp\left(-\frac{\chi_l}{kT}\right)$

$$\Rightarrow \quad \eta_\nu \propto P_e^{-1}\, T^{5/2}\, \exp\left[-\frac{\chi_l + 0.754}{k\,T}\right] \qquad P_e \propto \exp(\Omega\, T)$$

$$\Rightarrow \quad \frac{1}{\eta_\nu}\frac{d\,\eta_\nu}{dT} = \frac{5}{2}\frac{1}{T} + \frac{\chi_l + 0.754}{k\,T^2} - \Omega$$

$$\Rightarrow \quad \frac{1}{\eta_\nu}\frac{\partial\,\eta_\nu}{\partial P_e} = -\frac{1}{P_e}$$

- The strength of the line decreases as pressure increases.

4.3 Line strength

$$\kappa_{bf}(\mathrm{H}^-) \propto \alpha_{bf}(\mathrm{H}^-)\, P_e\, T^{-5/2}\, \exp\left[\frac{0.754}{k\,T}\right]$$

- Consider a line of an ion Z^y where Z^{y+1} is the dominant ionization of the species Z. $N_l \propto T^{-5/2}\, P_e\, \exp\left(\frac{I-\chi_l}{kT}\right)$

$$\Rightarrow \quad \eta_\nu \propto \exp\left[\frac{I - \chi_l - 0.754}{k\,T}\right]$$

$$\Rightarrow \quad \frac{1}{\eta_\nu}\frac{d\,\eta_\nu}{dT} = \frac{\chi_l + 0.754 - I}{k\,T^2}$$

- The line strength does not depend on pressure.

4.3 Line strength

$$\kappa_{bf}(\mathrm{H}^-) \propto \alpha_{bf}(\mathrm{H}^-)\, P_e\, T^{-5/2}\, \exp\,[\frac{0.754}{k\,T}]$$

- Consider finally, a line of an ion Z^y where Z^{y-1} is the dominant ionization state of species Z. $N_l \propto T^{5/2}\, P_e^{-1}\, \exp\,(-\frac{I+\chi_l}{kT})$

$$\Rightarrow \quad \eta_\nu \propto P_e^{-2}\, T^5\, \exp\,[-\frac{I + \chi_l + 0.754}{k\,T}]$$

$$\Rightarrow \quad \frac{1}{\eta_\nu}\frac{d\,\eta_\nu}{dT} = \frac{5}{T} + \frac{I + \chi_l + 0.754}{k\,T^2} - 2\,\Omega$$

$$\Rightarrow \quad \frac{1}{\eta_\nu}\frac{\partial\,\eta_\nu}{\partial P_e} = -\frac{2}{P_e}$$

- The line strength decreases strongly with increasing pressure.

4.3 Line strength

- If the continuum absorption is dominated by the ionization of neutral hydrogen:

$$\kappa_{bf}(\mathrm{H}, n) \propto \alpha_{bf}(\mathrm{H}, n)\ \exp\left[\frac{-\chi_n}{k\,T}\right]$$

- Consider the same situations as previously: a line of ion Z^y where Z^y is the dominating ionization state of species Z.

$$N_l \propto \exp\left(-\frac{\chi_l}{kT}\right)$$

$$\Rightarrow \qquad \eta_\nu \propto \exp\left[-\frac{\chi_l - \chi_n}{k\,T}\right]$$

$$\Rightarrow \qquad \frac{1}{\eta_\nu}\frac{d\,\eta_\nu}{dT} = \frac{\chi_l - \chi_n}{k\,T^2}$$

- The line strength is independent of pressure.

4.3 Line strength

$$\kappa_{bf}(\mathrm{H}, n) \propto \alpha_{bf}(\mathrm{H}, n) \; \exp\,[\frac{-\chi_n}{k\,T}]$$

- Line of an ion Z^y where Z^{y+1} is the dominant ionization state.

$$N_l \propto T^{-5/2}\, P_e \, \exp\,(\frac{I-\chi_l}{kT})$$

$$\Rightarrow \quad \eta_\nu \propto T^{-5/2}\, P_e \, \exp\,[\frac{I+\chi_n-\chi_l}{k\,T}]$$

$$\Rightarrow \quad \frac{1}{\eta_\nu}\frac{d\,\eta_\nu}{dT} = -\frac{5}{2}\frac{1}{T} - \frac{I+\chi_n-\chi_l}{k\,T^2} + \Omega$$

$$\Rightarrow \quad \frac{1}{\eta_\nu}\frac{\partial\,\eta_\nu}{\partial P_e} = \frac{1}{P_e}$$

- Line strength increases with pressure.

4.3 Line strength

$$\kappa_{bf}(\mathrm{H}, n) \propto \alpha_{bf}(\mathrm{H}, n)\ \exp\left[\frac{-\chi_n}{k\,T}\right]$$

- Consider a line of ion Z^y where Z^{y-1} is the dominant ionization state of species Z.

$$N_l \propto T^{5/2}\, P_e^{-1}\ \exp\left(-\frac{I+\chi_l}{kT}\right)$$

$$\Rightarrow \quad \eta_\nu \propto P_e^{-1}\, T^{5/2}\ \exp\left[-\frac{I + \chi_l - \chi_n}{k\,T}\right]$$

$$\Rightarrow \quad \frac{1}{\eta_\nu}\frac{d\,\eta_\nu}{dT} = \frac{5}{2}\frac{1}{T} + \frac{I + \chi_l - \chi_n}{k\,T^2} - \Omega$$

$$\Rightarrow \quad \frac{1}{\eta_\nu}\frac{\partial\,\eta_\nu}{\partial P_e} = -\frac{1}{P_e}$$

- The line strength decreases with increasing pressure.
- In B, A, and F stars, the hydrogen lines are broadened by the linear Stark effect (proportional to the electron pressure). The lines are stronger in stars of lower luminosity.

4.3 Line strength

- The strength of a line generally increases with the abundance of the element.

$$l_\nu \, \rho = \frac{\pi \, e^2}{m \, c} \, f_{l,u} \, N_l \, [1 - \exp\left(-h\,\nu/k\,T\right)] \, H(a,v)$$

H(a,v): Voigt – Hjerting function: $v = \Delta\,\nu/\Delta\,\nu_D, \; a = \Gamma/(4\,\pi\,\Delta\,\nu_D)$

- In LTE: $\mathcal{F}_\nu = 2\,\pi \int_0^\infty B_\nu[T(\tau_c)] \, E_2\left(\int_0^{\tau_c} (1+\eta_\nu)\,dt\right) (1+\eta_\nu)\,d\tau_c$

- Consider a model atmosphere with a linear dependence of the source function on optical depth:

$$B_\nu[T(\tau_c)] = B_0 + B_1\,\tau_c$$

$$\Rightarrow \quad \mathcal{F}_\nu = 2\,\pi \int_0^\infty (B_0 + B_1\,\tau_c)\, E_2[(1+\eta_\nu)\,\tau_c]\,(1+\eta_\nu)\,d\tau_c = \pi\left(B_0 + \frac{2}{3}\,\frac{B_1}{1+\eta_\nu}\right)$$

$$\Rightarrow \quad \mathcal{A}_\nu = \frac{\mathcal{F}_c - \mathcal{F}_\nu}{\mathcal{F}_c} = \frac{\eta_\nu}{1+\eta_\nu}\,\frac{1}{1+\frac{3\,B_0}{2\,B_1}}$$

$\Rightarrow$ When η tends towards infinity: $\mathcal{A}_0 = \frac{1}{1+\frac{3\,B_0}{2\,B_1}}$

4.3 Line strength

$$\mathcal{A}_\nu = \frac{\mathcal{F}_c - \mathcal{F}_\nu}{\mathcal{F}_c} = \frac{\eta_\nu}{1+\eta_\nu}\,\frac{1}{1+\frac{3\,B_0}{2\,B_1}}$$ & $$\mathcal{A}_0 = \frac{1}{1+\frac{3\,B_0}{2\,B_1}}$$ $\Rightarrow$ $$\mathcal{A}_\nu = \frac{\mathcal{A}_0\,\eta_\nu}{1+\eta_\nu}$$

- The equivalent width becomes:

$$\begin{aligned} EW &= 2\,\mathcal{A}_0\,\Delta\nu_D \int_0^\infty \frac{\eta_\nu}{1+\eta_\nu}\,dv \\ &= 2\,\mathcal{A}_0\,\Delta\nu_D \int_0^\infty \frac{\eta_0\,H(a,v)}{1+\eta_0\,H(a,v)}\,dv \end{aligned}$$

- Curve of growth:

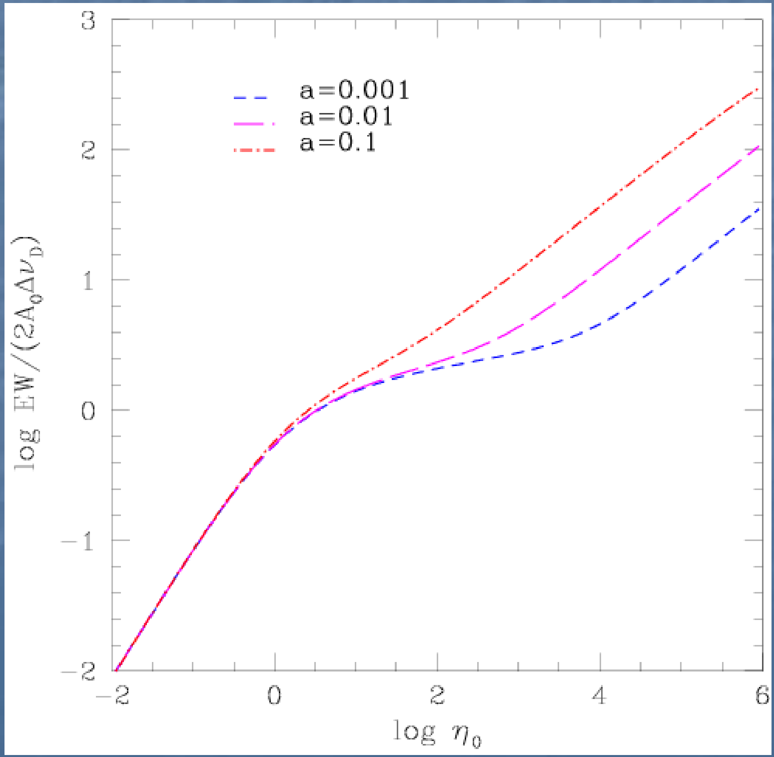

4.3 Line strength

- Curve of growth:

1. Linear increase of EW with the number of particles (Doppler core of the line gets deeper).
2. Saturation: opacity in the core reaches its maximum value.
3. Increase as the square root of the number of particles (increase of the wings of the line).

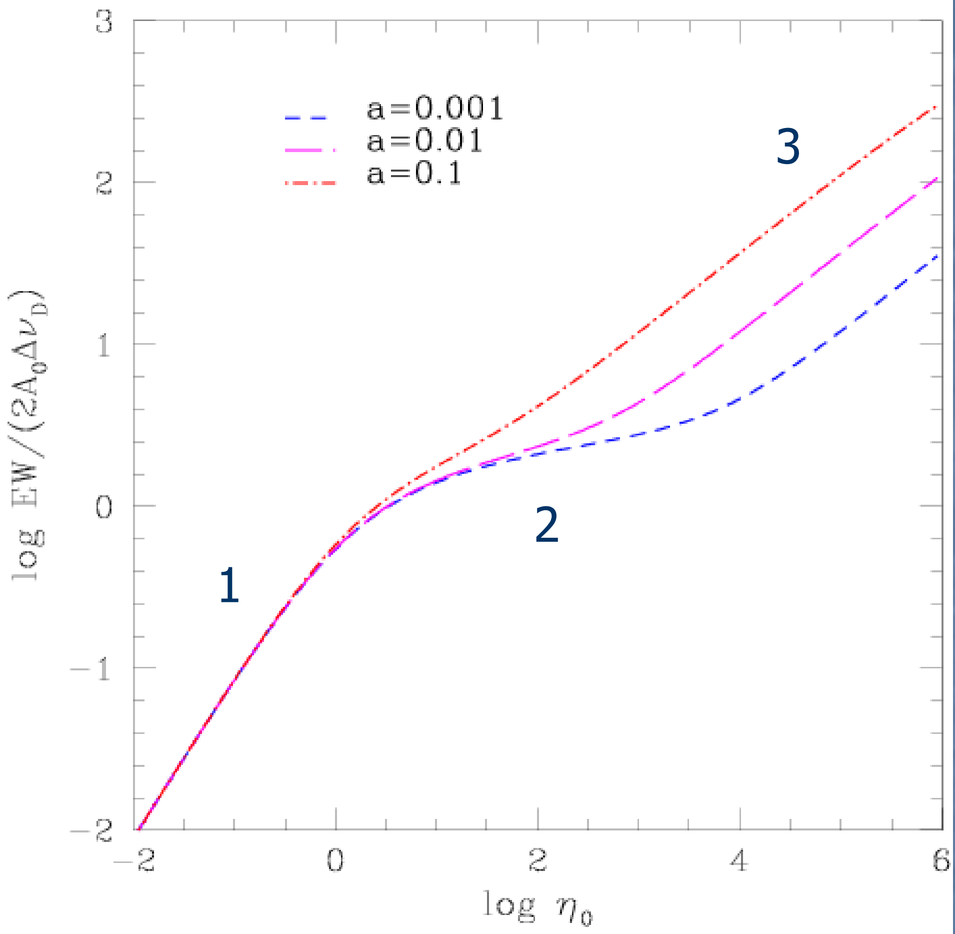

4.3 Line strength

- Other way to illustrate the concept of curve of growth: suppose the line forms in a reversal layer above the region where the continuum is formed $\Rightarrow$ $\mathcal{F}_\nu = \mathcal{F}_c \exp(-\tau_\nu)$

  with $$\tau_\nu = \int_0^L l_\nu\, \rho\, dx = \int_0^L N_l\, \alpha\, dx = A_Z \int_0^L \frac{N_l}{N_Z} N_H\, \alpha\, dx$$

- For a low number of absorbing particles, the optical depth is small and one finds: $\mathcal{F}_\nu \simeq \mathcal{F}_c (1 - \tau_\nu)$
- When the wings get important:

$$\alpha \simeq \left(\frac{\pi e^2}{m c}\right) \left(\frac{\gamma}{4\pi^2}\right) \frac{f}{\Delta\nu^2} \quad \Rightarrow \quad \begin{aligned} \tau_\nu &= \frac{\pi e^2}{m c} \frac{A_Z f}{\Delta\nu^2} \int_0^L \frac{N_l}{N_Z} N_H \frac{\gamma}{4\pi^2} dx \\ \mathcal{A}_\nu &= \frac{\mathcal{F}_c - \mathcal{F}_\nu}{\mathcal{F}_c} = 1 - \exp(-\tau_\nu) \end{aligned}$$

$$\Rightarrow \quad \begin{aligned} EW &= \int \mathcal{A}_\nu\, d\nu = \int (1 - \exp[-C <\gamma> A_Z f/\Delta\nu^2])\, d\nu \\ &= \left(\int (1 - \exp[-u^{-2}])\, du\right) (C <\gamma> A_Z f)^{1/2} \end{aligned}$$

4.4 Photospheric velocity fields

- Photospheric velocity fields can be classified into several categories.

1. Apparently chaotic motion: micro- and macro-turbulence.
2. Radial and non-radial pulsations (see lectures on *Astro-seismology* or *Variable Stars*)
3. Rotation of the star about its axis.

4.4.1 Micro- and macro-turbulence

- The Sun: spatial resolution allows distinguish granulation due to motion in the upper part of the convective zone. Brighter regions = ascending hot material, darker regions = cooler, descending material.

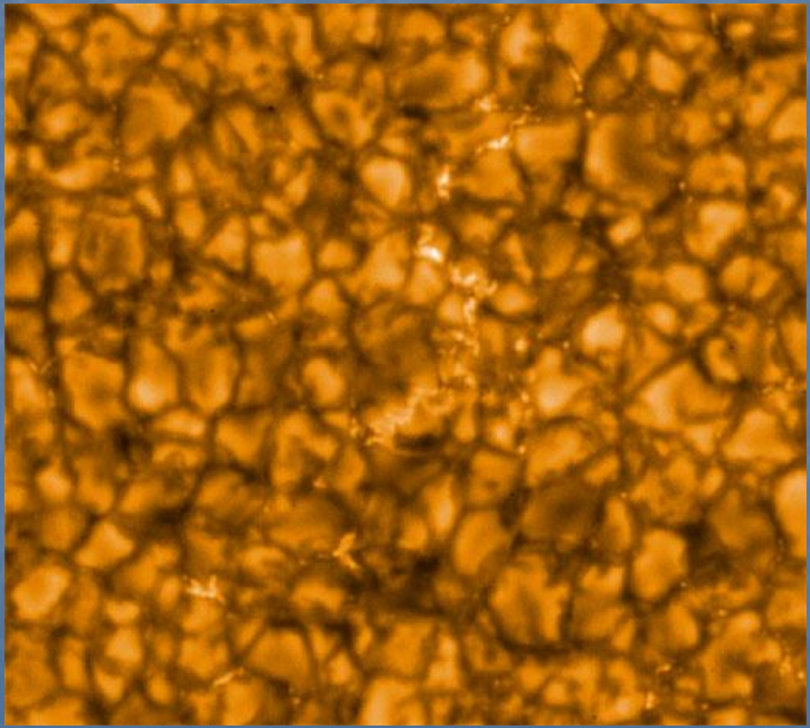

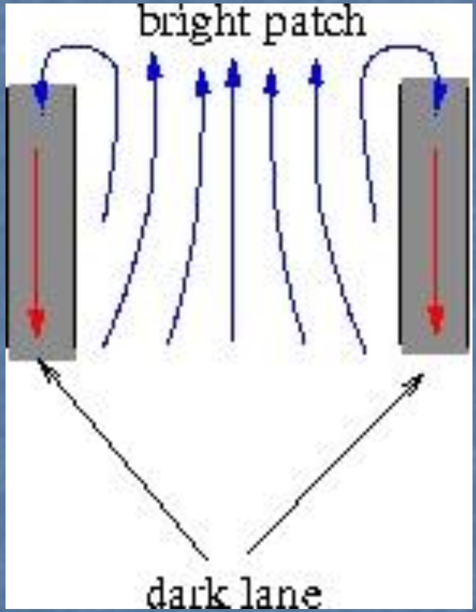

- The velocity field of the Sun's non-radial pulsations are superposed to these motions.

4.4.1 Micro- and macro-turbulence

- Red Supergiant Antares: resolved with VLTI

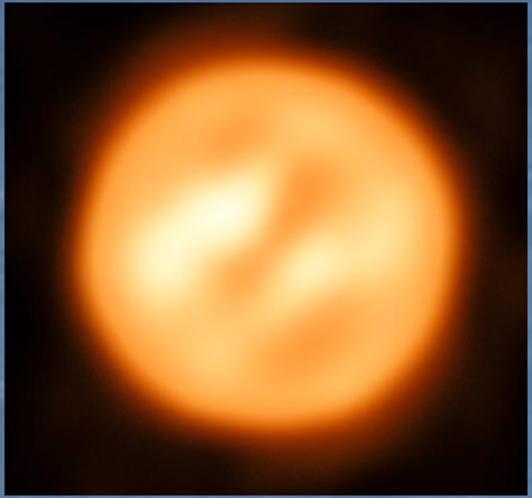

- Continuum and CO lines yield different pictures:

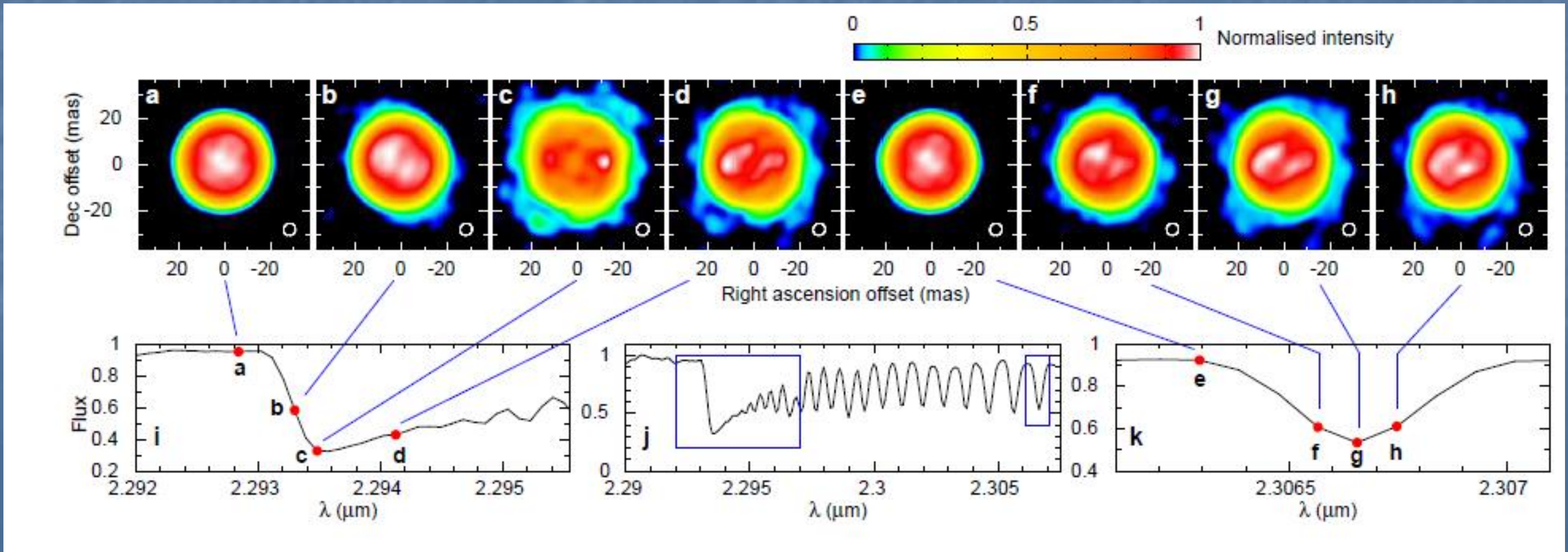

4.4.1 Micro- and macro-turbulence

- Detailed investigation of Antares reveals complex (large-scale) turbulent motion in the extended parts of the stellar atmosphere:

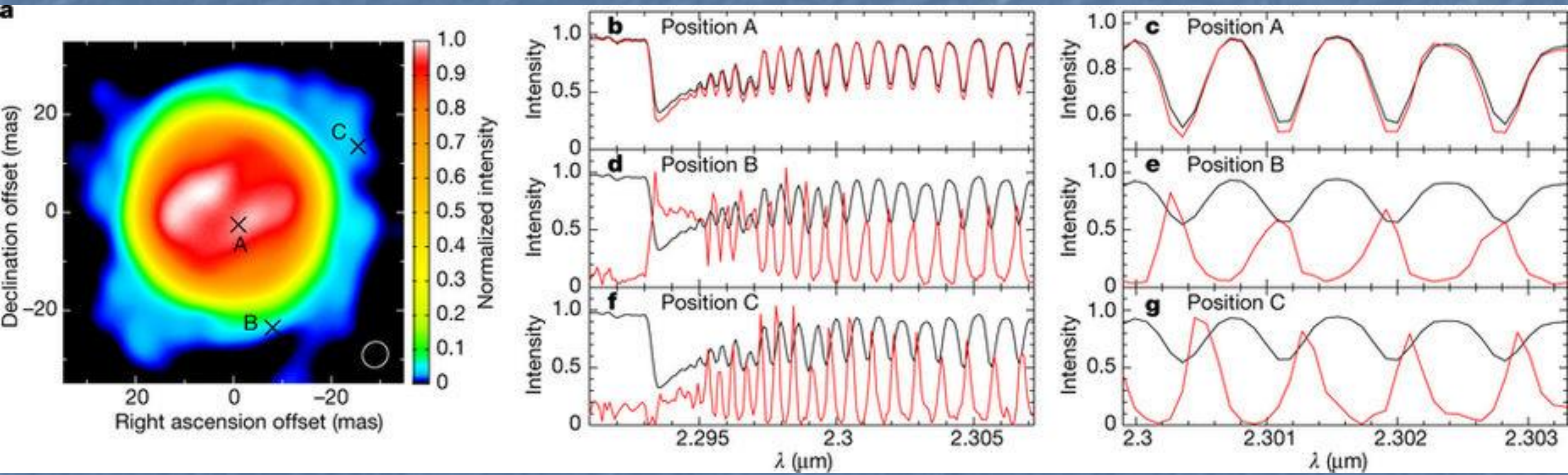

4.4.1 Micro- and macro-turbulence

- Other stars: the individual granulation cells cannot be resolved, but the effect of the velocity field on the line profiles can be measured.
- One distinguishes

1. micro-turbulence ("turbulent elements" are small compared to the length corresponding to $\tau = 1$), e.g. Alfvèn waves. Micro-turbulence broadens the line profiles (Gaussian of width a few km s^{-1}).
2. macro-turbulence ("turbulent elements" are of comparable size to the length corresponding to $\tau = 1$). In this case, each "turbulent element" produces its own spectrum, shifted in wavelength by the corresponding Doppler shift.

These motions do not necessarily correspond to genuine hydrodynamic turbulence, but may arise from the combination of motions of different origins.

4.4.1 Micro- and macro-turbulence

- One of the consequences of macro-turbulence due to granulation: “C-shape” of photospheric lines (bi-sector shifted by about 100 m s^{-1} between the wings and the core of the line).

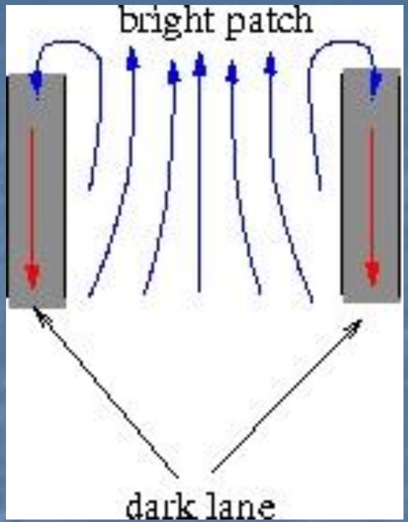

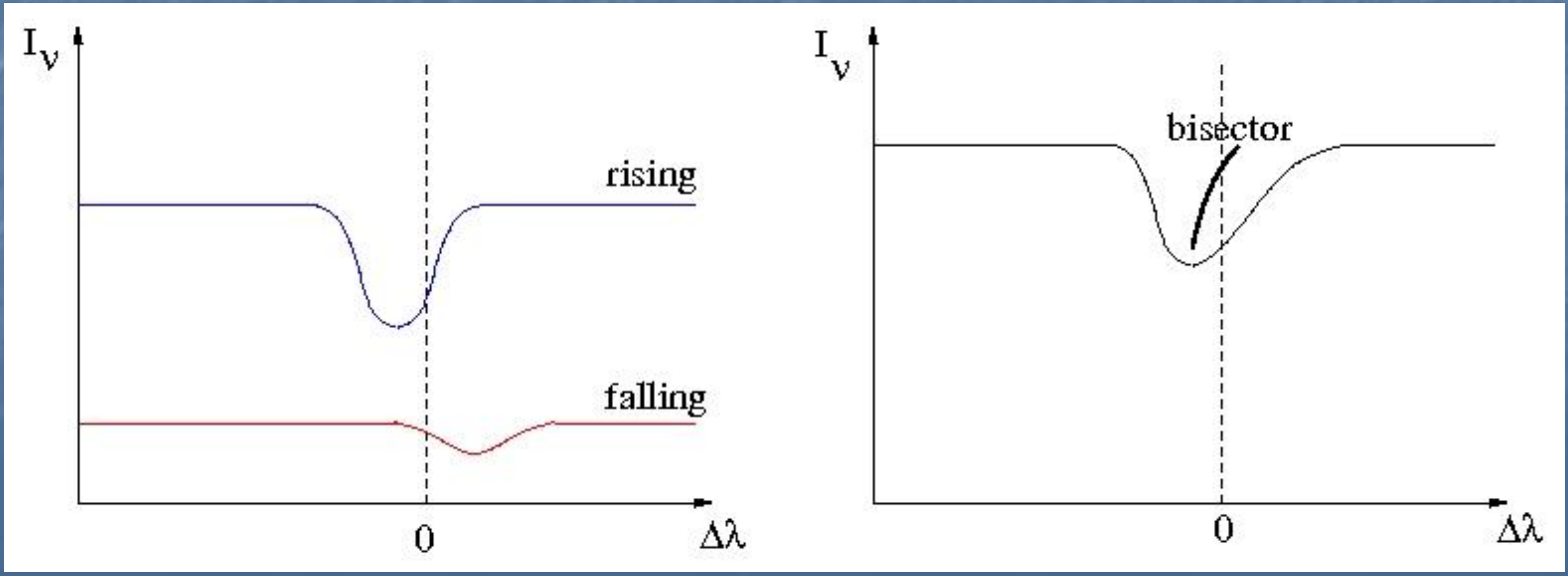

4.4.1 Micro- and macro-turbulence

- Let $\Theta(\Delta\lambda)$ be the fraction of the photons emitted in an interval shifted by a Doppler shift $\Delta\lambda$.

$$\Rightarrow \quad \mathcal{F}_\nu = \oint I_\nu * \Theta(\Delta\lambda)\, \cos\theta \, d\omega$$

I_ν is the specific intensity in the absence of macro-turbulence.

- Suppose that the macro-turbulent cells follow a Gaussian distribution of standard deviation v_0:

$$N(\Delta\lambda)\, d\Delta\lambda = \frac{1}{\sqrt{\pi}\,\zeta_0\, \cos\theta} \exp\left[-\left(\frac{\Delta\lambda}{\zeta_0\, \cos\theta}\right)^2\right] d\Delta\lambda \qquad \zeta_0 = \frac{\lambda\, v_0}{c}$$

- Model of purely radial or tangential macro-turbulence: velocity of a cell is either radial (fraction A_R) or tangential ($A_T = 1 - A_R$):

$$\begin{aligned}\Theta(\Delta\lambda) &= A_R\,\Theta_R(\Delta\lambda) + A_T\,\Theta_T(\Delta\lambda) \\ &= \frac{A_R}{\sqrt{\pi}\,\zeta_R\, \cos\theta} \exp\left[-\left(\frac{\Delta\lambda}{\zeta_R\, \cos\theta}\right)^2\right] + \frac{A_T}{\sqrt{\pi}\,\zeta_T\, \sin\theta} \exp\left[-\left(\frac{\Delta\lambda}{\zeta_T\, \sin\theta}\right)^2\right]\end{aligned}$$

4.4.1 Micro- and macro-turbulence

$$\begin{aligned}\Theta(\Delta\lambda) &= A_R\,\Theta_R(\Delta\lambda) + A_T\,\Theta_T(\Delta\lambda)\\ &= \frac{A_R}{\sqrt{\pi}\,\zeta_R\,\cos\theta}\,\exp\left[-\left(\frac{\Delta\lambda}{\zeta_R\,\cos\theta}\right)^2\right] + \frac{A_T}{\sqrt{\pi}\,\zeta_T\,\sin\theta}\,\exp\left[-\left(\frac{\Delta\lambda}{\zeta_T\,\sin\theta}\right)^2\right]\end{aligned}$$

$$\Rightarrow \mathcal{F}_\nu = 2\,\pi\left[A_R\int_0^{\pi/2}\Theta_R(\Delta\lambda) * I_\nu\,\sin\theta\,\cos\theta\,d\theta + A_T\int_0^{\pi/2}\Theta_T(\Delta\lambda) * I_\nu\,\sin\theta\,\cos\theta\,d\theta\right]$$

$$\begin{aligned}\mathcal{F}_\nu &= 2\,\pi\,I_\nu * \left[A_R\int_0^{\pi/2}\Theta_R(\Delta\lambda)\,\sin\theta\,\cos\theta\,d\theta + A_T\int_0^{\pi/2}\Theta_T(\Delta\lambda)\,\sin\theta\,\cos\theta\,d\theta\right]\\ &= \frac{2\,\pi\,I_\nu}{\sqrt{\pi}} * \left[\frac{A_R}{\zeta_R}\int_0^{\pi/2}\exp\left[-\left(\frac{\Delta\lambda}{\zeta_R\,\cos\theta}\right)^2\right]\sin\theta\,d\theta + \frac{A_T}{\zeta_T}\int_0^{\pi/2}\exp\left[-\left(\frac{\Delta\lambda}{\zeta_T\,\sin\theta}\right)^2\right]\cos\theta\,d\theta\right]\\ &= \pi\,I_\nu * M(\Delta\lambda)\end{aligned}$$

with

$$M(\Delta\lambda) = \frac{2\,A_R\,\Delta\lambda}{\sqrt{\pi}\,\zeta_R^2}\int_0^{\zeta_R/\Delta\lambda}\exp\left(-1/u^2\right)du + \frac{2\,A_T\,\Delta\lambda}{\sqrt{\pi}\,\zeta_T^2}\int_0^{\zeta_T/\Delta\lambda}\exp\left(-1/u^2\right)du$$

if $\zeta_R = \zeta_T = \zeta$, then: $M(\Delta\lambda) = \frac{2\,\Delta\lambda}{\sqrt{\pi}\,\zeta^2}\int_0^{\zeta/\Delta\lambda}\exp\left(-1/u^2\right)du$

4.4.1 Micro- and macro-turbulence

$$\mathcal{F}_\nu = \pi I_\nu * M(\Delta\lambda)$$

$$M(\Delta\lambda) = \frac{2\,\Delta\lambda}{\sqrt{\pi}\,\zeta^2}\int_0^{\zeta/\Delta\lambda} \exp(-1/u^2)\,du \Rightarrow$$

$$m(\sigma) = 2\int_0^\infty M(\Delta\lambda)\,\cos(2\pi\,\Delta\lambda\,\sigma)\,d(\Delta\lambda)$$

$$m(\sigma) = \frac{1-\exp[-(\pi\,\zeta\,\sigma)^2]}{(\pi\,\zeta\,\sigma)^2}$$

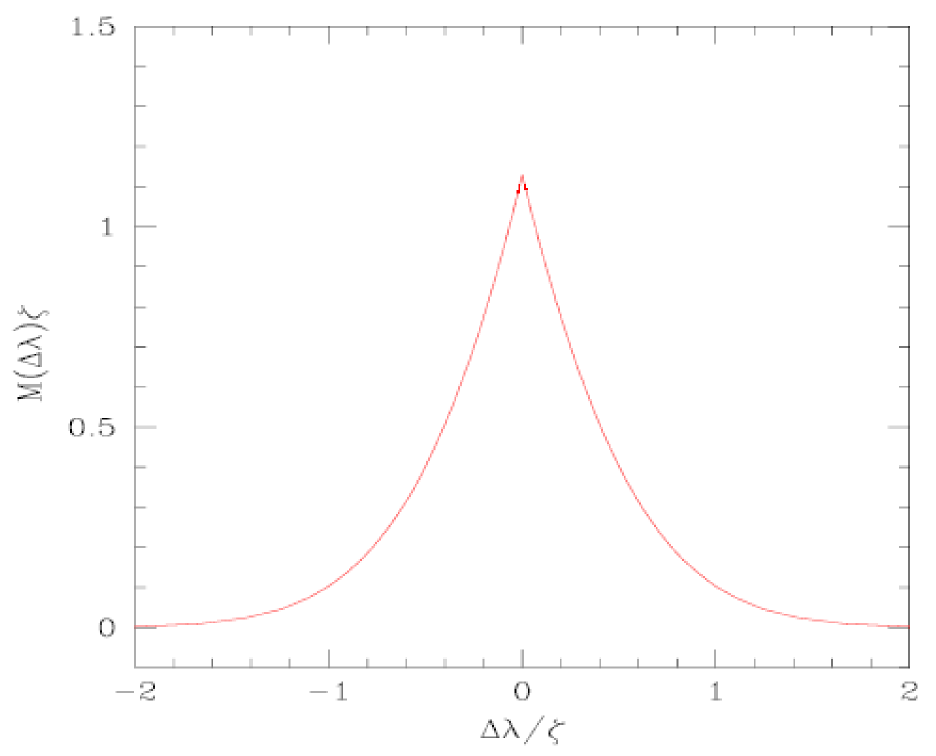

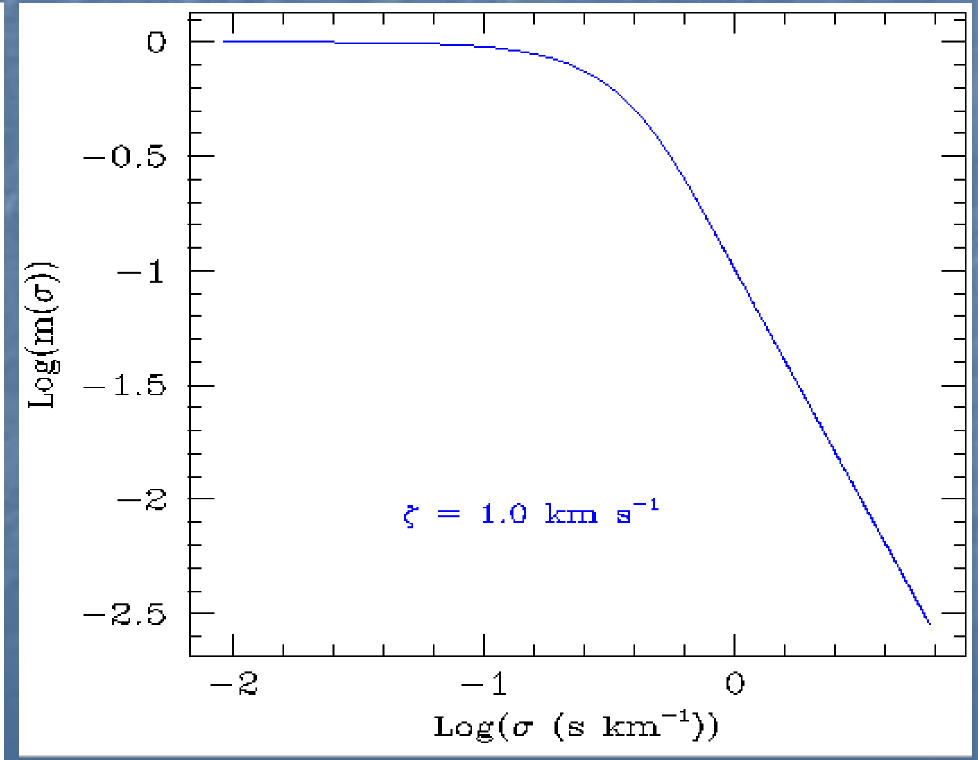

4.4.2 Rotation

- Stellar rotation velocities range between a few km s^{-1} and several hundred km s^{-1}.
- Sun: angular velocity depends on the latitude (differential rotation).
- Rotation modifies the shape of a star, leading to a non uniform distribution of the surface gravity and hence the surface temperature (gravitational darkening effect).

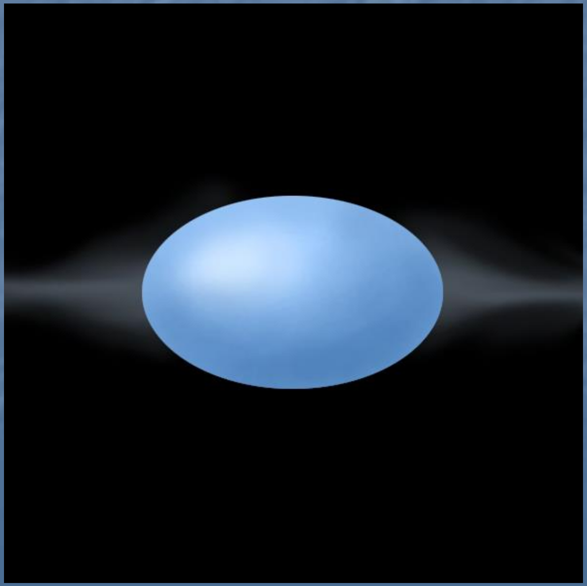

Example: Achernar (α Eri, B6Vep), rotational velocity = 250 km/s

4.4.2 Rotation

- In principle, one has to discretize the stellar surface into a grid of points with different temperatures and gravities, and to compute the specific intensity in each point according to its parameters.

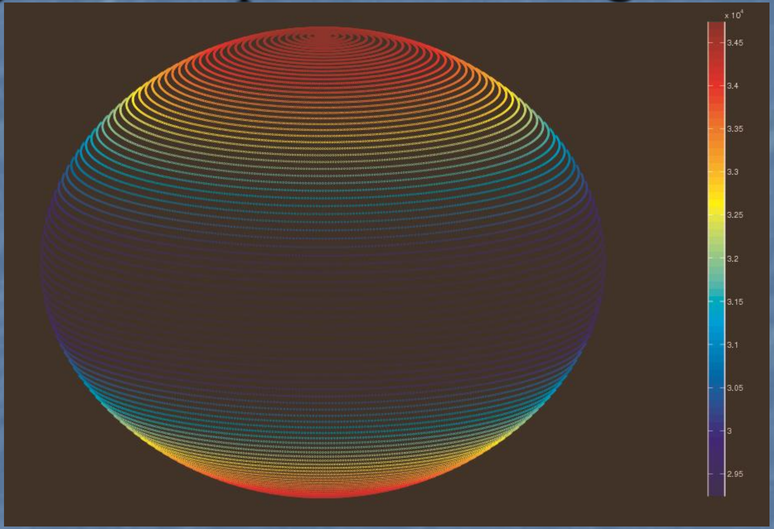

- Here, we consider the simpler (idealized) situation of stellar surface rotating as a solid body.
- In each point of the surface $\vec{R}$ (x, y, z), one can thus write:

$$\vec{v} = \vec{\Omega} \wedge \vec{R}$$

where $\vec{\Omega}$ is a constant vector.

4.4.2 Rotation

$$\vec{v} = \vec{\Omega} \wedge \vec{R}$$

$$\Rightarrow \quad v_z = y\,\Omega_x - x\,\Omega_y$$

- $\Omega_x = 0$ and $\Omega_y = \Omega \sin i$
- Let us consider the radial velocity (positive for receding motion)

$$\Rightarrow \quad v_z = x\,\Omega\,\sin i$$

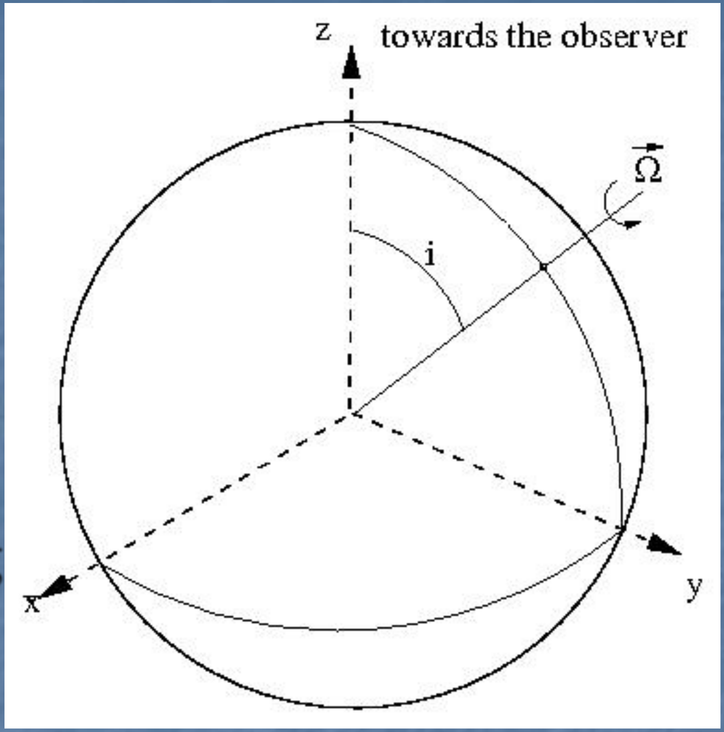

- One has to evaluate the flux at a wavelength shifted by the Doppler shift corresponding to the local value of *x*.

4.4.2 Rotation

- One has to evaluate the flux at a wavelength shifted by the Doppler shift corresponding to the local value of *x*.

$$v_z = x\,\Omega\,\sin i$$

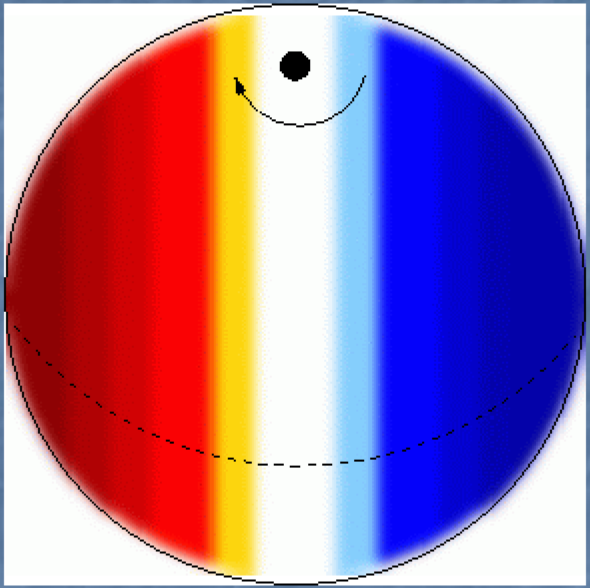

- In the absence of macro-turbulence, consider the ratio between the specific intensity of the line at Δλ and the continuum:

$$H(v) = H(\Delta\lambda) = I_\nu(\Delta\lambda)/I_c$$

4.4.2 Rotation

$$\frac{\mathcal{F}_\nu}{\mathcal{F}_c} = \frac{\oint H(v - v_z)\, I_c\, \cos\theta\, d\omega}{\oint I_c\, \cos\theta\, d\omega}$$

- $x = R \sin\theta \cos\varphi$ & $y = R \sin\theta \sin\varphi$ $\Rightarrow$

$$\begin{aligned}\mathcal{F}_\nu &= \oint H(v - v_z)\, I_c\, \cos\theta\, d\omega = \int\!\!\int H(v - v_z)\, I_c\, \frac{dx\, dy}{R^2} \\ &= \int_{-R}^{R} H(v - v_z) \left(\int_{-\sqrt{R^2 - x^2}}^{\sqrt{R^2 - x^2}} I_c\, \frac{dy}{R} \right) \frac{dx}{R}\end{aligned}$$

- We introduce a function $G(\Delta\lambda)$ such that

$$G(\Delta\lambda) = \frac{1}{v_{\text{eq}}\, \sin i}\, \frac{\int_{-\sqrt{R^2 - x^2}}^{\sqrt{R^2 - x^2}} I_c\, \frac{dy}{R}}{\oint I_c\, \cos\theta\, d\omega} \qquad \text{for} \qquad |v_z| \leq v_{\text{eq}}\, \sin i = R\,\Omega\, \sin i$$

$$G(\Delta\lambda) = 0 \qquad \text{for} \qquad |v_z| > v_{\text{eq}}\, \sin i$$

$$\Rightarrow \quad \frac{\mathcal{F}_\nu}{\mathcal{F}_c} = \int_{-\infty}^{+\infty} H(v - v_z)\, G(v_z)\, dv_z = H(v) * G(v)$$

The line profile widened by rotation is the convolution of the intrinsic profile and the function *G*.

4.4.2 Rotation

$$\frac{\mathcal{F}_\nu}{\mathcal{F}_c} = \int_{-\infty}^{+\infty} H(v - v_z)\, G(v_z)\, dv_z = H(v) * G(v)$$

- For a linear limb-darkening law $I_c = I_c^0\,(1 - \epsilon + \epsilon\,\cos\theta)$

$$\Rightarrow \quad \oint I_c\,\cos\theta\, d\omega = I_c^0\,\pi\,(1 - \frac{\epsilon}{3})$$

$$\& \quad \int_{-\sqrt{R^2-x^2}}^{\sqrt{R^2-x^2}} I_c\,\frac{dy}{R} = 2\,I_c^0\,(1-\epsilon)\left(1 - \left(\frac{v_z}{v_{\rm eq}\,\sin i}\right)^2\right)^{1/2} + \frac{\pi\,\epsilon\,I_c^0}{2}\left(1 - \left(\frac{v_z}{v_{\rm eq}\,\sin i}\right)^2\right)$$

- We thus obtain:

$$G(v_z) = \frac{2\,(1-\epsilon)}{\pi\,(1-\frac{\epsilon}{3})\,v_{\rm eq}\,\sin i}\left(1 - \left(\frac{v_z}{v_{\rm eq}\,\sin i}\right)^2\right)^{1/2} + \frac{\epsilon}{2\,(1-\frac{\epsilon}{3})\,v_{\rm eq}\,\sin i}\left(1 - \left(\frac{v_z}{v_{\rm eq}\,\sin i}\right)^2\right)$$

$$\Rightarrow \quad g(\sigma) = \frac{2\,(1-\epsilon)}{1-\frac{\epsilon}{3}}\,\frac{J_1(2\,\pi\,\Delta\lambda_L\,\sigma)}{2\,\pi\,\Delta\lambda_L\,\sigma} - \frac{2\,\epsilon\,\cos\,(2\,\pi\,\Delta\lambda_L\,\sigma)}{(1-\frac{\epsilon}{3})\,(2\,\pi\,\Delta\lambda_L\,\sigma)^2} + \frac{2\,\epsilon\,\sin\,(2\,\pi\,\Delta\lambda_L\,\sigma)}{(1-\frac{\epsilon}{3})\,(2\,\pi\,\Delta\lambda_L\,\sigma)^3}$$

$$J_s(x) = \frac{1}{\pi}\int_0^{\pi} \cos\,(s\,\psi - x\,\sin\psi)\, d\psi \qquad s\,J_s(x) = [J_{s-1}(x) + J_{s+1}(x)]\,\frac{x}{2}$$

4.4.2 Rotation

- If we account for the effects of macro-turbulence:

$$\begin{aligned}\mathcal{F}_\nu &= \oint I_\nu(\lambda - \Delta\lambda_{\rm rot}) * \Theta(\Delta\lambda)\ \cos\theta\, d\omega \\ &= \oint I_\nu(\lambda) * \Theta(\Delta\lambda - \Delta\lambda_{\rm rot})\ \cos\theta\, d\omega\end{aligned}$$

- With a linear limb-darkening law $I_\nu(\lambda) = H(\lambda)\, I_c^0\, (1 - x + x\ \cos\theta)$, we obtain

$$\begin{aligned}\mathcal{F}_\nu &= \oint H(\lambda)\, I_c^0\, (1 - x + x\ \cos\theta) * \Theta(\Delta\lambda - \Delta\lambda_{\rm rot})\ \cos\theta\, d\omega \\ &= H(\lambda) * \oint I_c^0\, (1 - x + x\ \cos\theta)\, \Theta(\Delta\lambda - \Delta\lambda_{\rm rot})\ \cos\theta\, d\omega \\ &= H(\lambda) * M(\Delta\lambda)\end{aligned}$$

- The function $M(\Delta\lambda)$ includes now the effects of rotation and of macro-turbulence.

4.5 Observational determination

- Use of the different observational diagnostics to determine the fundamental parameters of the stars.
- Effective temperature:

1. Slope of the Paschen continuum (if the interstellar reddening is known)
2. Relative strength of pairs of lines sensitive to temperature

- Pressure:

1. Strength of lines sensitive to gravity (this allows to evaluate the "spectroscopic mass" of the star):

$$\frac{M}{M_\odot} = \left(\frac{R}{R_\odot}\right)^2 \frac{g}{g_\odot}$$

4.5 Observational determination

- Simultaneous determination of temperature and pressure: equivalent widths of two lines of the same ion with different sensitivities on *T* and *g* (lines arising from levels that have different excitation potentials).

  One searches the intersection between isocurves of the EWs.

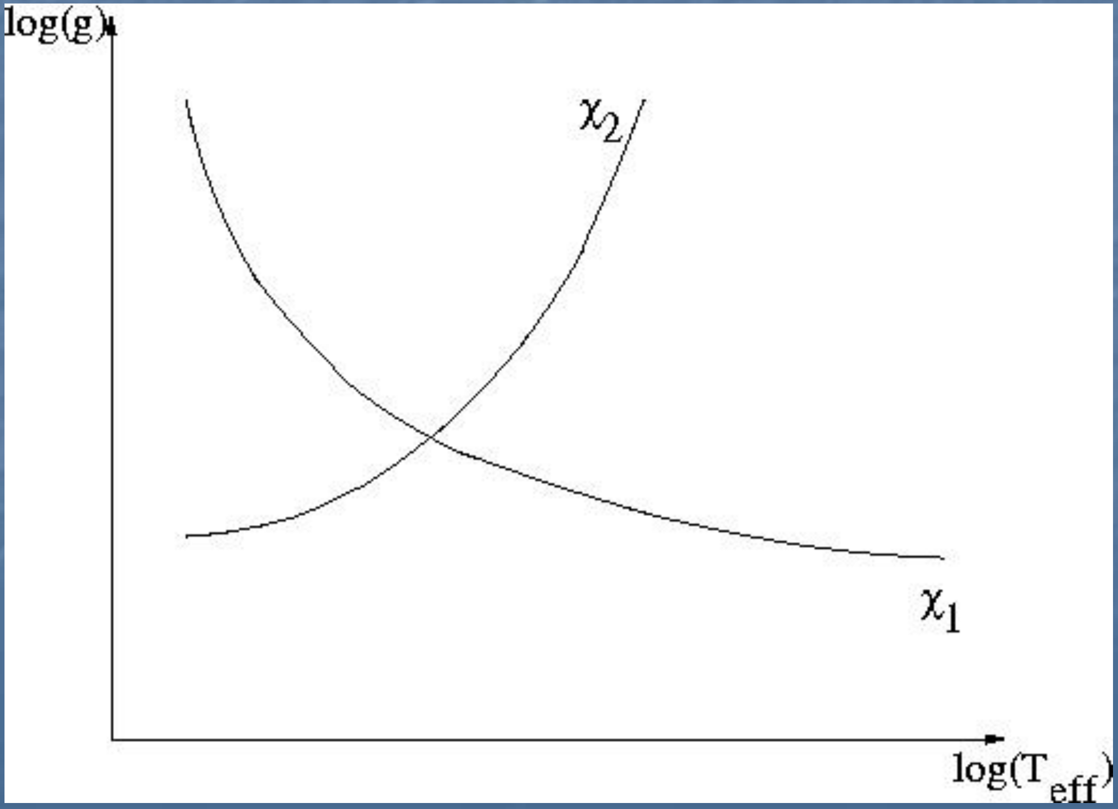

4.5 Observational determination

- Determination of the chemical composition:

1. Empirical curve of growth: the curve of growth is intrinsically the same for all lines of an ion. In the linear part of the curve, one finds:

$$EW \propto \lambda^2 \, f \, \frac{N_l}{\kappa_\nu}$$

Hence, $$\log \frac{EW}{\lambda} = C + \log A_{Z,j} + \log \left(g_l \, f_{l,u} \, \lambda \right) - \frac{\chi}{kT} - \log \kappa_\nu$$

The different curves of growth are shifted horizontally and one determines the shift $\Delta \, \log A_{Z,j}$ of each line to minimise the dispersion of the points around the curve.

$$\begin{aligned} \Delta \, \log A_{Z,j} &= \log A^1_{Z,j} - \log A_{Z,j} \\ &= \log \frac{g_l \, f_{l,u} \, \lambda}{g^1_l \, f^1_{l,u} \, \lambda_1} - \frac{\chi_l - \chi^1_l}{kT} - \log \frac{\kappa_\nu}{\kappa_1} \end{aligned}$$

2. Global fit of the spectrum with a model atmosphere code.

4.5 Observational determination

- Solar abundances: logarithm of the hydrogen abundance arbitrarily set to 12.0.

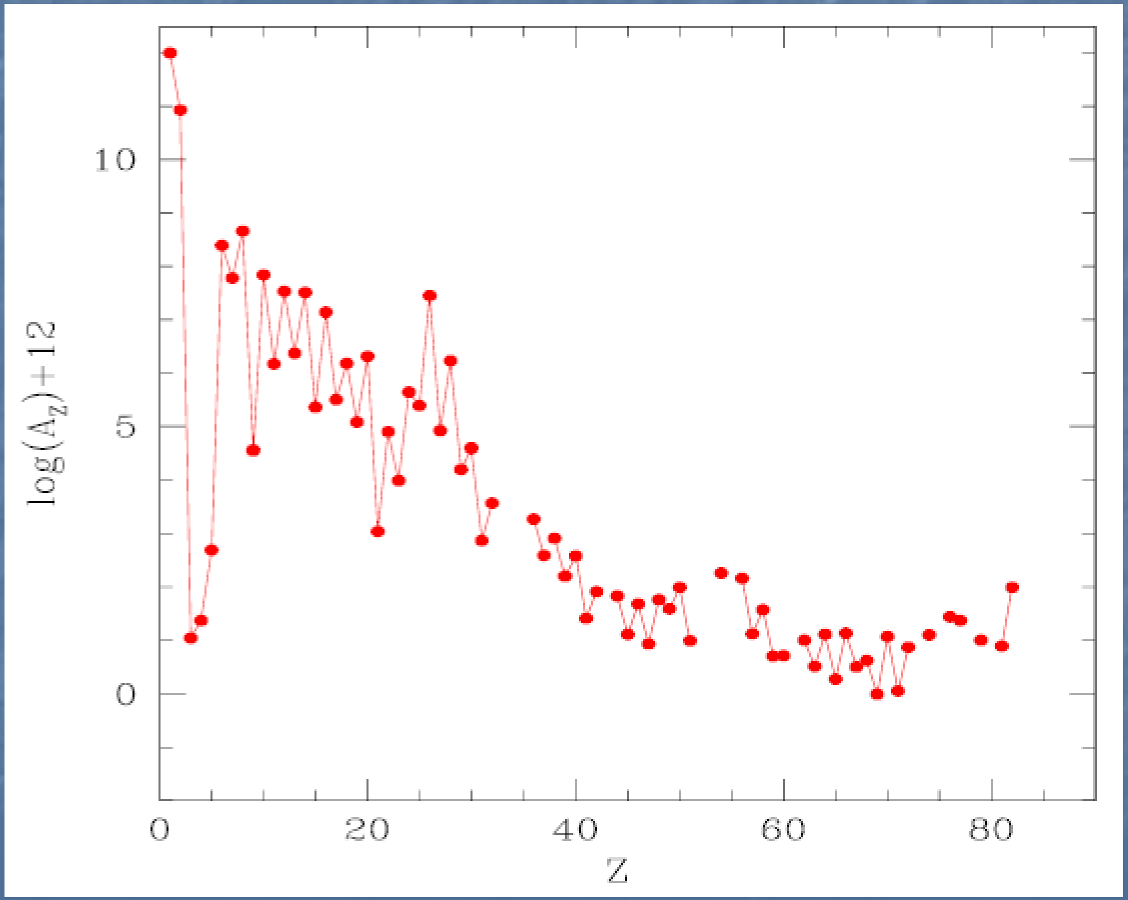

4.5 Observational determination

- Projected rotational velocity: study lines free of blends and weakly affected by collisional broadening. In fast rotators, gravity darkening lowers the contribution of the equatorial regions.
- Different methods have been used:

1. Measure the full width at half maximum of the line.
2. Cross correlate with the spectrum of a star of known rotational velocity.
3. Comparison with model atmospheres.
4. Fourier transform.

$$D(\Delta\lambda) = H(\Delta\lambda) * M(\Delta\lambda) * L(\Delta\lambda) = \frac{\mathcal{F}_\nu}{\mathcal{F}_c}$$

$$\Rightarrow \quad d(\sigma) = h(\sigma)\, g(\sigma)\, l(\sigma)$$

4.5 Observational determination

$$d(\sigma) = h(\sigma)\, g(\sigma)\, l(\sigma)$$

- The Fourier transform $g(\sigma)$ has zeros, the first of which is set by the value of $v_{eq} \sin i$
- Application to real situations: macro-turbulence and noise.

$$D(\Delta\lambda) = H(\Delta\lambda) * M(\Delta\lambda) * L(\Delta\lambda)$$

$$d(\sigma) = h(\sigma)\, m(\sigma)\, l(\sigma)$$

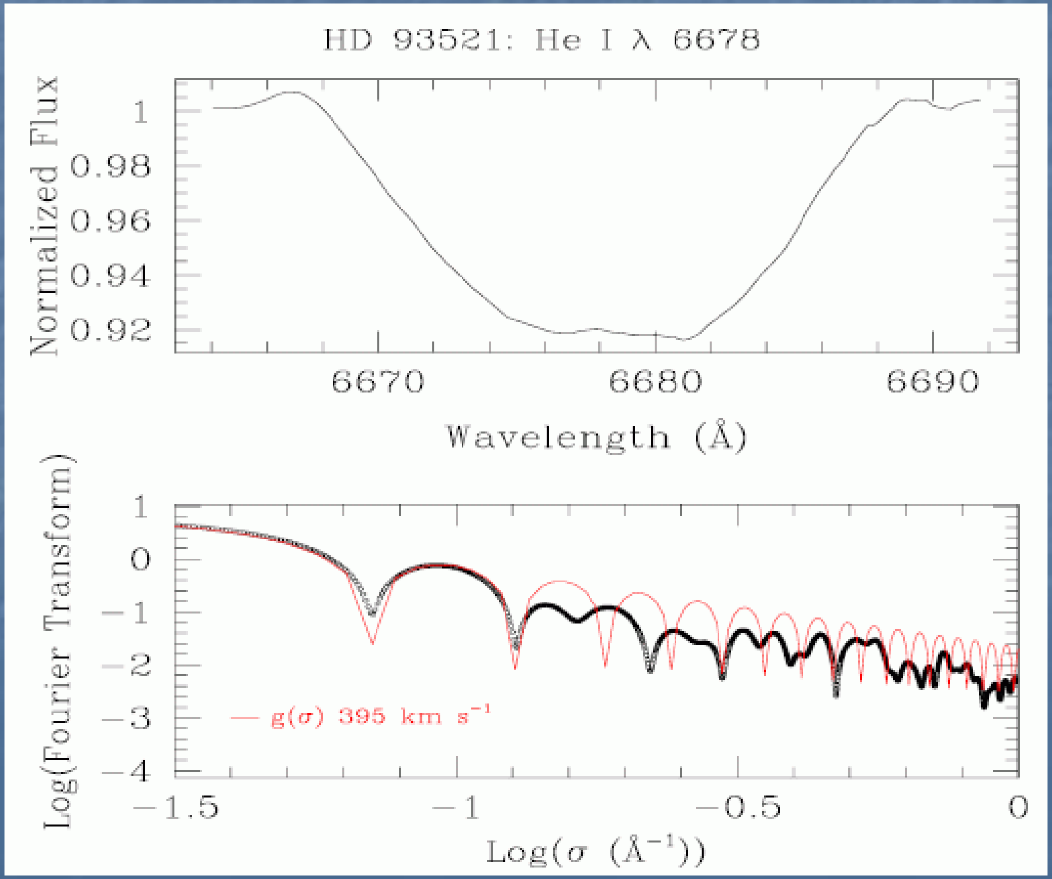

4.5 Observational determination

- Case of a binary consisting of two stars with very different rotational velocities:

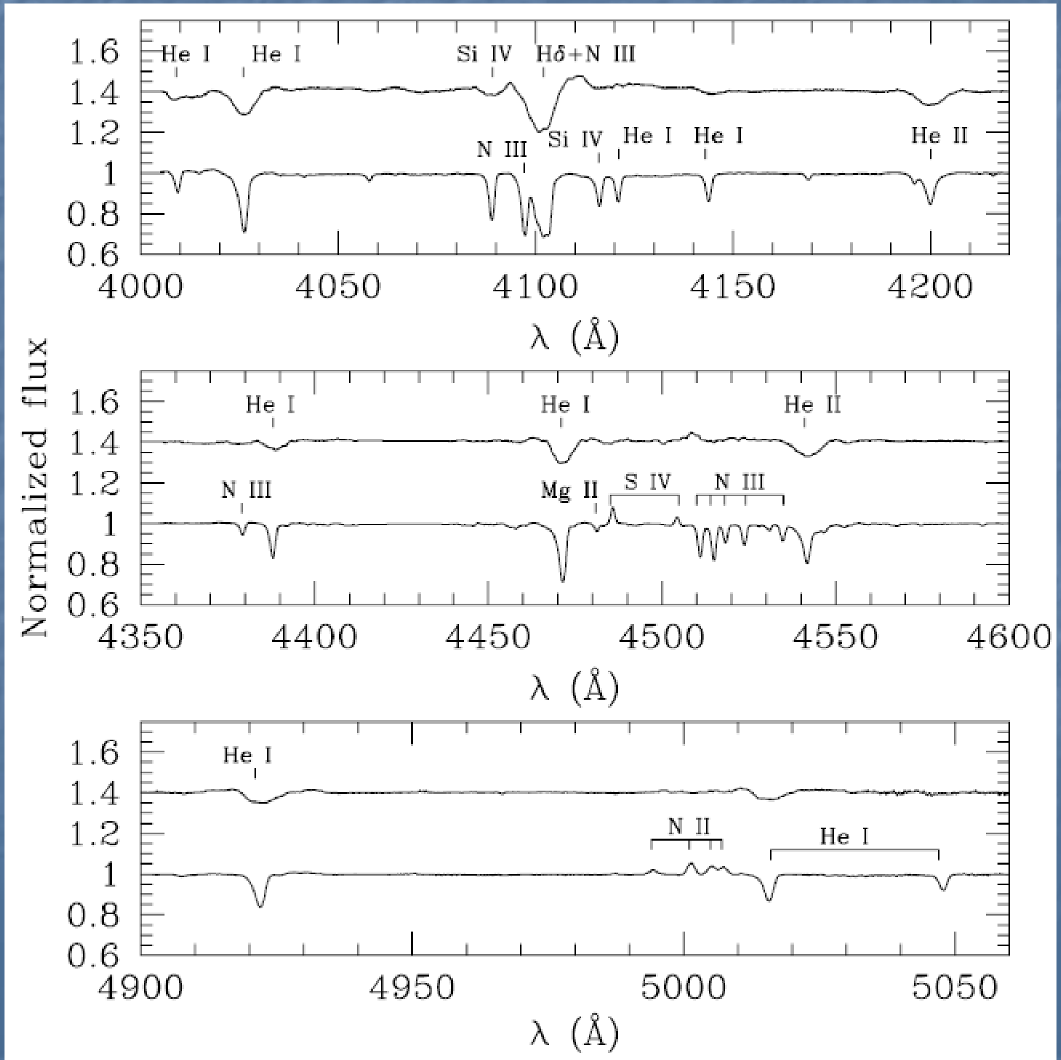

310 ± *20* km/s

66 ± *9* km/s

V. Expanding spherical atmospheres

- Radiative transfer in the continuum:

1. Grey atmospheres.
2. Feautrier method.

- Radiative transfer in spectral lines:

1. Optically thin spectral lines.
2. Optically thick spectral lines: the Sobolev approximation.

- Beyond the Sobolev approximation.
- The effect of free electron scattering.
- Structures in stellar winds.

V. Expanding spherical atmospheres

- The spectra of Wolf-Rayet, O and Of stars display the spectral signatures of stellar winds (P-Cygni profiles)

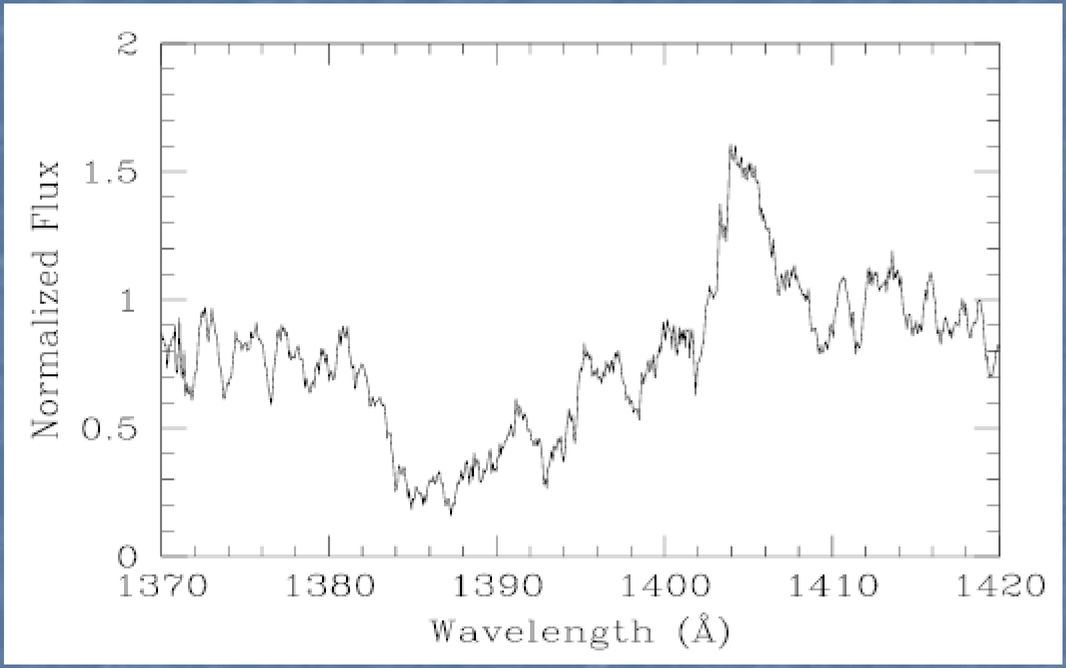

- Stellar wind = combination of an important mass-loss rate with a fast expansion. Acceleration through radiation pressure in the UV lines.

5.1 Radiative transfer in the continuum

- The expansion of the wind has essentially no effect on the transfer of the radiation in the continuum.

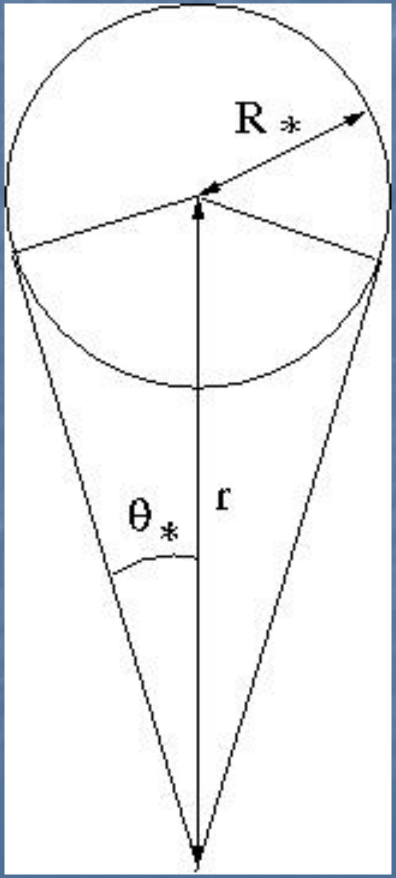

Dilution of continuum radiation in an extended atmosphere.

$$w = \frac{1}{2}\left(1 - \sqrt{1 - \left(\frac{R_*}{r}\right)^2}\right)$$

Moments of the continuum radiation field in an extended atmosphere.

$$\begin{aligned} J_\nu &= w\, I_\nu \\ H_\nu &= \frac{1}{4} I_\nu \left(\frac{R_*}{r}\right)^2 \\ K_\nu &= \frac{1}{6} I_\nu \left(1 - \left(1 - \left(\frac{R_*}{r}\right)^2\right)^{3/2}\right) \end{aligned}$$

At very large distance, all moments have the same limit: $\frac{1}{4} I_\nu \left(\frac{R_*}{r}\right)^2$

5.1 Radiative transfer in the continuum

- Equation of radiative transfer in spherical geometry:

$$\frac{\partial I_\nu}{\partial r}\frac{\cos\theta}{\kappa_\nu\,\rho} - \frac{\partial I_\nu}{\partial \theta}\frac{\sin\theta}{\kappa_\nu\,\rho\,r} = -I_\nu + S_\nu$$

with $\mu = \cos\theta$

$$\mu\,\frac{\partial I_\nu}{\partial r} + (1-\mu^2)\,\frac{1}{r}\,\frac{\partial I_\nu}{\partial \mu} = \kappa_\nu\,\rho\,(S_\nu - I_\nu)$$

$$\Rightarrow \quad \frac{\partial\,(r^2\,H_\nu)}{\partial r} = r^2\,\kappa_\nu\,\rho\,(S_\nu - J_\nu)$$

$d\tau = -\kappa_\nu \rho dr \Rightarrow$

$$\frac{\partial\,(r^2\,H_\nu)}{\partial \tau_\nu} = r^2\,(J_\nu - S_\nu)$$

$$\Rightarrow \quad \frac{\partial K_\nu}{\partial \tau_\nu} - \frac{1}{r\,\kappa_\nu\,\rho}\,(3\,K_\nu - J_\nu) - H_\nu = 0$$

5.1 Radiative transfer in the continuum

- Generalized Eddington factor: $f_\nu = K_\nu / J_\nu$

$$\frac{\partial K_\nu}{\partial \tau_\nu} - \frac{1}{r\,\kappa_\nu\,\rho}(3\,K_\nu - J_\nu) - H_\nu = 0 \quad \Rightarrow \quad \frac{\partial (f_\nu\,J_\nu)}{\partial \tau_\nu} - (3\,f_\nu - 1)\,\frac{J_\nu}{r\,\kappa_\nu\,\rho} - H_\nu = 0$$

tends towards 1/3 very deep in the atmosphere and towards 1 in the outer layers of the atmosphere. $J_\nu = H_\nu = K_\nu$

Solution of the transfer equation depends on the behaviour of the generalized Eddington factor.

5.1 Radiative transfer in the continuum

- Grey atmosphere in radiative equilibrium ($J = S$):

$$\frac{\partial\,(r^2\,H_\nu)}{\partial \tau_\nu} = r^2\,(J_\nu - S_\nu) \quad \Rightarrow \quad \frac{\partial\,(r^2\,H)}{\partial r} = 0$$

Hence,

$$r^2\,H = Cte = \frac{L_*}{16\,\pi^2}$$

$$\frac{\partial\,(f_\nu\,J_\nu)}{\partial \tau_\nu} - (3\,f_\nu - 1)\,\frac{J_\nu}{r\,\kappa_\nu\,\rho} - H_\nu = 0 \quad \Rightarrow \quad \frac{\partial\,(f\,J)}{\partial r} + (3\,f - 1)\,\frac{J}{r} + \kappa\,\rho\,H = 0$$

- In the outer regions of the atmosphere ($f = 1$)

$$\frac{\partial\,(r^2\,J)}{\partial r} = -\,\kappa\,\rho\,r^2\,H$$

$$\Rightarrow \quad J(\tau) = \frac{L_*}{16\,\pi^2\,r^2}\,(\tau + 1)$$

5.1 Radiative transfer in the continuum

- In the inner regions of the atmosphere (*f = 1/3*)

$$\frac{\partial J}{\partial r} = -3\,\kappa\,\rho\,H \quad \Rightarrow \quad J(\tau) = \frac{L_*}{16\,\pi^2\,R^2}\,3\int_0^\tau \frac{R^2}{r'^2}\,d\tau' + Cte$$

Value of the constant of integration? Connect the two solutions assuming that the opacity varies as some negative power of *r*.

$$\kappa\,\rho = C\,r^{-n}$$

$$\tau(r) = C\,r^{-n+1}/(n-1) \quad \Rightarrow \quad J(\tau) \to \frac{3\,(n-1)}{n+1}\,\frac{L_*\,\tau}{16\,\pi^2\,r^2}$$

for $\tau \to \infty$

The solution hence becomes:

$$J(\tau) = \frac{3\,(n-1)}{n+1}\,\frac{L_*}{16\,\pi^2\,r^2}\left(\tau + \frac{n+1}{3\,(n-1)}\right)$$

5.1 Radiative transfer in the continuum

- Temperature profile of an extended atmosphere in LTE (crude approximation): $J(\tau) = \sigma T^4(\tau)/\pi$

$$J(\tau) = \frac{3\,(n-1)}{n+1}\,\frac{L_*}{16\,\pi^2\,r^2}\,\left(\tau + \frac{n+1}{3\,(n-1)}\right)$$

$$\Rightarrow \quad T(\tau) = T(\tau=1)\,\tau^{\frac{1}{2\,(n-1)}}\left[\frac{3\,(n-1)\,\tau + n + 1}{4\,n-2}\right]^{1/4}$$

- Temperature decreases outwards and the spectral distribution appears “flatter” than for a plane-parallel atmosphere of same effective temperature.

5.1 Radiative transfer in the continuum

- Feautrier method: we introduce a new variable

$$dX_\nu = q_\nu \, d\tau_\nu$$

with the sphericity parameter:

$$\ln\left(\frac{r^2 q_\nu}{R_*^2}\right) = \int_{R_*}^{r} \frac{3 f_\nu - 1}{f_\nu} \frac{dr'}{r'}$$

$$\left.\begin{aligned} &\frac{\partial (f_\nu J_\nu)}{\partial \tau_\nu} - (3 f_\nu - 1) \frac{J_\nu}{r \kappa_\nu \rho} - H_\nu = 0 \\ &\frac{\partial (r^2 H_\nu)}{\partial \tau_\nu} = r^2 (J_\nu - S_\nu) \end{aligned}\right\} \Rightarrow \begin{aligned} \frac{\partial}{\partial X_\nu}(r^2 q_\nu f_\nu J_\nu) &= r^2 H_\nu \\ \frac{\partial^2}{\partial X_\nu^2}(r^2 q_\nu f_\nu J_\nu) &= \frac{r^2}{q_\nu} (J_\nu - S_\nu) \end{aligned}$$

Resolution of this equation requires knowledge of $f_\nu(r)$.

This problem is solved by numerically integrating the transfer equation along a straight line of impact parameter p.

5.1 Radiative transfer in the continuum

$$\frac{\partial I_\nu}{\partial r}\frac{\cos\theta}{\kappa_\nu\,\rho} - \frac{\partial I_\nu}{\partial \theta}\frac{\sin\theta}{\kappa_\nu\,\rho\, r} = -I_\nu + S_\nu$$

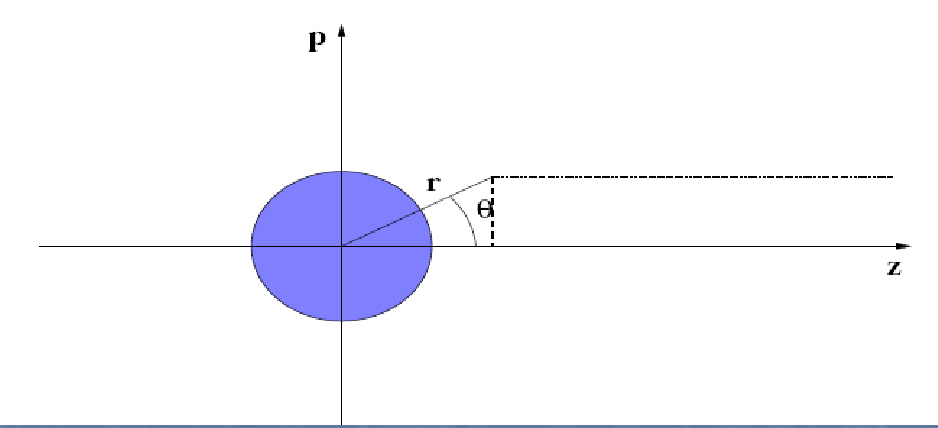

Numerical resolution of the transfer equation along a straight line p = Cte.

$$\frac{\partial}{\partial r} = \frac{\partial z}{\partial r}\frac{\partial}{\partial z} + \frac{\partial p}{\partial r}\frac{\partial}{\partial p} \quad \Rightarrow \quad \frac{\partial}{\partial r} = \mu\,\frac{\partial}{\partial z} + \sqrt{1-\mu^2}\,\cancel{\frac{\partial}{\partial p}}$$

$$\frac{\partial}{\partial \mu} = \frac{\partial z}{\partial \mu}\frac{\partial}{\partial z} + \frac{\partial p}{\partial \mu}\frac{\partial}{\partial p} \quad \Rightarrow \quad \frac{\partial}{\partial \mu} = r\,\frac{\partial}{\partial z} - \frac{\mu\, r}{\sqrt{1-\mu^2}}\,\cancel{\frac{\partial}{\partial p}}$$

$$\Rightarrow \quad \frac{\partial I_\nu}{\partial z} = \kappa_\nu\,\rho\,(S_\nu - I_\nu)$$

$\Rightarrow$ knowledge of $I_\nu(p, z)$ and numerical determination of f_ν

5.2 Radiative transfer in the lines

- Consider a spherical atmosphere in radial expansion.
- The Doppler shift in the observer's frame is given by:

$$v_z = \mu \, v(r) = \cos(\theta) \, v(r)$$

- *(p, z)* coordinates:

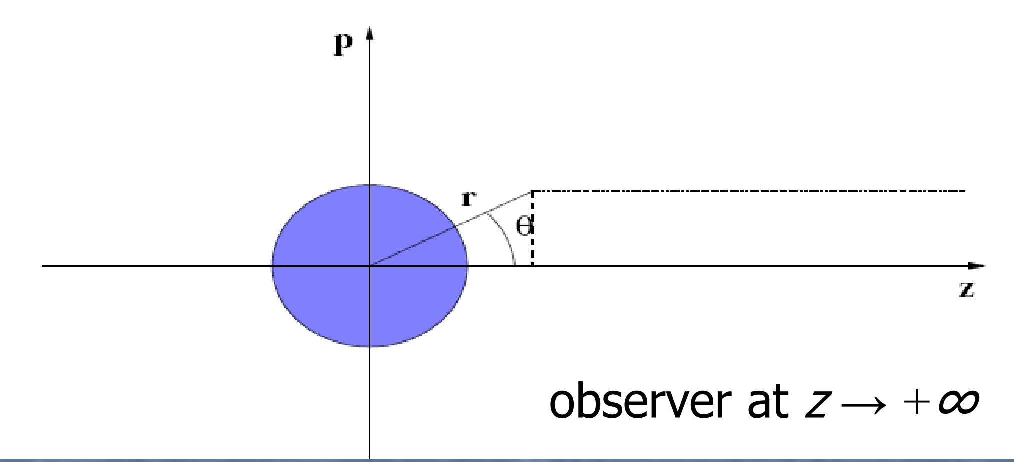

- Photons are observed at a wavelength λ_0 shifted by the Doppler shift.

5.2 Radiative transfer in the lines

- Spherical atmosphere in radial expansion: P-Cygni profiles.

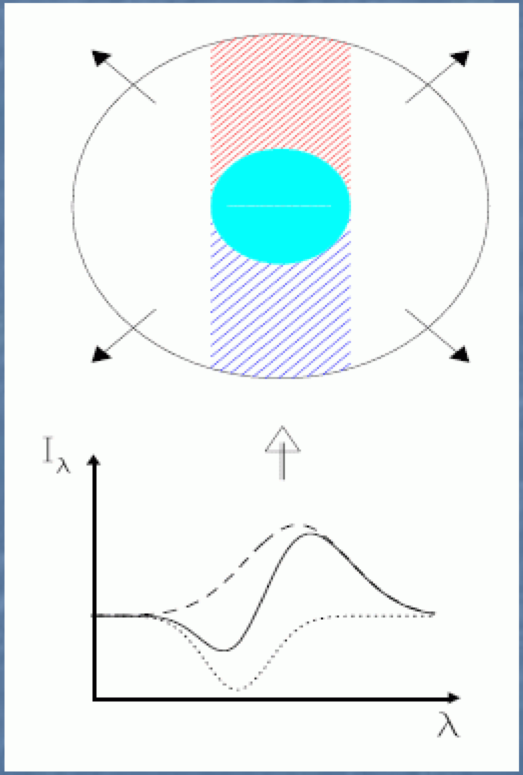

5.2 Radiative transfer in the lines

- Optically thin atmosphere: each photon emitted immediately leaves the atmosphere.
- Energy received by the observer located at $z \to +\infty$:

$$E_\nu = \int\int\int_V \eta(r)\,\phi\left[\nu - \nu_0\,(1 + \frac{\mu\, v(r)}{c})\right]\, dV$$

- Emissivity depends on the density which depends on the position in the wind through the continuity equation:

$$\eta(r) = \eta_0\,(\rho/\rho_0)^\alpha \quad \& \quad v(r) = v_0\,(r/R_*)^n$$

$$\Rightarrow \quad \eta = \eta_0\,(r/R_*)^{-(n+2)\,\alpha}$$

- Formulation of Doppler shift:

$$\chi = \frac{\nu - \nu_0}{\Delta\nu_D} \quad \& \quad \Delta\nu_D = \nu_0\,\frac{v_D}{c}$$

5.2 Radiative transfer in the lines

- Energy received by observer at $z \rightarrow +\infty$:

$$E_\chi = \eta_0 \, R_*^{(n+2)\,\alpha} \int\int\int_V \phi\left(\chi - \mu\,\frac{v(r)}{v_D}\right)\, r^{-(n+2)\,\alpha}\, dV$$

- φ sharply peaked function ⇒ emission at Doppler shift χ forms near the surface with the "right" radial velocity in the observer's frame of reference: v_z isovelocity surfaces = locus of the points having the same radial velocity in the observer's frame of reference (depends on velocity law!).
- The emission at a given wavelength does not arise in a specific point, but rather over a surface of same v_z.
- In certain cases, a given sightline intersects the same isovelocity surface twice ⇒ coupling between the radiative transfer at these points.

5.2 Radiative transfer in the lines

- v_z isovelocity surfaces.

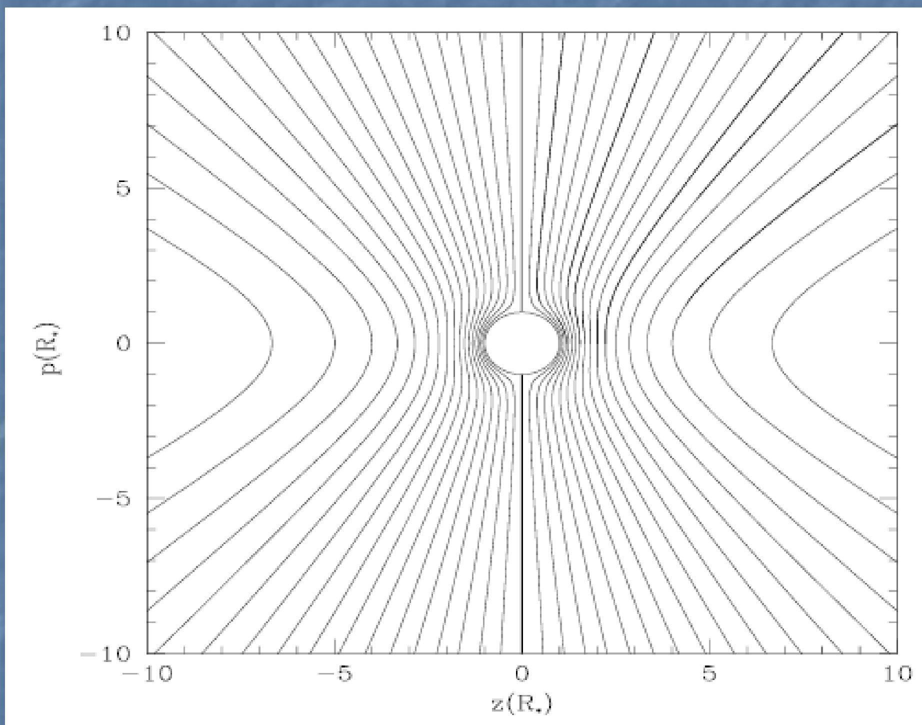

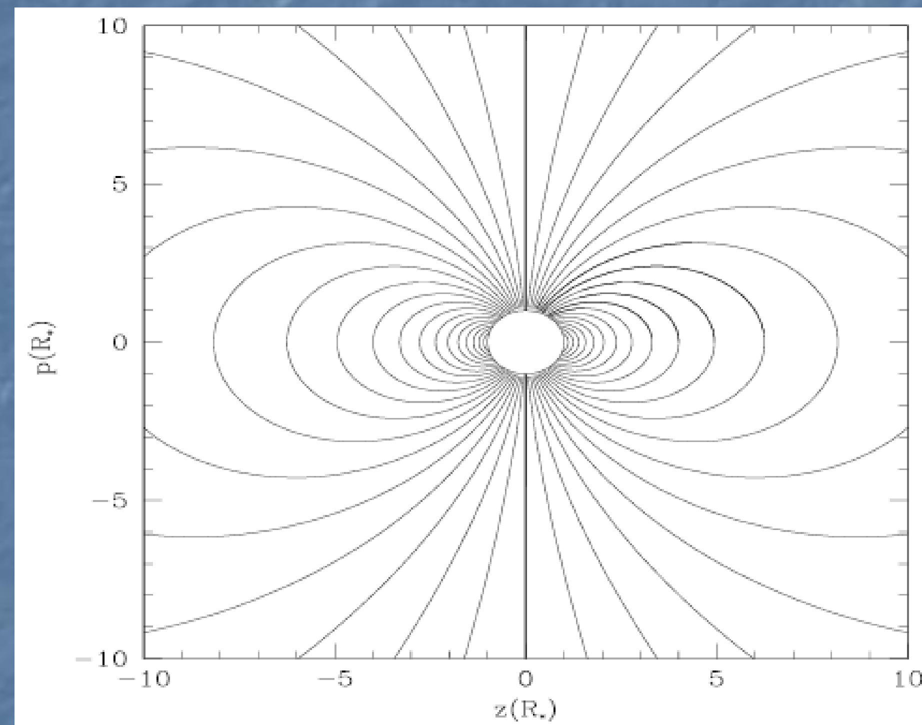

$$v = v_\infty \left(1 - \frac{R_*}{r}\right)$$

$$v = v_0 \left(\frac{r}{R_*}\right)^{-1/2}$$

5.2 Radiative transfer in the lines

- <u>Optically thick atmosphere</u>: the presence of a velocity gradient simplifies the resolution of the transfer equations (<u>Sobolev approximation</u>).
- Optical depth from point *(p, z)* towards the observer at $z \rightarrow +\infty$:

$$\tau(z,p,\chi) = \int_z^\infty l_\nu(r')\,\rho(r')\,dz' = \int_z^\infty \eta_l(r')\,\phi(\chi')\,dz'$$

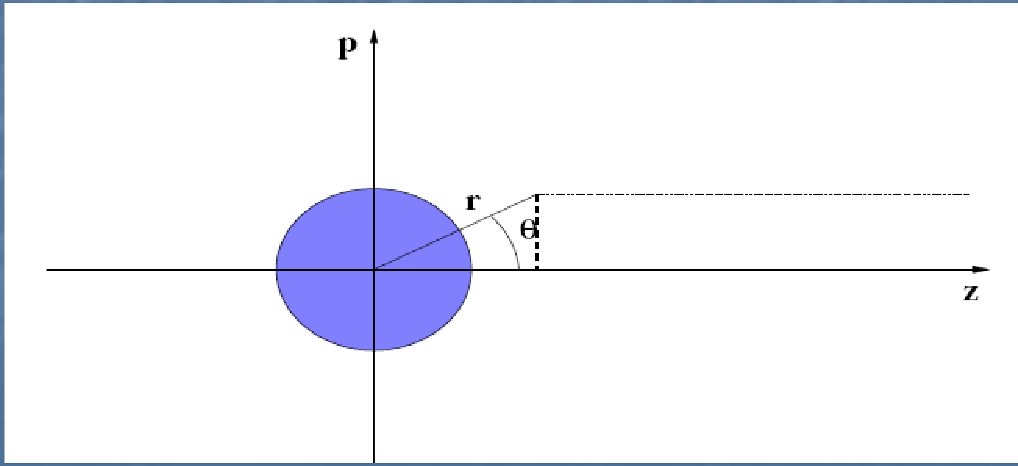

with $r' = \sqrt{z'^2 + p^2},\ \mu' = z'/r'$ $\quad \chi' = \chi - \mu'\,v(r')/v_D = \chi - v_z(r')/v_D$

5.2 Radiative transfer in the lines

$$\tau(z,p,\chi) = \int_z^\infty l_\nu(r')\,\rho(r')\,dz' = \int_z^\infty \eta_l(r')\,\phi(\chi')\,dz'$$

- The most important contributions to this integral arise from the points such that

$$\frac{z_0}{r_0}\,v(r_0)/v_D = \chi \qquad r_0 = \sqrt{z_0^2 + p^2}.$$

- i.e. the points of the iso-radial velocity surface.

$$\Rightarrow \quad \tau(z,p,\chi) \simeq \eta_l(r_0)\int_z^\infty \phi(\chi')\,dz'$$

- Moreover,

$$\begin{aligned}
\left(\frac{\partial\chi'}{\partial z'}\right)_p &= -\frac{1}{v_D}\left(\frac{\partial v_z}{\partial z'}\right)_p = -\frac{1}{v_D}\left(\frac{\partial}{\partial z'}[\mu'(z',p)\,v(r')]\right)_p \\
&= -\frac{1}{v_D}\left(\frac{\partial}{\partial z'}[\frac{z'}{\sqrt{z'^2+p^2}}\,v(\sqrt{z'^2+p^2})]\right)_p \\
&= -\frac{1}{v_D}\left[\mu'^2\,\frac{\partial\,v(r')}{\partial r'} + (1-\mu'^2)\,\frac{v(r')}{r'}\right] = -Q(r',\mu')
\end{aligned}$$

5.2 Radiative transfer in the lines

$$\tau(z,p,\chi) = \int_z^\infty l_\nu(r')\,\rho(r')\,dz' = \int_z^\infty \eta_l(r')\,\phi(\chi')\,dz'$$

- If the photon interaction region is small,

$$\begin{aligned}
\tau(z,p,\chi) &\simeq \frac{\eta_l(r_0)}{Q(r_0,\mu_0)} \int_{-\infty}^{\chi - v_z/v_D} \phi(\xi')\,d\xi' \\
&= \frac{\tau_0(r_0)}{1+\mu^2\left[\frac{d\log v/v(r_0)}{d\log r/r_0} - 1\right]_0} \int_{-\infty}^{\chi - v_z/v_D} \phi(\xi')\,d\xi' \\
&= \frac{\tau_0(r_0)}{1+\mu^2\left[\frac{d\log v/v(r_0)}{d\log r/r_0} - 1\right]_0} \Phi(\chi - v_z/v_D)
\end{aligned}$$

with $\tau_0(r_0) = \eta_l(r_0)\,\frac{r_0\,v_D}{v(r_0)}$ & $\Phi(\chi - v_z/v_D) = \int_{-\infty}^{\chi - v_z/v_D} \phi(\xi')\,d\xi'$

5.2 Radiative transfer in the lines

- Optical depth from an arbitrary point and along an arbitrary direction:

$$\tau(\vec{r},\vec{n},\chi) = \frac{\eta_l(r_0)}{Q(\vec{r},\vec{n})}\,\Phi(\zeta)$$ where $$\zeta = \chi - \frac{\vec{n}\cdot\vec{v}}{v_D}$$

- The general solution of the transfer equation...

$$I_\nu(\tau_\nu) = \exp(-\tau_\nu)\int_0^{\tau_\nu} S_\nu(t_\nu)\,\exp(t_\nu)\,dt_\nu + I_\nu(0)\,\exp(-\tau_\nu)$$

...can be simplified:

$$\begin{aligned}
I_\nu(\vec{r},\vec{n}) &= S_\nu(r)\left[1-\exp\left(-\frac{\eta_l(r)\,\Phi(\zeta)}{Q(\vec{r},\vec{n})}\right)\right]\\
I_\nu(\vec{r},\vec{n}) &= S_\nu(r)\left[1-\exp\left(-\frac{\eta_l(r)\,\Phi(\zeta)}{Q(\vec{r},\vec{n})}\right)\right] + I_c\,\exp\left(-\frac{\eta_l(r)\,\Phi(\zeta)}{Q(\vec{r},\vec{n})}\right)
\end{aligned}$$

5.2 Radiative transfer in the lines

$$
\begin{aligned}
I_\nu(\vec{r},\vec{n}) &= S_\nu(r)\left[1-\exp\left(-\frac{\eta_l(r)\,\Phi(\zeta)}{Q(\vec{r},\vec{n})}\right)\right] \\
I_\nu(\vec{r},\vec{n}) &= S_\nu(r)\left[1-\exp\left(-\frac{\eta_l(r)\,\Phi(\zeta)}{Q(\vec{r},\vec{n})}\right)\right] + I_c\,\exp\left(-\frac{\eta_l(r)\,\Phi(\zeta)}{Q(\vec{r},\vec{n})}\right)
\end{aligned}
$$

- The mean intensity can now be computed via an integration over solid angle...

$$
J(r) = \frac{1}{4\pi}\oint d\omega \int_{-\infty}^{+\infty} \phi(\zeta)\left\{S(r)\left[1-\exp\left(-\frac{\eta_l(r)\,\Phi(\zeta)}{Q(\vec{r},\vec{n})}\right)\right] + I_{\rm inc}\,\exp\left(-\frac{\eta_l(r)\,\Phi(\zeta)}{Q(\vec{r},\vec{n})}\right)\right\} d\zeta
$$

$$
I_{\rm inc} = I_c \text{ for } -\vec{n}\in\Omega_* \text{ and } I_{\rm inc} = 0 \text{ otherwise}
$$

- ...and one can express it in terms of the escape probabilities of the photons:

$$
J(r) = (1-\beta(r))\,S(r) + \beta_c\,I_c
$$

5.2 Radiative transfer in the lines

$$J(r) = (1 - \beta(r))\, S(r) + \beta_c\, I_c$$

- The probability that a photon escapes from the interaction region is:

$$\begin{aligned}
\beta(r) &= \frac{1}{2}\int_{-1}^{1} d\mu \int_{-\infty}^{\infty} \phi(\zeta)\, \exp\left(-\tau\right) d\zeta \\
&= \frac{1}{2}\int_{-1}^{1} d\mu \int_{0}^{1} \exp\left[-\eta_l(r)\, \Phi/Q(r,\mu)\right] d\Phi \\
&= \eta_l(r)^{-1} \int_{0}^{1} \left[1 - \exp\left(-\eta_l(r)/Q(r,\mu)\right)\right] Q(r,\mu)\, d\mu
\end{aligned}$$

- The probability that a photospheric photon enters the interaction region is:

$$\begin{aligned}
\beta_c(r) &= \frac{1}{2}\int_{-1}^{-\cos\theta_*} d\mu \int_{0}^{1} \exp\left[-\eta_l(r)\, \Phi/Q(r,\mu)\right] d\Phi \\
&= \frac{1}{2}\, \eta_l(r)^{-1} \int_{\cos\theta_*}^{1} \left[1 - \exp\left(-\eta_l(r)/Q(r,\mu)\right)\right] Q(r,\mu)\, d\mu
\end{aligned}$$

$$\cos\theta_* = \sqrt{1 - \left(\frac{R_*}{r}\right)^2}$$

- To first order:

$$\beta_c(r) = w(r)\, \beta(r)$$

5.2 Radiative transfer in the lines

- Flux of the line as observed by an observer at infinity:

$$
\begin{aligned}
\mathcal{F}_\chi &= \frac{2\,\pi}{R_*^2} \int_0^\infty I(\infty, p, \chi)\, p\, dp \\
&= \frac{2\,\pi}{R_*^2} \left(\int_{R_*}^\infty S(r_0)\, [1 - \exp\left(-\tau(-\infty, p, \chi)\right)]\, p\, dp + \int_0^{R_*} S(r_0)\, [1 - \exp\left(-\tau(-\infty, p, \chi)\, \Phi(\chi_c)\right)]\, p\, dp \right. \\
&\quad \left. + I_c \int_0^{R_*} \exp\left[-\tau(-\infty, p, \chi)\, \Phi(\chi_c)\right] p\, dp \right)
\end{aligned}
$$

- Allows to compute the line profiles in the framework of the Sobolev approximation. In general, the equations of statistical equilibrium must be solved because the atmosphere is not in LTE.

5.3 Beyond the Sobolev approximation

- CoMoving Frame (CMF) method allows to overcome the limitations of the Sobolev approximation when the velocity gradients are small.
- However, the CMF is not an inertial frame of reference.
- Complex method (especially because of the nLTE effects).
- Currently, most popular approach for analysing the spectra of Wolf-Rayet and Of stars.

5.3 Beyond the Sobolev approximation

- Spectra of Wolf-Rayet stars: WN and WC sequences:

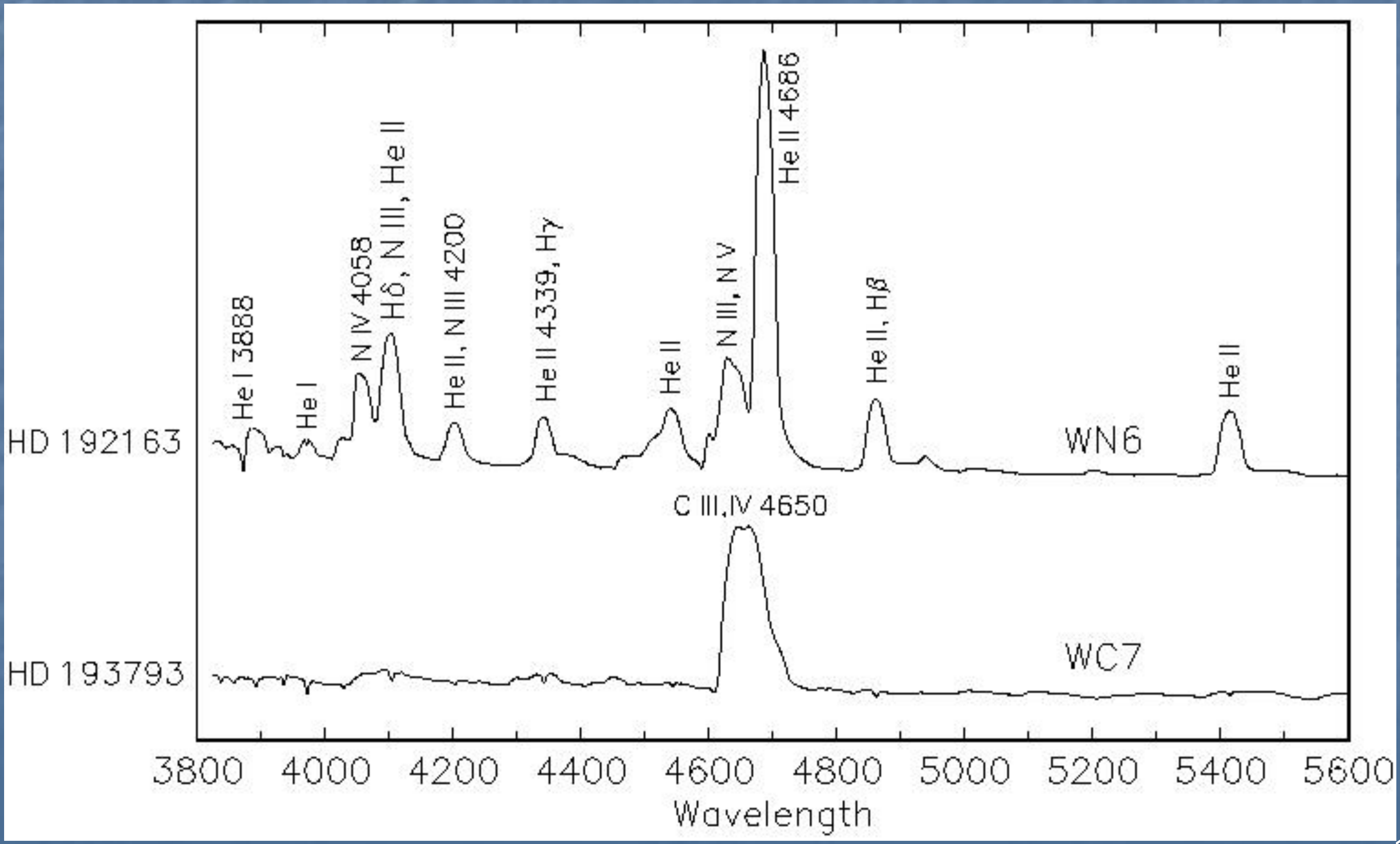

5.3 Beyond the Sobolev approximation

- Progression of the spectra as a function of the strength of the stellar wind:

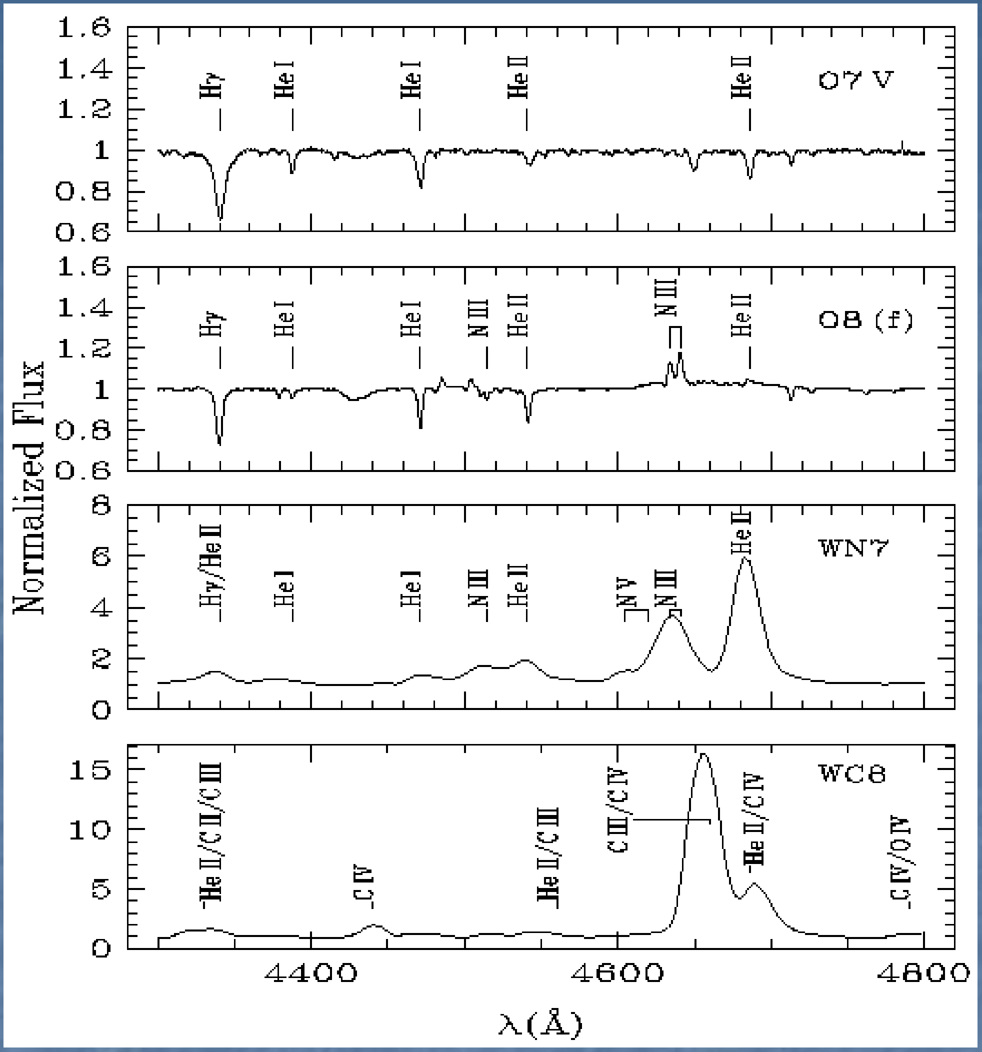

$$\rho(2\,R_*) = \frac{\dot{M}}{16\,\pi\,R_*^2\,v_\infty\,(0.5)^\beta}$$

Spectral type	v_∞ ($\mathrm{km\,s^{-1}}$)	R_* ($R_\odot$)	β	$\dot{M}$ ($M_\odot\,\mathrm{yr}^{-1}$)	$\rho(2\,R_*)$ ($\mathrm{g\,cm^{-3}}$)
O4 V	3000	12.0	1.0	0.25×10^{-6}	3×10^{-15}
O4 If$^+$	2300	19.6	0.8	1.8×10^{-6}	9×10^{-15}
WN7	1385	16.7	1.0	7.9×10^{-5}	1×10^{-12}
WC4	2800	1.06	1.0	9.5×10^{-5}	1.5×10^{-10}

5.3 Beyond the Sobolev approximation

- Analysis with CMFGEN of the spectrum of a WC star:

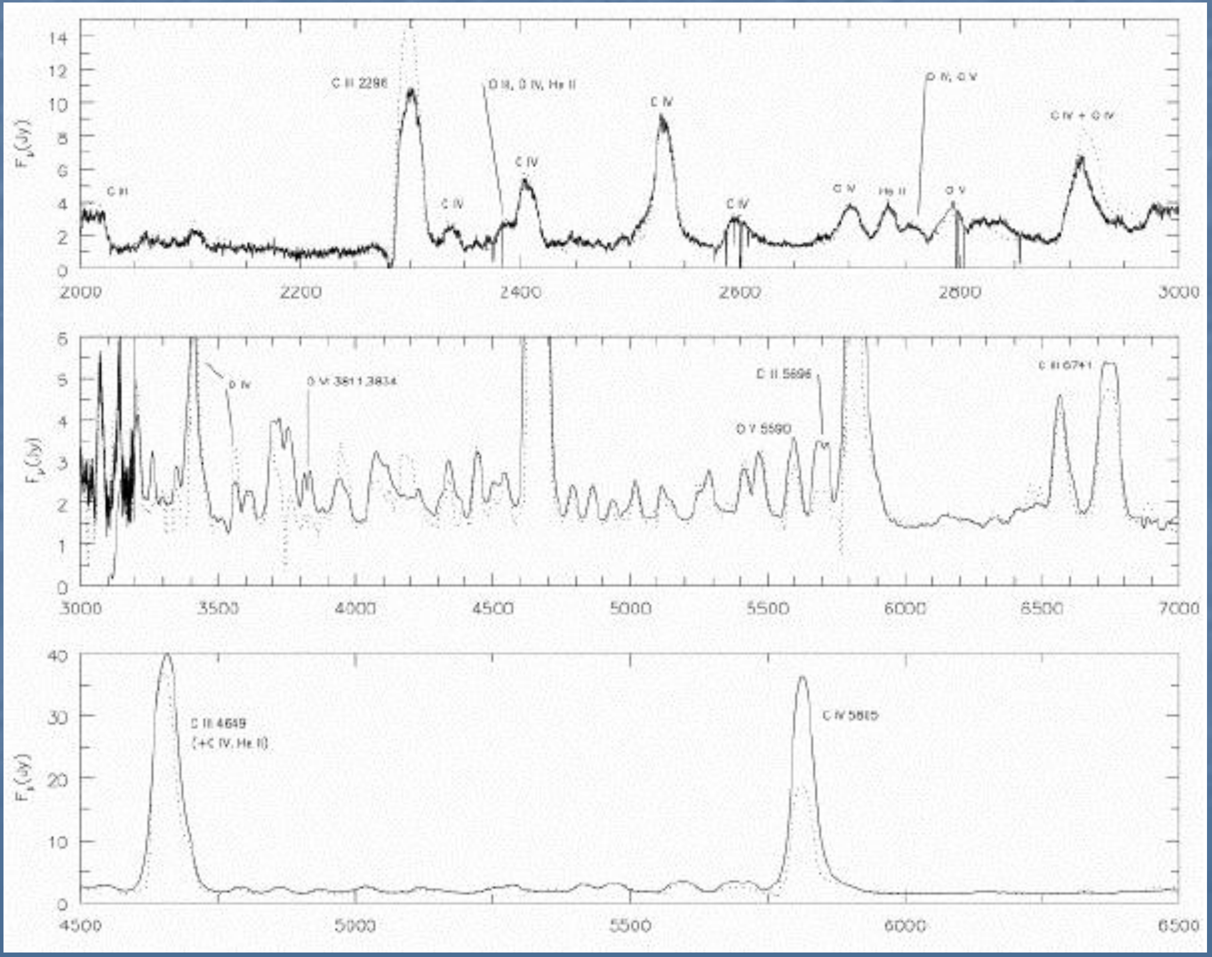

5.4 Scattering by free electrons

- Free electrons contribute significantly to the opacity of the stellar wind. They produce notably the scattering wings in the profiles of strong emission lines.

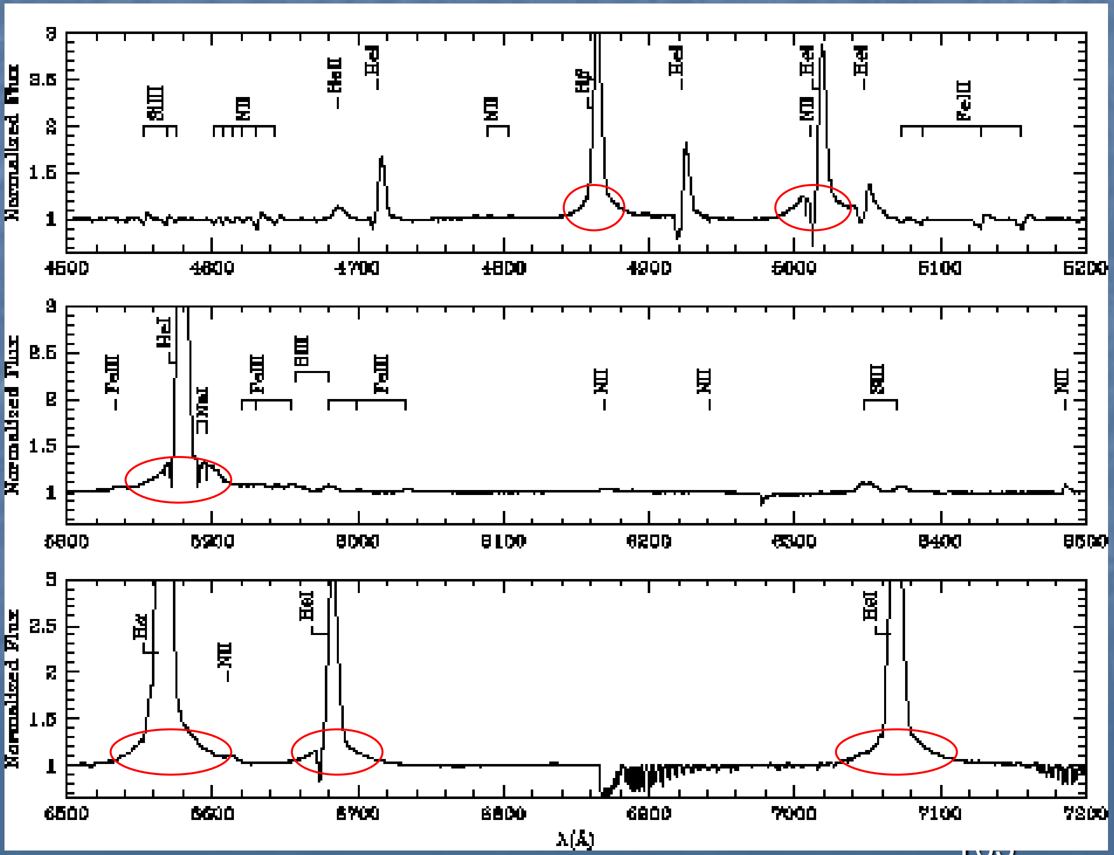

5.4 Scattering by free electrons

- The free electrons produce “red” wings for the emission: Auer & van Blerkom effect
- Doppler shift of a photon at first scattering: $\chi = \mu \times (v/c)$

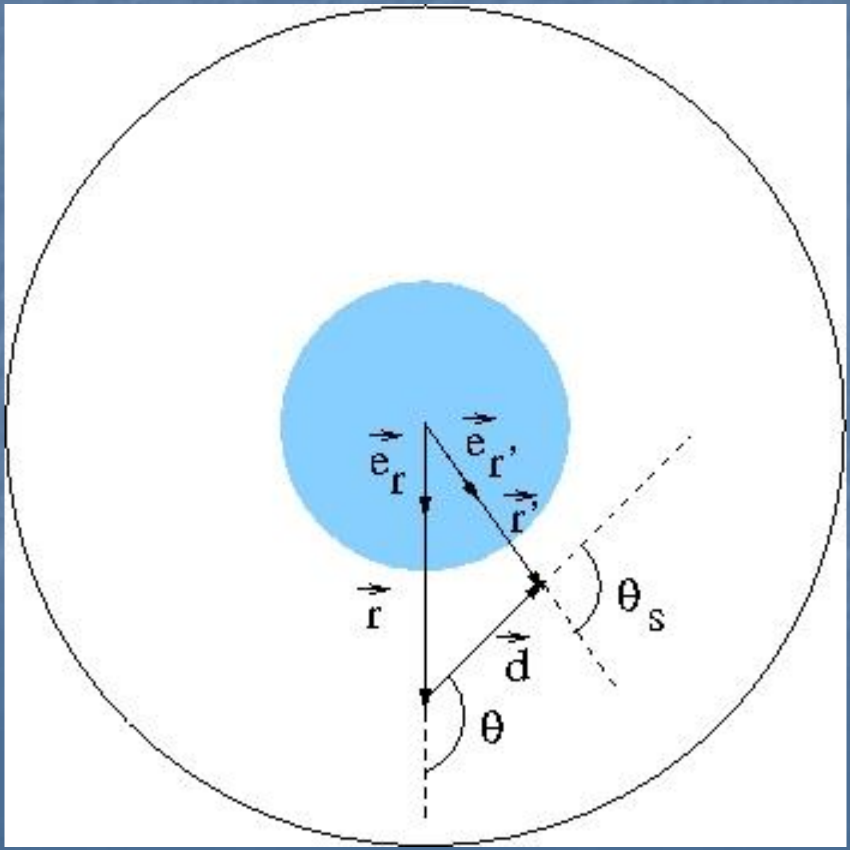

$$\mu = \cos\theta = \vec{e_r} \cdot \vec{d}/d$$

On average: $< \mu >= 0$

At the 2nd scattering event:

$$< \mu_s > \geq < \mu >$$

$$< \mu_s > \geq 0$$

5.5 Structures in the stellar winds

- Are stellar winds really homogeneous and spherically symmetric?

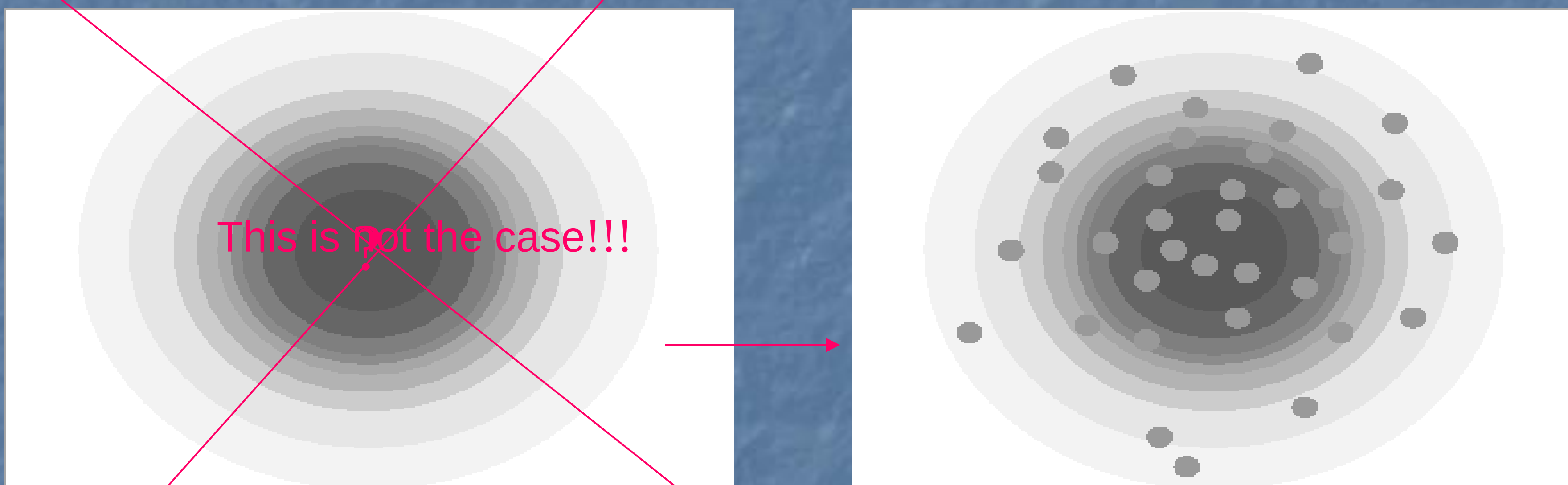

- Winds contain a huge number of small clumps of higher than average density.
- This fragmentation must be taken into account to correctly evaluate the mass-loss rate.

VI. Stellar magnetic fields

- Stellar atmospheres and interiors contain highly ionized plasma where charged particles move around = ideal conditions for generation of magnetic fields, but how can we measure them?

1. Polarization.
2. The Zeeman effect
3. Magnetic fields in stars

6.1 Polarization

- Polarization describes the evolution of the orientation of the electric field vector in an electromagnetic wave upon propagation.

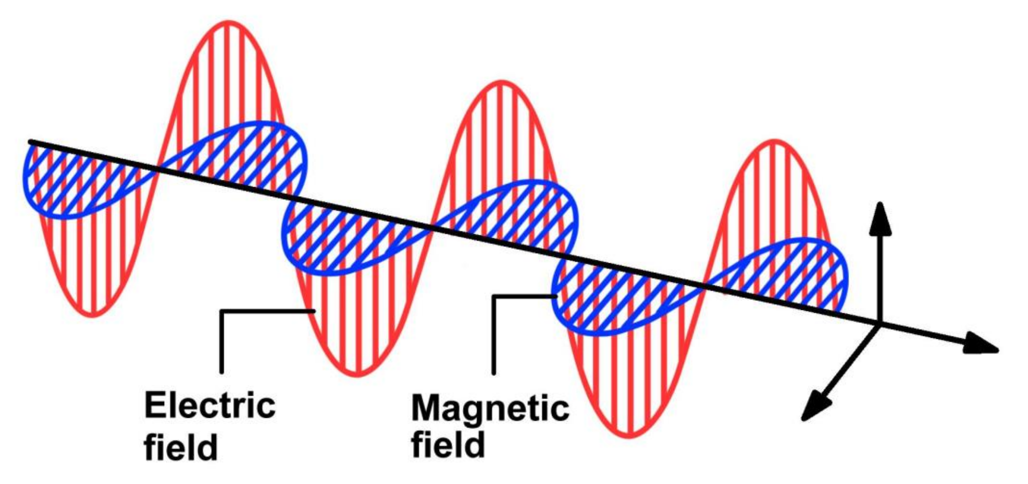

- Jones vector:

$$\vec{E} = \begin{pmatrix} E_x \\ E_y \end{pmatrix} = \begin{pmatrix} \zeta_x \exp\left[i\left(\omega\, t - k\, z\right)\right] \\ \zeta_y \exp\left[i\left(\omega\, t - k\, z + \delta\right)\right] \end{pmatrix}$$

- $\delta = 0 \rightarrow$ linearly polarized, $\delta = \pm\pi/2 \rightarrow$ circularly polarized.

6.1 Polarization

- Jones vector formulation valid for a single wave. In optical astronomy, one rather deals with the specific intensity described by the Stokes vector:

$$\vec{I} = \begin{pmatrix} I \\ Q \\ U \\ V \end{pmatrix} = \begin{pmatrix} < E_x^* E_x + E_y^* E_y > \\ < E_x^* E_x - E_y^* E_y > \\ < E_x^* E_y + E_y^* E_x > \\ < i\,(E_y^* E_x - E_x^* E_y > \end{pmatrix} = \begin{pmatrix} < \zeta_x^2 + \zeta_y^2 > \\ < \zeta_x^2 - \zeta_y^2 > \\ < 2\,\zeta_x\,\zeta_y \cos\delta > \\ < 2\,\zeta_x\,\zeta_y\,\sin\delta > \end{pmatrix}$$

- *I* specific intensity, *Q* & *U* linear polarization, *V* circular polarization.
- Modification of polarization properties described by Mueller matrices:

$$\vec{I}_{\rm obs} = \underline{\underline{\mathcal{M}}}_N\,\underline{\underline{\mathcal{M}}}_{N-1} \cdots \underline{\underline{\mathcal{M}}}_1\,\vec{I}_{\rm inc}$$

6.1 Polarization

- Polarization is also affected by free electron scattering, diffusion by interstellar dust grains and the instrument itself.
- Any reflection or interaction that breaks the symmetry modifies the polarization.
- Polarization levels of stars are often very low (less than a few percent).
- (Spectro)Polarimetry is a photon starving discipline requiring telescopes and instruments with low instrumental polarization and large telescopes.

6.2 The Zeeman effect

- Pieter Zeeman discovered the splitting of spectral lines under the action of a magnetic field (1896).

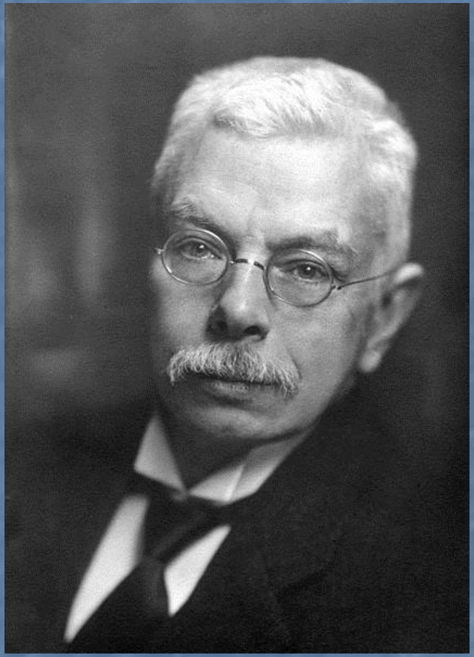

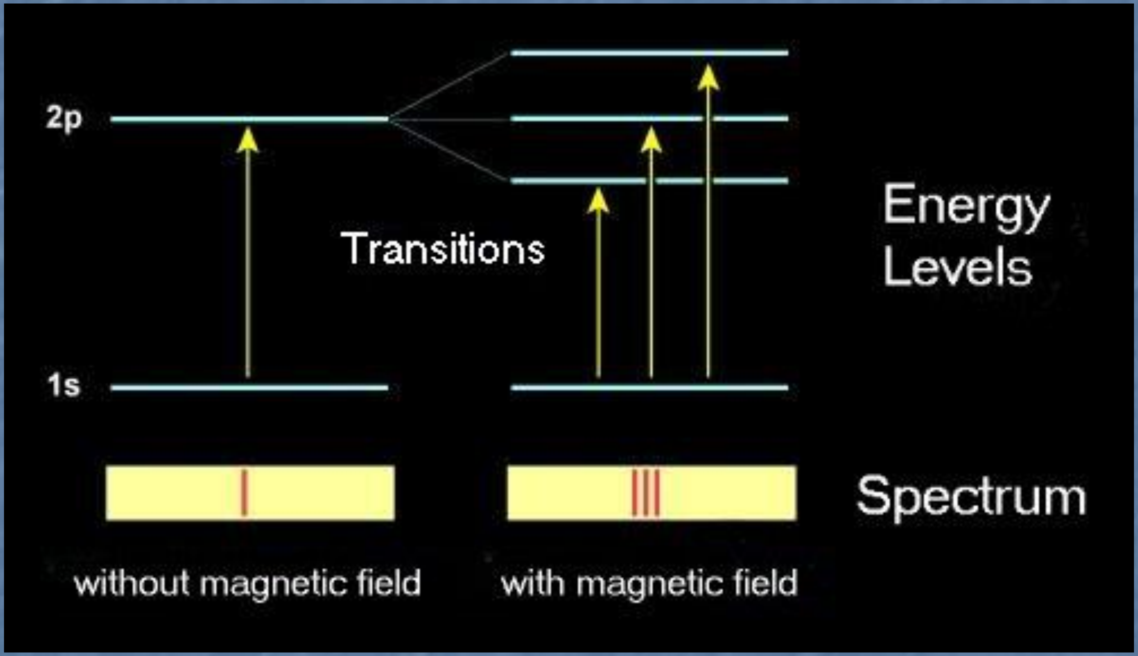

6.2 The Zeeman effect

- Consider an energy level of total angular momentum $\vec{J} = \vec{L} + \vec{S}$
- In the absence of a magnetic field, the level is 2 *J* + 1 times degenerate.
- When an external magnetic field is applied, the Hamiltonian describing the energy needs to be modified by adding a term

$$\mathcal{H}_B = \mu_B \, (\vec{L} + 2\,\vec{S}) \cdot \vec{B}$$

$$\mu_B = \frac{e\,h}{4\,\pi\,m\,c} = 9.27\,10^{-21}\,\mathrm{erg\,G^{-1}}$$

- The energy levels split into 2 *J* + 1 sublevels separated by

$$\Delta\,E = \mu_B\, g_{LS}\, B\, M$$

- Where *M* = *-J,-J +1,…,0,…,J – 1, J* and the Landé factor is given by

$$g_{LS} = \frac{3}{2} + \frac{S\,(S+1) - L\,(L+1)}{2\,J\,(J+1)}$$

6.2 The Zeeman effect

- The splitting of the energy levels leads to the splitting of the corresponding transitions:

$$\Delta E = (g_u\, M_u - g_l\, M_l)\, \mu_B\, B$$

- Where $\Delta M = M_u - M_l = -1, 0, +1.$
- $\Delta M=0$ corresponds to π components (no wavelength shift on average) which are linearly polarized for lines of sight perpendicular to the B field.
- $\Delta M=\pm 1$ corresponds to the $\sigma_\pm$ components shifted in wavelength by $\Delta\lambda_B = 4.67\,10^{-13}\,\lambda_0^2\,\overline{g}\,B$ around λ_0 and circularly polarized in opposite directions for lines of sight parallel to the B field and linearly polarized (perpendicular to the π component) for lines of sight perpendicular to the B field.

6.2 The Zeeman effect

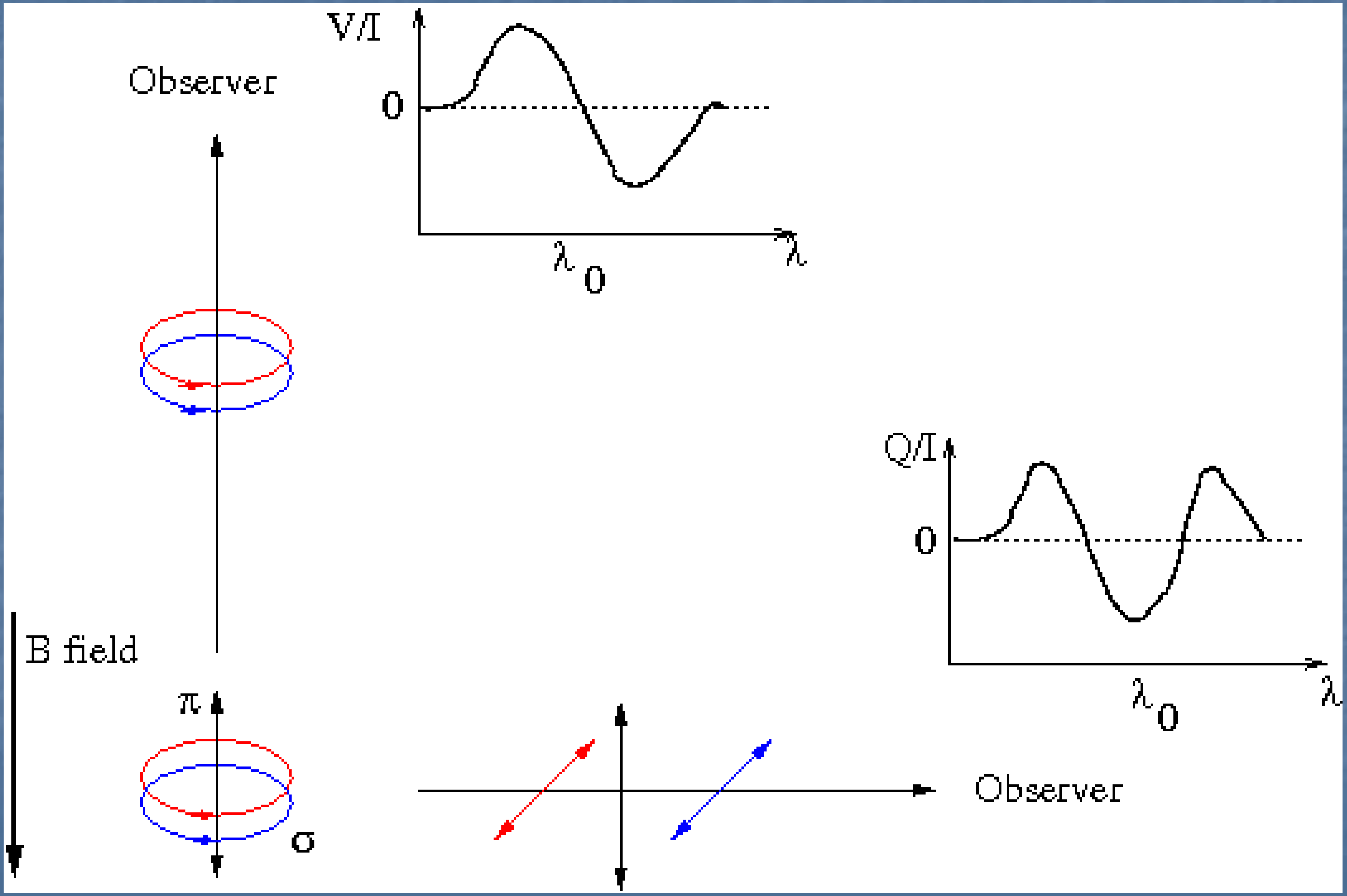

6.2 The Zeeman effect

- The Zeeman effect due to a stellar magnetic field can be detected either via line splitting or broadening (if the individual subcomponents are not resolved) or via spectropolarimetry.

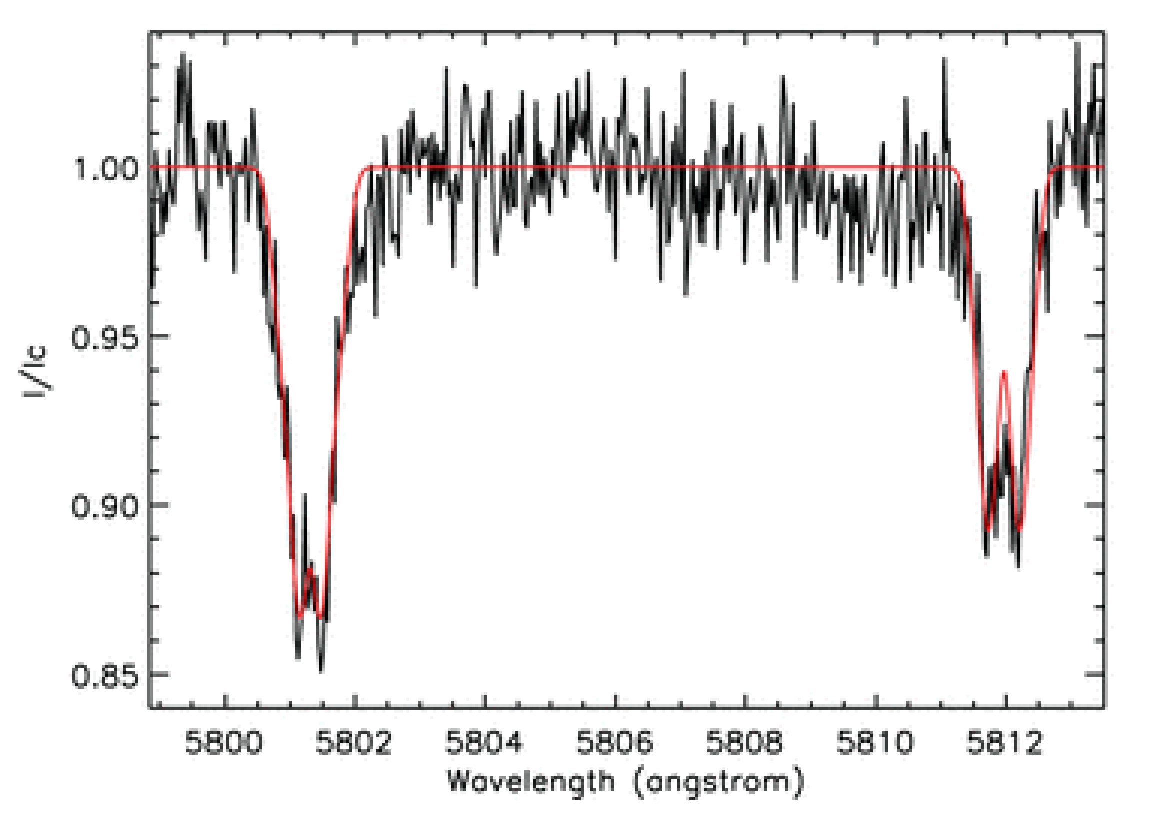

6.2 The Zeeman effect

- The significance of the spectropolarimetric signature can be improved via Least Square Deconvolution.
- Rotational modulation of the spectropolarimetric signal allows to map the magnetic field via Zeeman Doppler imaging.

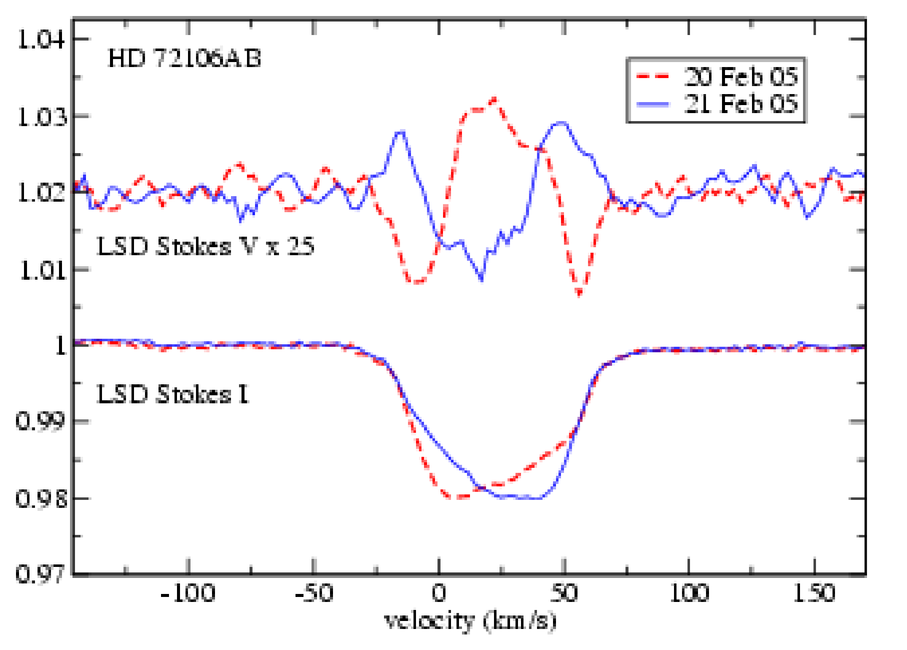

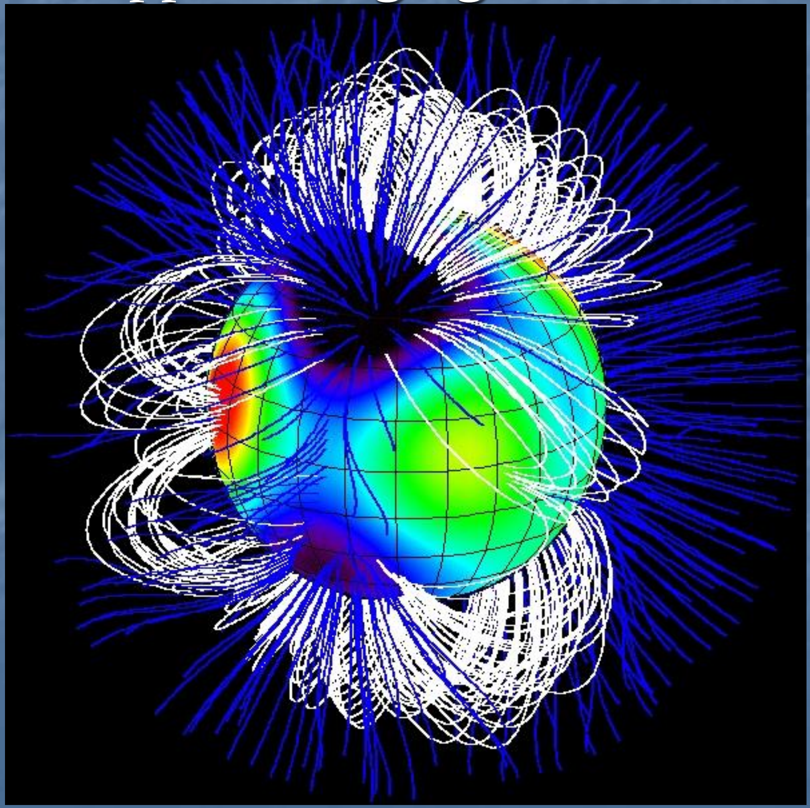

6.3 Stellar magnetic fields

- First detection of solar magnetic field in sunspots by G.E. Hale in 1908.

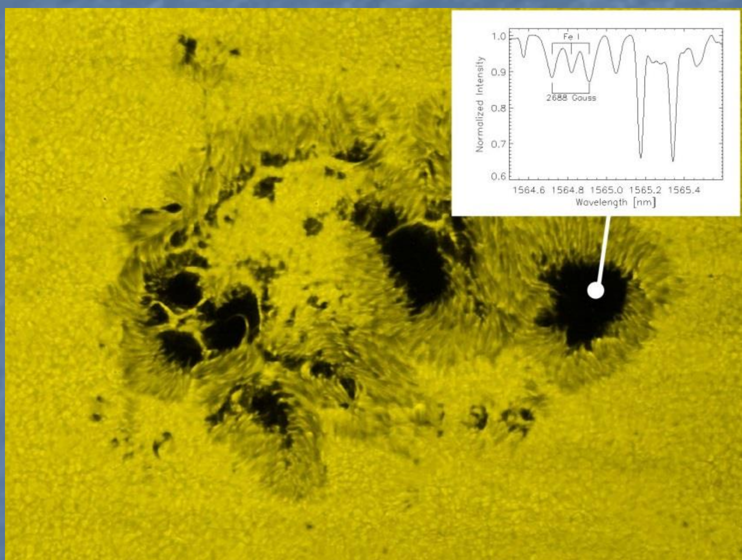

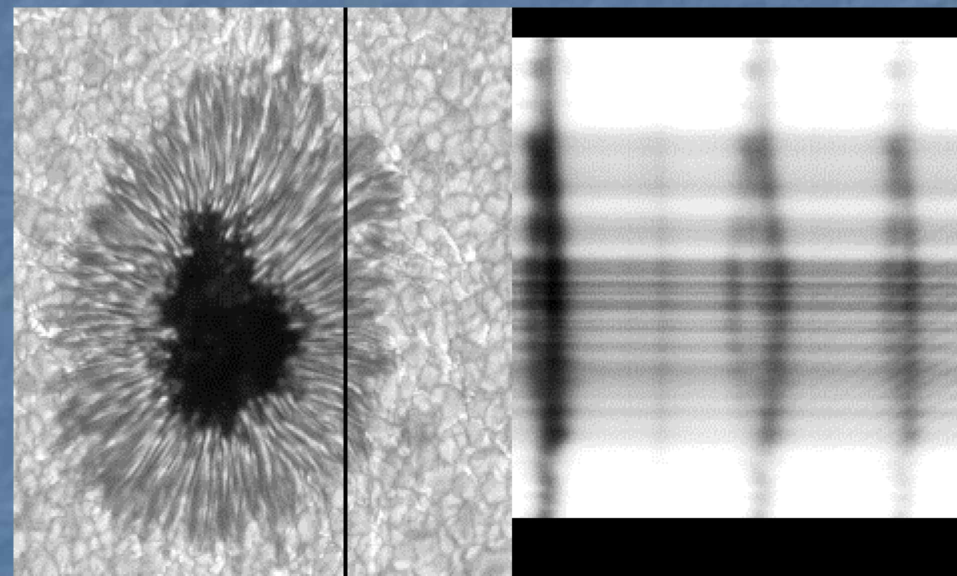

- First detection of large-scale stellar magnetic field by H. Babcock in 1947.
- Nowadays, modern spectropolarimeters: NARVAL @ TBL, ESPaDOnS @ CFHT and HARPSpol @ 3.6m ESO (La Silla).

6.3 Stellar magnetic fields

- Cool stars produce highly variable and complex magnetic fields via a dynamo effect at the interface between the differentially rotating core and the convective envelope.

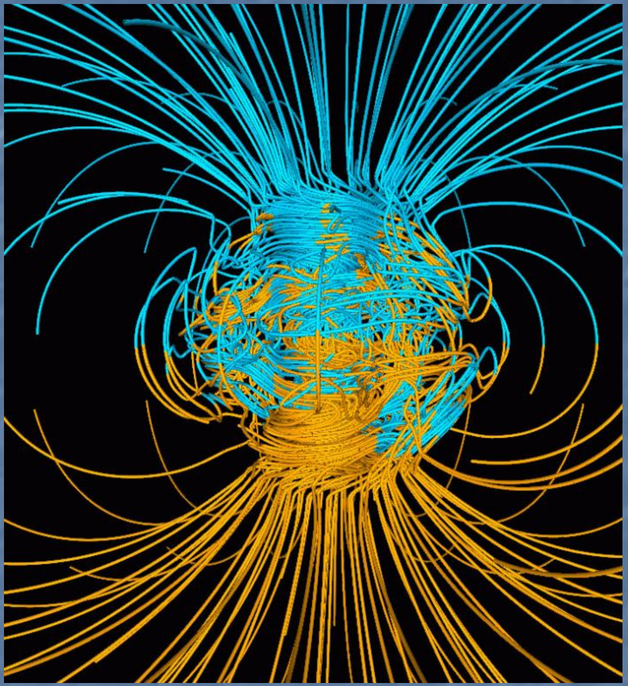

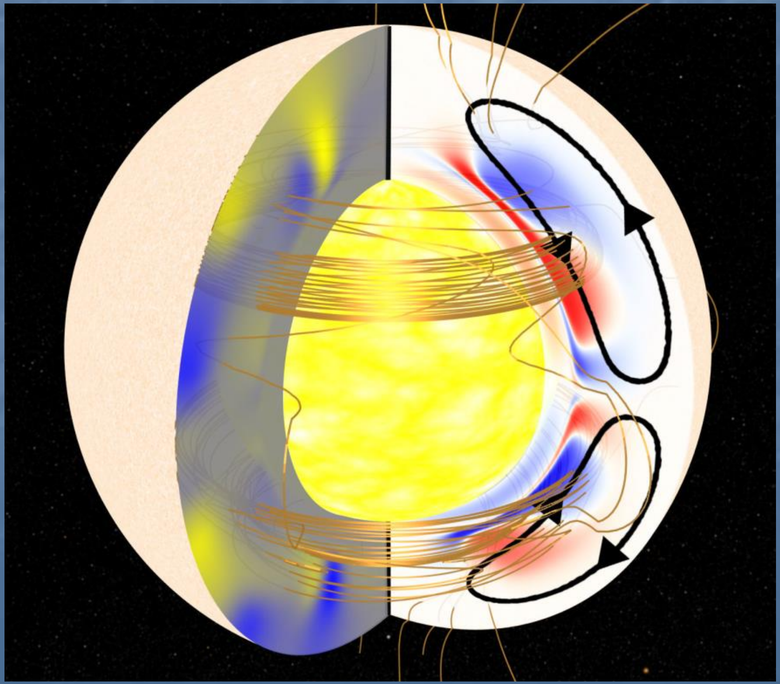

6.3 Stellar magnetic fields

- Tepid and hot stars feature rather simple (dipolar) magnetic morphologies. Less than 10% of these stars have a detectable magnetic field. These stars lack the convective envelope and their fields are thought to be fossil.

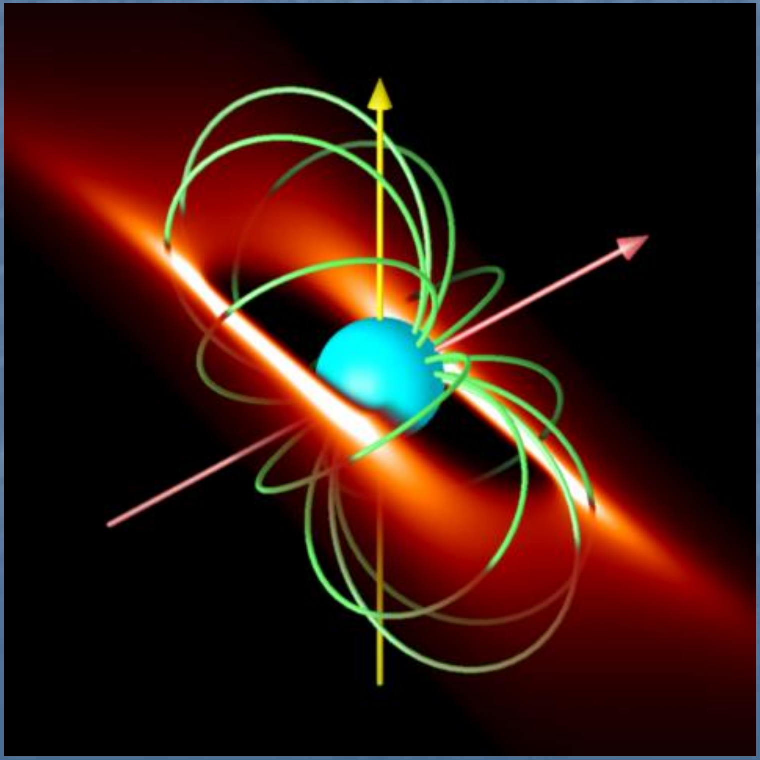

Exercises

Exercise 1

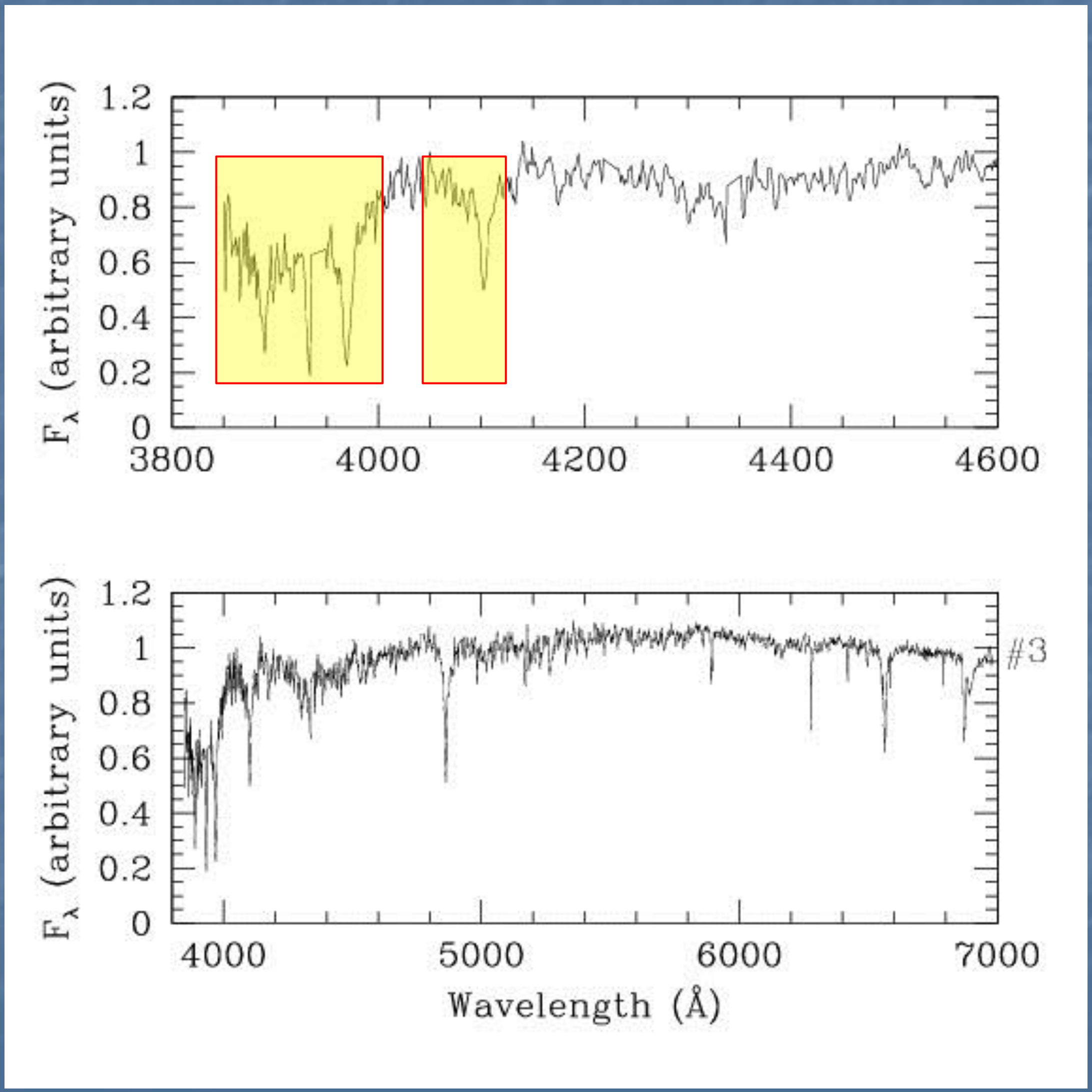

Comparison with Fig. 1.11: spectral type F –G.

Relative intensity of the H8 (3888 Å) line compared with Ca II H & K suggests spectral type F5 (Fig. 1.15). Weakness of Sr II λ 4077 indicates luminosity class V (Fig. 1.15).

Classification: F5V

Exercise 1

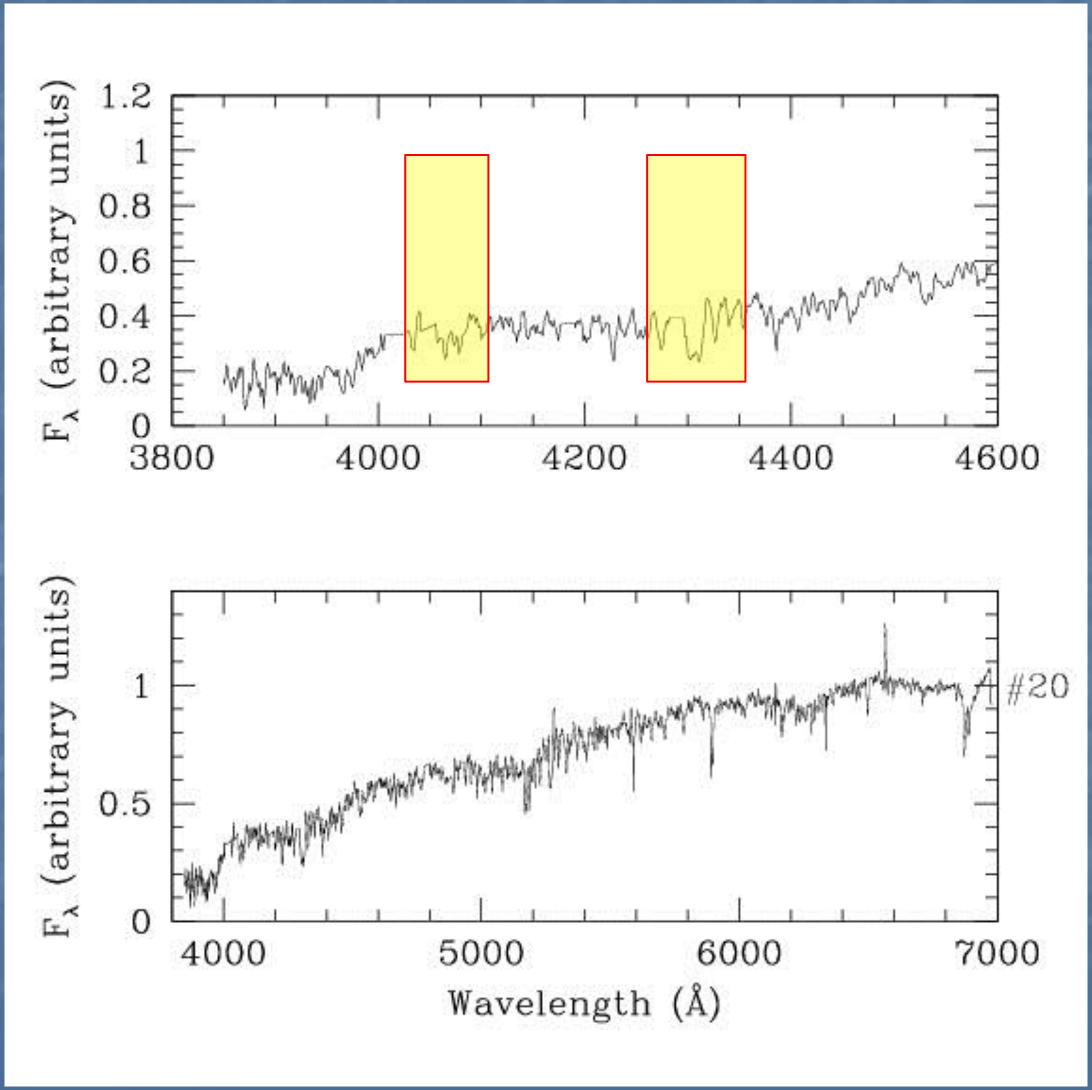

Comparison with Fig. 1.11: strength of G band (4300 Å) suggests spectral type K.

Ratio Fe I λ 4325/ Hγ (4340 Å) suggests type K0 or slightly later (Fig. 1.15). Weakness of Sr II λ 4077 indicates luminosity class V–III (Fig. 1.16).

Classification: K0–1V–III with peculiarity: Hα (6563 Å) in emission.

Exercise 1

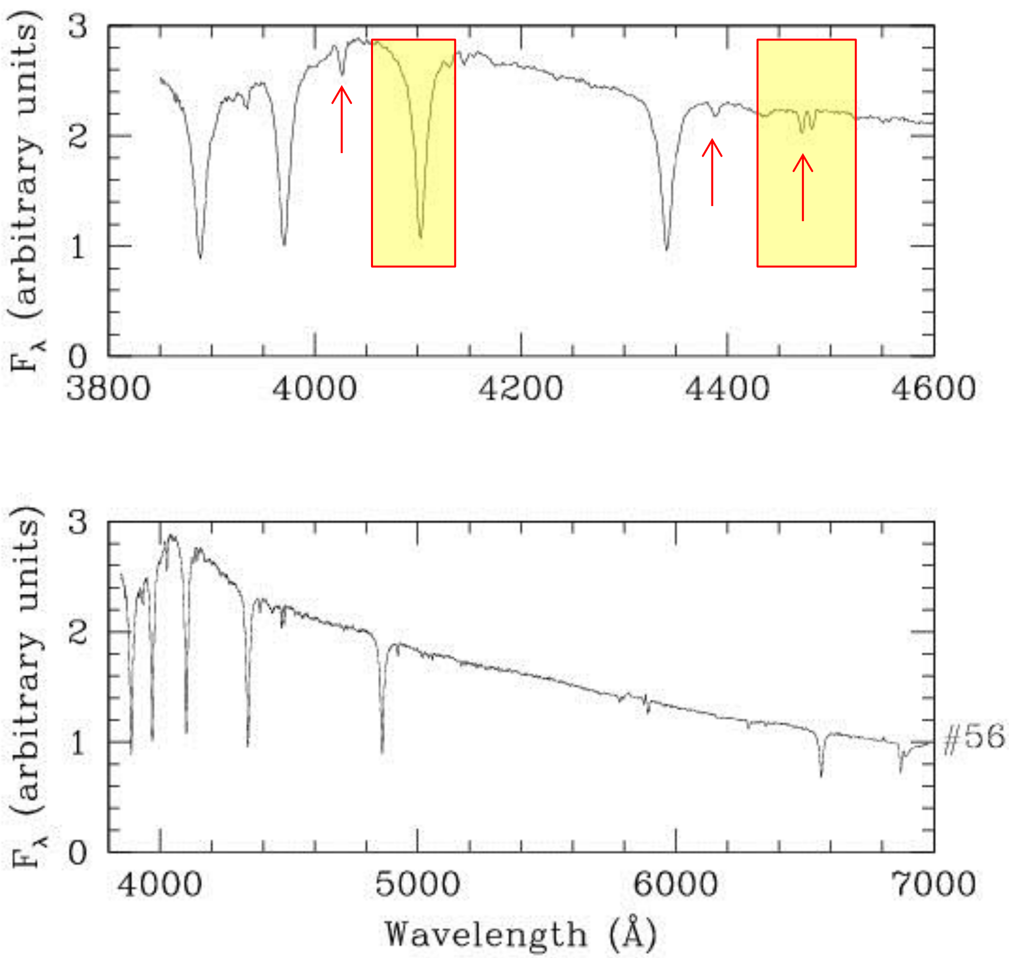

Comparison with Fig. 1.11: hot star (A – B). Presence of He I (λλ 4026, 4388, 4471) lines reveals a B star.

Ratio He I λ 4471/Mg II 4481 indicates spectral type B5 – 7 (Fig. 1.14). Width of the Balmer lines indicates luminosity class V (Fig. 1.14).

Classification: B5 – 7 V

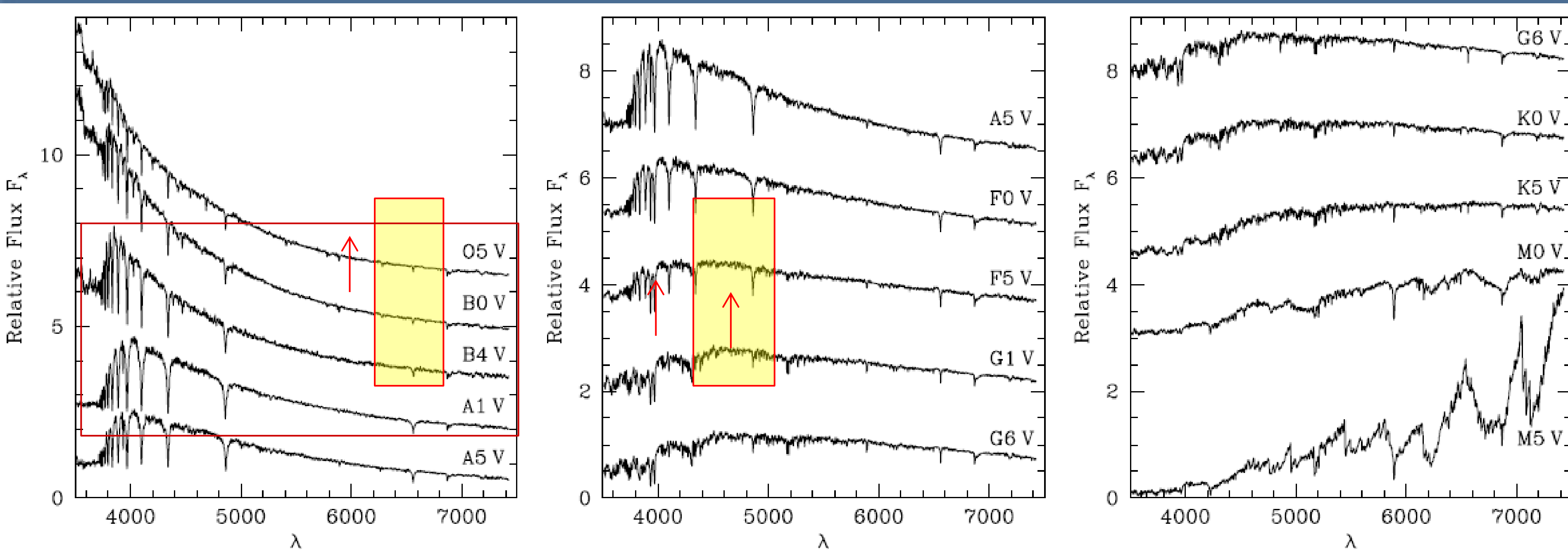

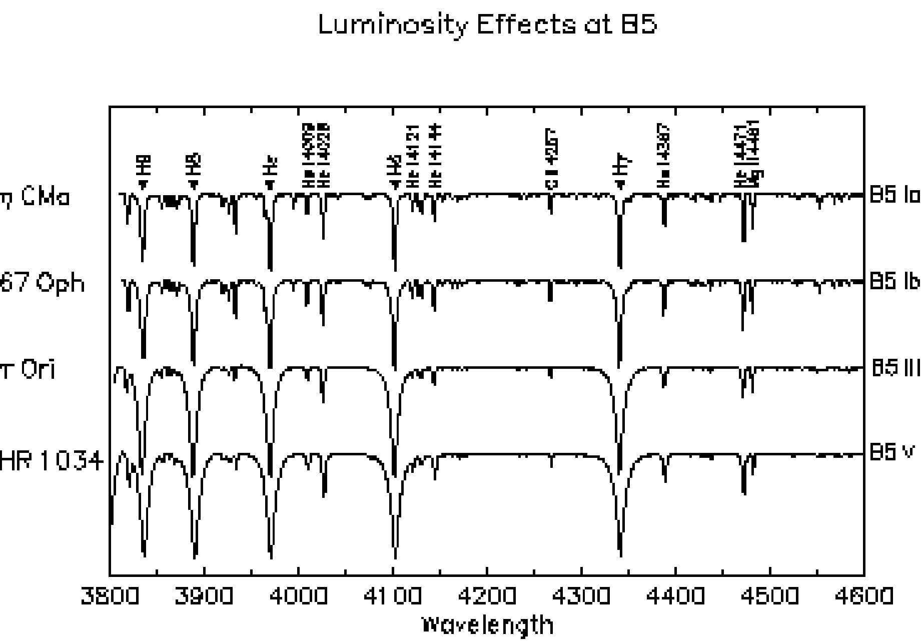

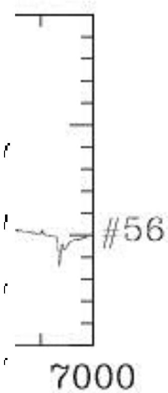

type B5 – 7 (Fig. 1.14).
Width of the Balmer lines indicates luminosity class V (Fig. 1.14).

Classification: B5 – 7 V

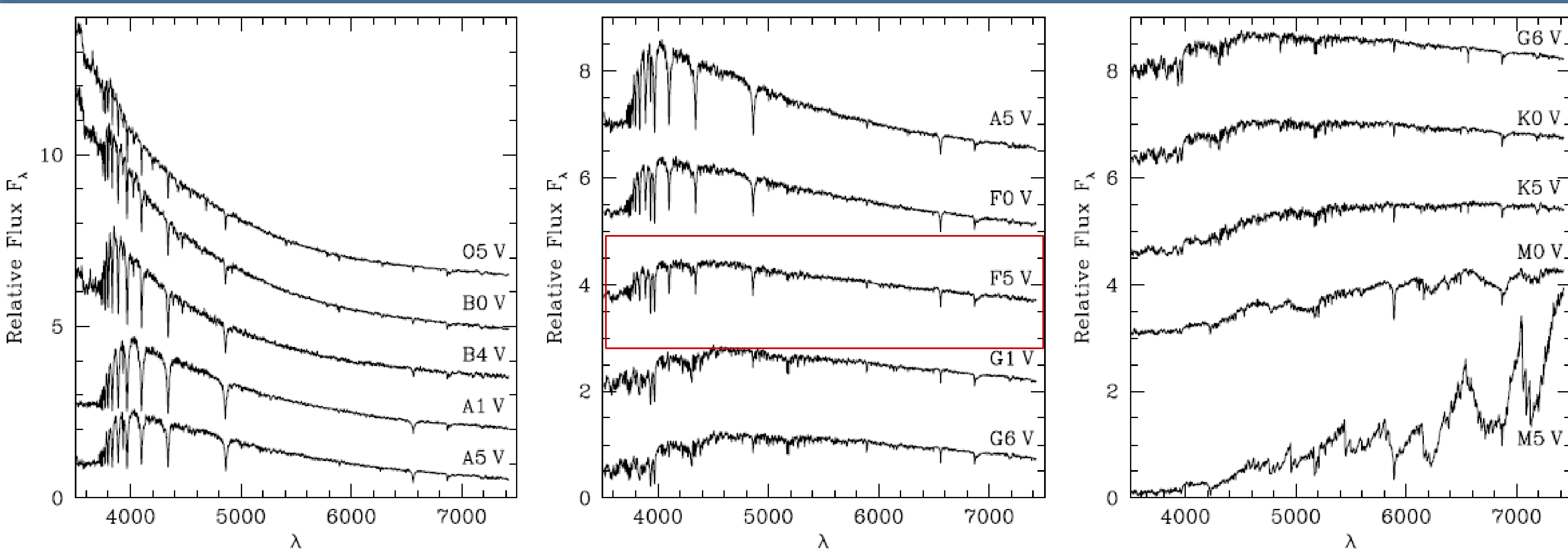

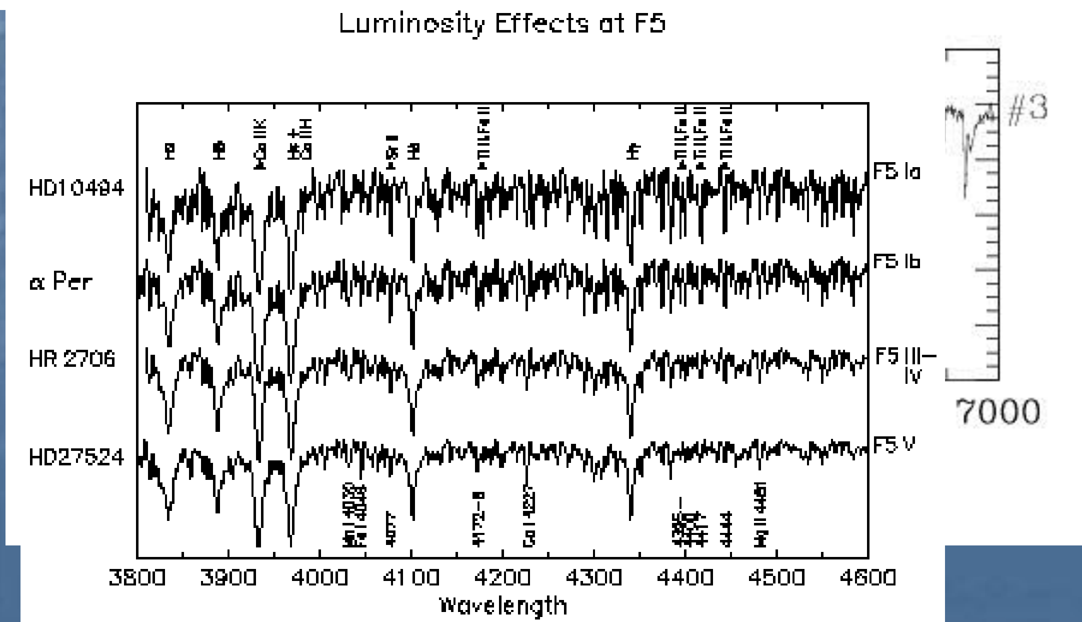

of Sr II λ 4077 indicates luminosity class V (Fig. 1.15).

Classification: F5V

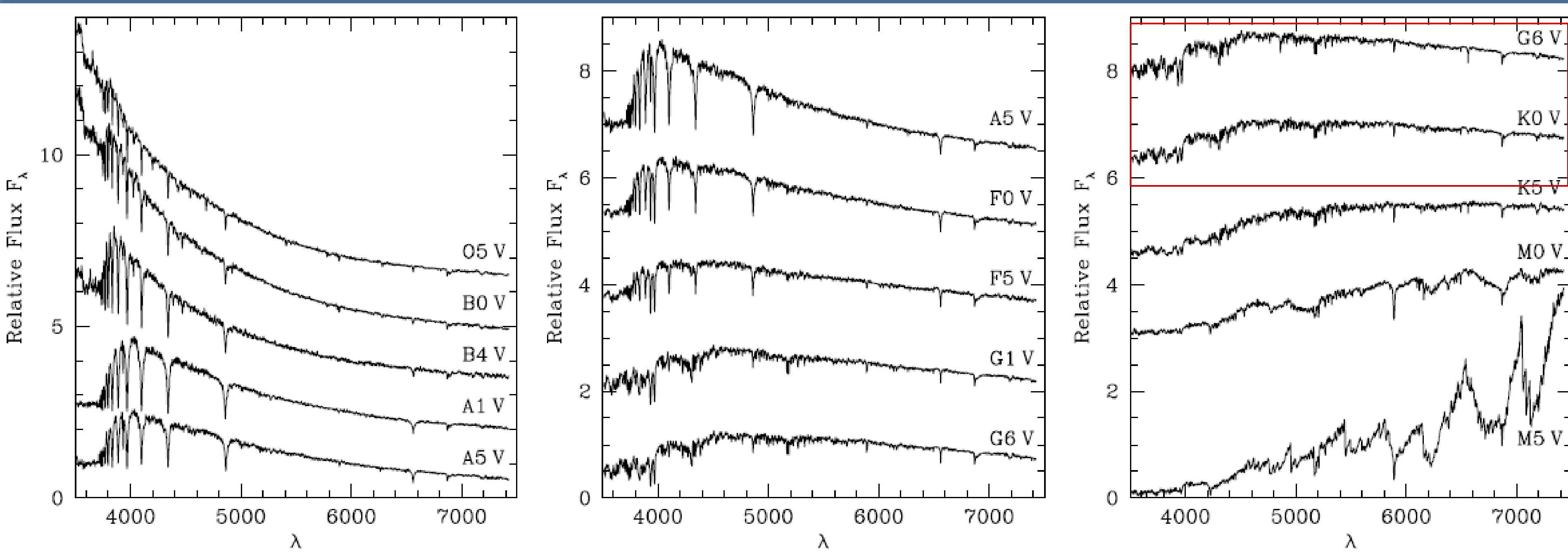

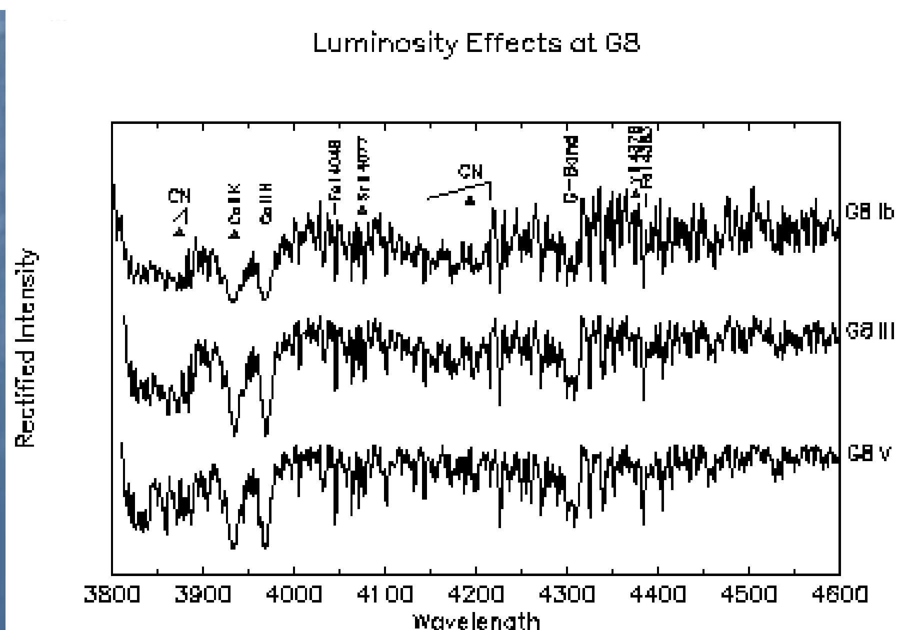

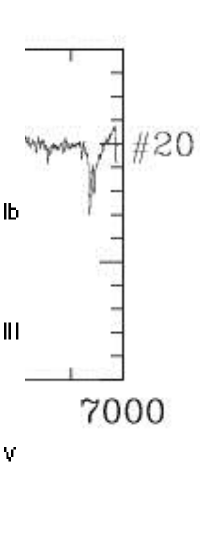

1.15). Weakness of Sr II λ 4077 indicates luminosity class V–III (Fig. 1.16).

Classification: K0–1V–III with peculiarity: Hα (6563 Å) in emission.

Chapter 3

- Source function at various wavelengths and as a function of the optical depth.

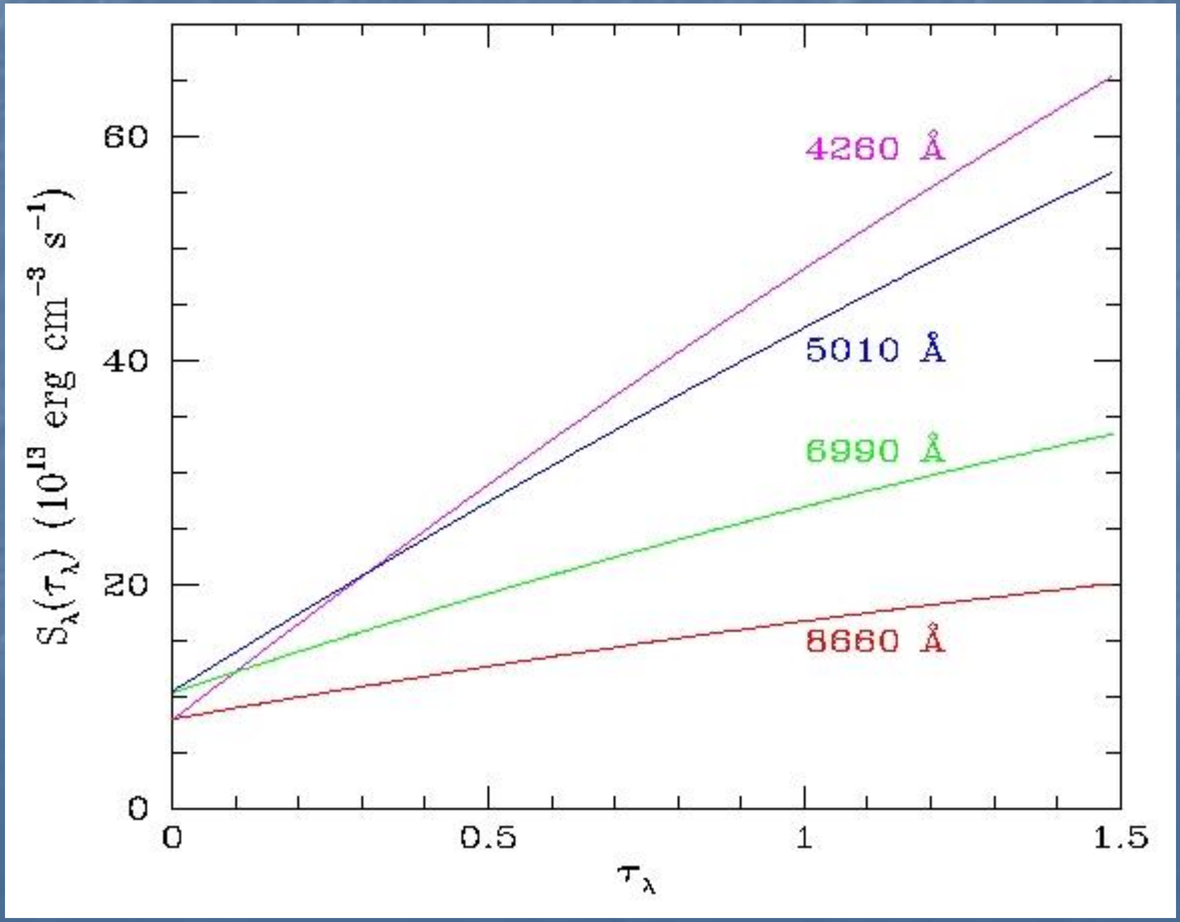

Chapter 3

- Temperature as a function of the optical depth in an ETL atmosphere for different wavelengths.

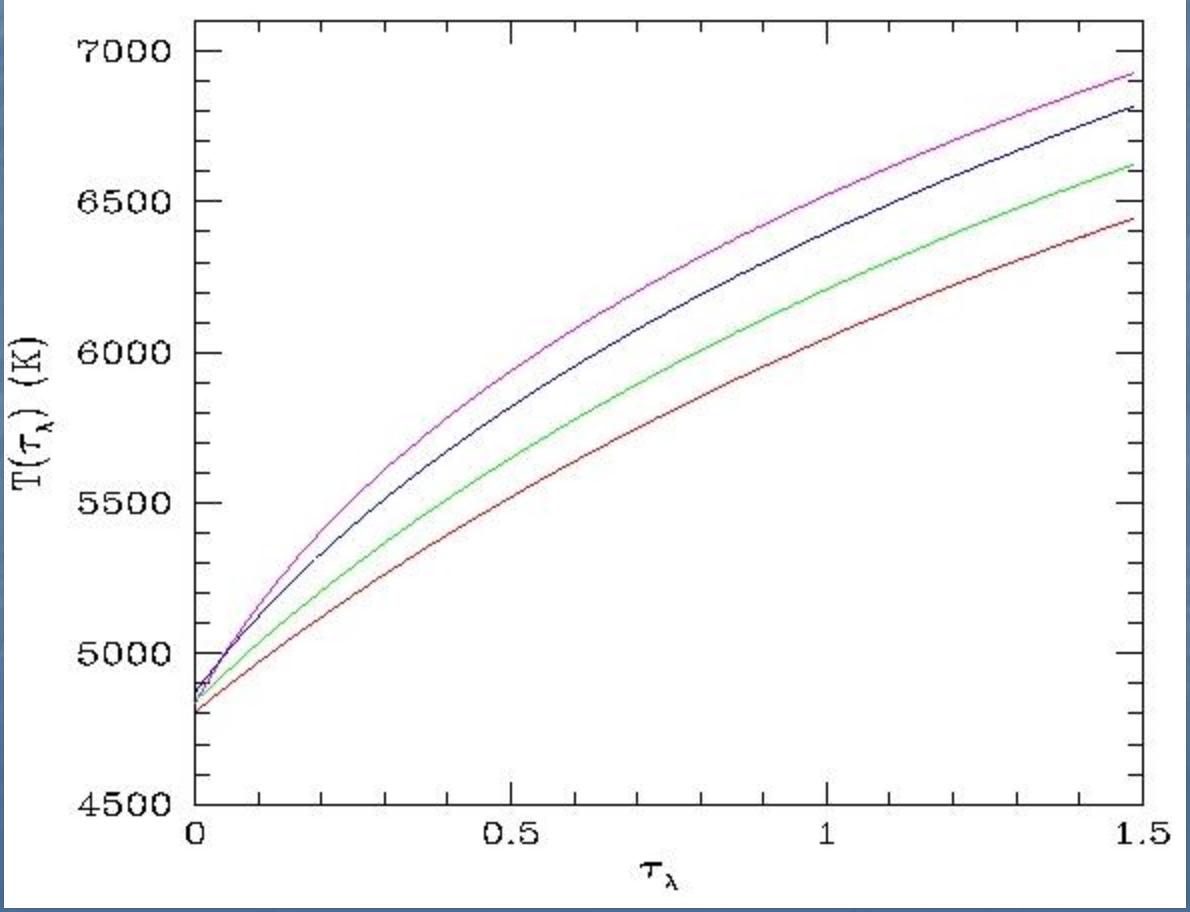

Chapter 3

- Opacity as a function of the wavelength at 3 different temperatures.

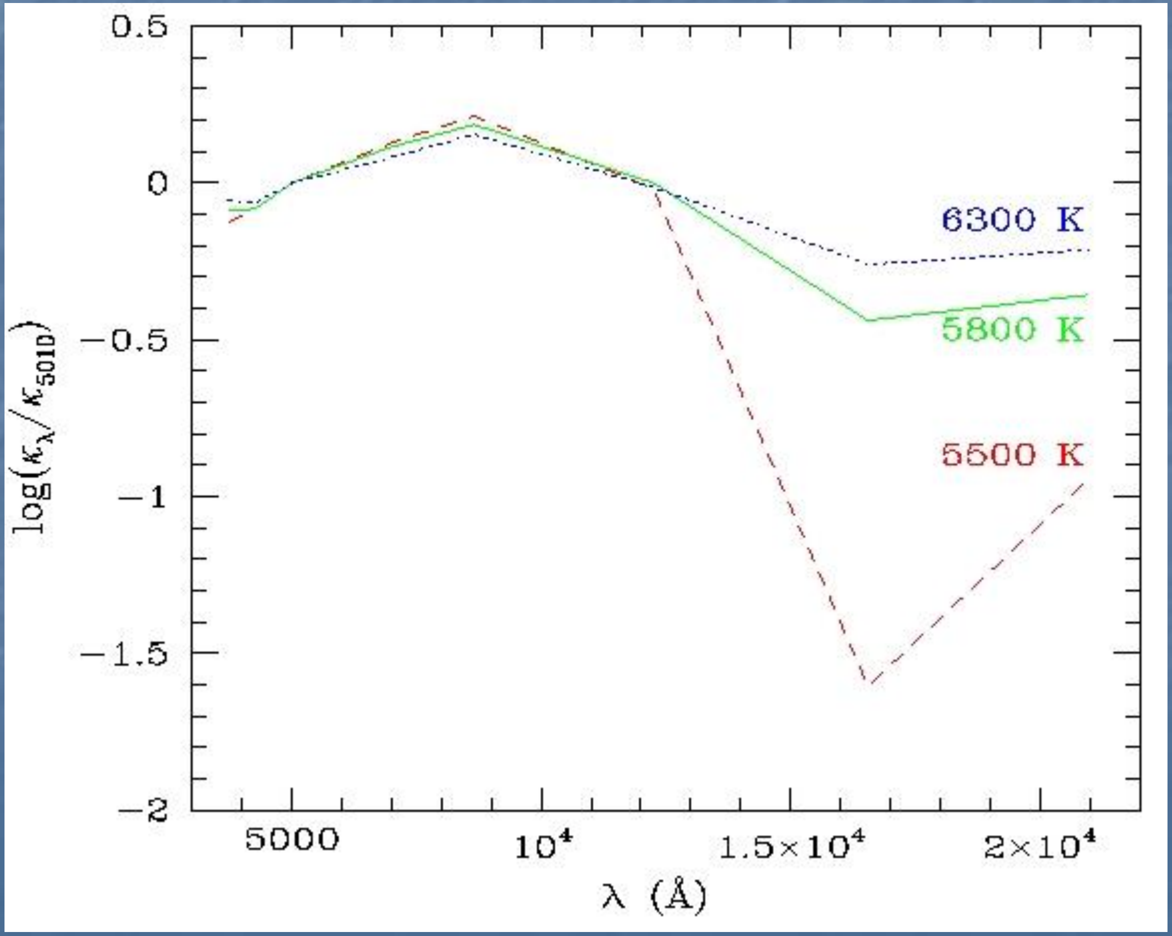

Chapter 5

- Mean intensity of a grey atmosphere as a function of optical depth: comparison of the exact solution vs. Eddington approximation + Eddington approximation with Λ_τ operator.

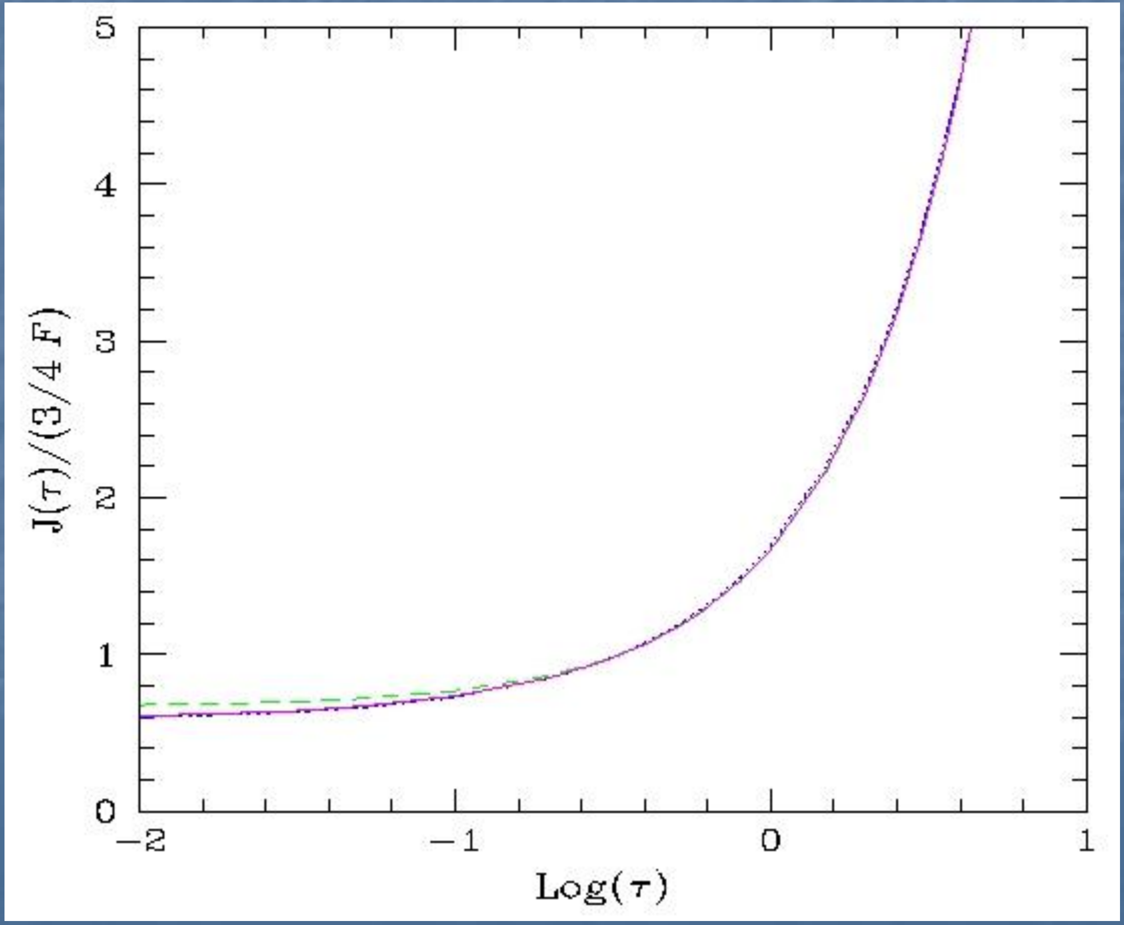

Chapter 5

- Relative error on $J(\tau)$ for a grey atmosphere using the Eddington approximation without and with application of the Λ_τ operator

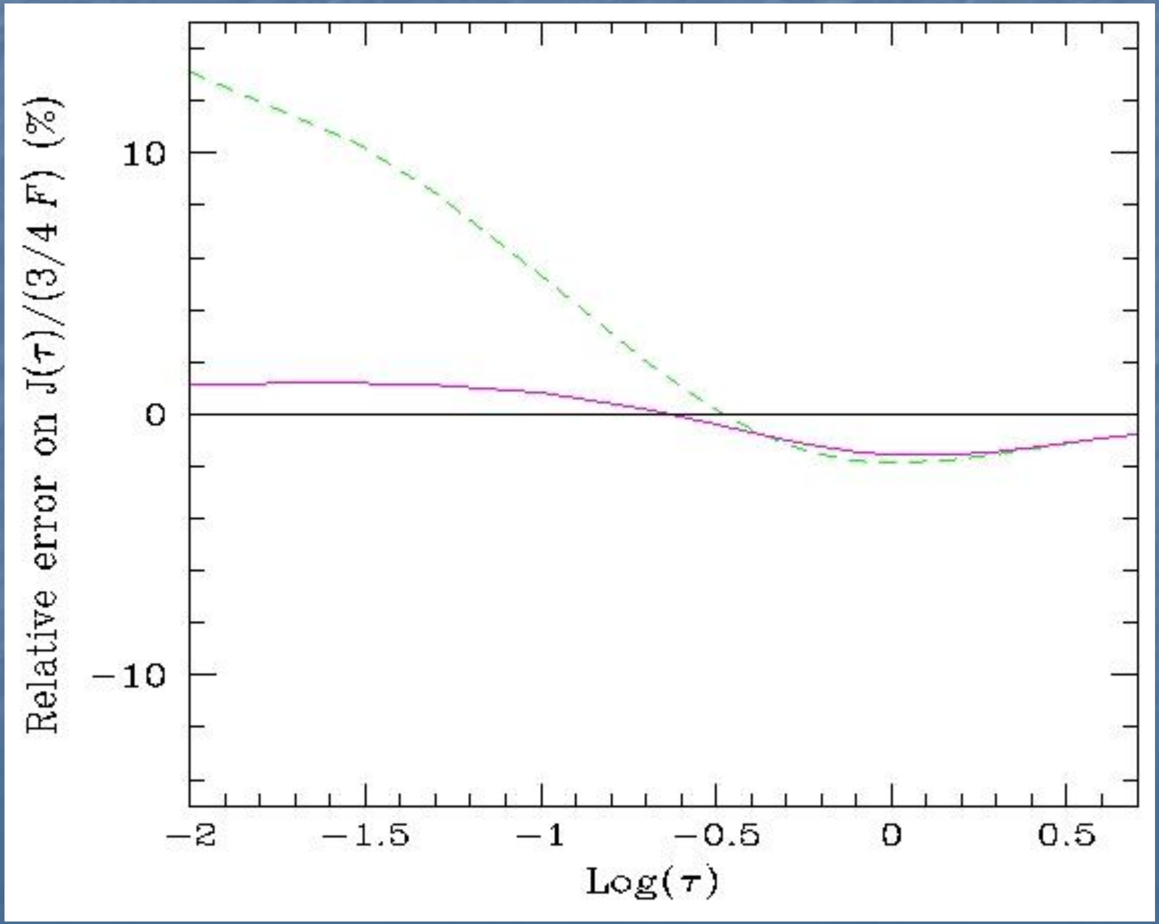

Chapter 5

- Emerging intensity $I^+(0,\mu)$ of a grey atmosphere. Exact solution vs. Eddington approximation or Eddington approximation combined with an application of the Λ_τ operator